

Deeptanshu Dwivedi

# Control and operation of dividing-wall columns with vapor split manipulation

Doctoral thesis  
for the degree of philosophiae doctor

Trondheim, January 2013

Norwegian University of Science and Technology  
The Faculty of Natural Sciences and Technology  
Department of Chemical Engineering

**NTNU**

Norwegian University of Science and Technology

Doctoral thesis  
for the degree of philosophiae doctor

The Faculty of Natural Sciences and Technology  
Department of Chemical Engineering

© 2013 Deeptanshu Dwivedi.

ISBN 978-82-471-4130-4 (printed version)  
ISBN 978-82-471-4131-1 (electronic version)  
ISSN 1503-8181

Doctoral theses at NTNU, 2013:20

Printed by NTNU-trykk

# Summary

Thermally coupled distillation arrangements with dividing-wall implementation provide significant energy and capital savings compared to energy intensive conventional distillation arrangements. In this thesis, the focus is to study control and operation of such arrangements for three and four product separation. The study comprises of mainly simulation study for the Petlyuk arrangements while for the four-product Kaibel arrangement, simulation as well as experimental works are reported.

The first contribution deals with selecting control structures for a three-product Petlyuk (dividing-wall) column. Alternate control structures are considered, with and without the vapor split as a degree of freedom. This work also demonstrates the usefulness of the graphical  $V_{min}$  diagram to visualize minimum boilup requirement and choose the appropriate control structure.

Next, for a four-product Kaibel column separating methanol, ethanol, propanol and *n*-butanol, a start-up procedure and steady state operation is demonstrated using experimental setup. A control structure with four temperature controllers is used for control and it can handle feed rate disturbances as well as setpoint changes. The experiment data also compares well with an equilibrium stage model.

Dividing-wall distillation columns offer large potential energy savings over conventional column sequences, typically up to 30 % for three-product (Petlyuk) columns and 40 % for four-product (Kaibel) columns. However, the energy required for a separation depends on using an optimal vapor split. Hence, the energy saving potential may be lost if the column is operated away from its optimal point, for example, due to feed composition changes. The following work demonstrates experimentally that the vapor split can be effectively used as a degree of freedom during operation for example, for temperature control in the prefractionator section. Together with an adjustable liquid split, the vapor split control allows for minimizing the energy requirements.

Finally, a control study on a four-product extended Petlyuk column operating close to minimum energy is reported. The study assumes an “ideal” case with all steady state degrees of freedom available for control, including the vapor split valves, which is required to achieve minimum energy under all conditions. Four decentralized control structures are proposed and tested against a wide range of disturbances. This work demonstrates again the use of the graphical  $V_{min}$  tool which can be used to visualize the minimum boilup requirement for four-product Petlyuk arrangements.

# Acknowledgements

This work could not have been completed without the assistance of several individuals. First and foremost is my supervisor, Prof. Sigurd Skogestad. Prof. Sigurd Skogestad has been a real source of motivation during this work. His doors were always open for suggestions and guidance and his passion for learning has truly inspired me. He has definitely left a lasting impression on me as a both a person and a researcher. Next, I would really like to thank my co-supervisor Dr Ivar J Halvorsen (from SINTEF, ICT). He has been there help me tackle each hurdle I faced, be it simulation studies, or experimental work. I will always be grateful to him for his unselfish and unfailing desire to help.

I would also like to acknowledge with gratitude, Dr. Jens P Strandberg who built the experimental column and Prof. Heinz Presig, who helped in the initial design of the column. I am also thankful to Ms. Kathinka Lystad (from SINTEF), who assisted me in the analysis of the samples and Mr. Odd Ivar Hovin and Mr. Jan-Morten Roel from the workshop who were always eager to help me fix the experimental setup. I am also grateful to Mr. Filip Vos and Mr. Jon Anta Buljo Hansen who assisted with the experiments.

I gratefully acknowledge the funding source that made this work possible. This work has been financed by The Research Council of Norway through the GASSMAKS project: Basic Energy Efficient Distillation Technology.

It was an absolute privilege to have the company of Process Systems Engineering group members most of whom became my close friends and I will always cherish the tremendous warmth I received from them. They helped create an environment of sharing, as we learned together the lessons of life as well as Process Control.

Finally, I would like to thank my parents, Dr. P N Dwivedi and Mrs. Satrupa Dwivedi, who have always stood by me, even though living far away.

My two sisters, Meenakshi and Deepti shared their experiences, sometimes to boost my morale and sometimes to motivate me to work harder. And I am really fortunate to have with me the constant support of my wife, Richa for the last one year, who instilled in me confidence and a strong desire to finish this work.

Deeptanshu Dwivedi  
January 2013  
Trondheim, Norway

# Contents

<b>Summary</b>	<b>i</b>
<b>Acknowledgements</b>	<b>iii</b>
<b>1 Introduction</b>	<b>1</b>
1.1 Motivation . . . . .	1
1.2 Organization of thesis . . . . .	2
1.3 List of Contributions . . . . .	3
References . . . . .	4
<b>2 Energy efficient distillation</b>	<b>5</b>
2.1 Single Column . . . . .	5
2.2 Optimal Sequence of multiple columns . . . . .	6
2.3 Thermal coupling . . . . .	8
2.3.1 Indirect Coupling . . . . .	9
2.3.2 Direct Coupling . . . . .	9
2.4 $V_{min}$ diagrams . . . . .	13
2.5 Minimum energy and thermal efficiency for three-product separation using alternate configurations . . . . .	16
2.5.1 Minimum energy in conventional arrangements . . . . .	16
2.5.2 Minimum energy in Petlyuk arrangements . . . . .	16
2.5.3 Thermal efficiency in alternate configurations . . . . .	16
2.5.4 A Case Study . . . . .	17
2.6 Conclusion . . . . .	18
References . . . . .	19
<b>3 Control structure selection for three-product Petlyuk (dividing- wall) column</b>	<b>21</b>
3.1 Introduction . . . . .	21
3.2 Case Study . . . . .	24

---

3.3	Control Structures for three-product Petlyuk column . . . . .	27
3.3.1	Control Objectives . . . . .	27
3.3.2	Setpoints for the controlled variables . . . . .	31
3.3.3	Control Structures . . . . .	32
3.4	Closed loop simulation results . . . . .	34
3.4.1	Simulation of structure CS1 . . . . .	35
3.4.2	Simulation of structure CS2 . . . . .	36
3.4.3	Simulation of structure CS3 . . . . .	36
3.4.4	Simulation of structure CS4 . . . . .	36
3.5	Analysis of energy usage . . . . .	36
3.6	Discussion . . . . .	41
3.6.1	Change in difficult split . . . . .	41
3.6.2	Multivariable Control (MPC) . . . . .	42
3.6.3	Other control structures . . . . .	43
3.7	Conclusions . . . . .	44
	References . . . . .	44
<b>4</b>	<b>Steady state and dynamic operation of four-product dividing-wall (Kaibel) columns: Experimental Verification</b>	<b>47</b>
4.1	Introduction . . . . .	47
4.2	Experimental setup . . . . .	51
4.3	Control Structure . . . . .	54
4.4	Experiments . . . . .	56
4.4.1	Start-up . . . . .	56
4.4.2	Closed-loop operation . . . . .	58
4.5	Steady state experiments and comparison with simulations .	65
4.6	Discussion . . . . .	68
4.6.1	Practical issues related to operation . . . . .	68
4.6.2	Plant-model mismatch . . . . .	70
4.6.3	Optimal operation . . . . .	70
4.7	Conclusions . . . . .	71
4.7.1	Acknowledgement . . . . .	72
4.7.2	Model Details . . . . .	72
	References . . . . .	73
<b>5</b>	<b>Active vapor split control for dividing-wall columns</b>	<b>79</b>
5.1	Introduction . . . . .	79
5.2	Experimental Setup . . . . .	85
5.3	Experiment . . . . .	86
5.3.1	Vapor Split valve behavior . . . . .	86
5.3.2	Total Reflux experiments . . . . .	86



5.3.3	4-Product Kaibel Column experiments . . . . .	93
5.4	Discussion . . . . .	95
5.4.1	Feedback implementation of vapor split . . . . .	95
5.4.2	Use of two vapor valves . . . . .	95
5.5	Conclusions . . . . .	95
5.5.1	Acknowledgement . . . . .	96
	References . . . . .	96
<b>6</b>	<b>Control structure selection for four-product Petlyuk column</b>	<b>99</b>
6.1	Introduction . . . . .	99
6.2	Case Study . . . . .	104
6.2.1	Steady state composition profiles . . . . .	104
6.3	$V_{min}$ diagrams . . . . .	105
6.4	Control structures for three-product Petlyuk columns . . . . .	107
6.5	Proposed control structures for the four-product extended Petlyuk column . . . . .	109
6.5.1	Control Structure 1 (CS1) . . . . .	110
6.5.2	Control Structure 2 (CS2) . . . . .	111
6.5.3	Control Structure 3 (CS3) . . . . .	112
6.5.4	Control Structure 4 (CS4) . . . . .	113
6.6	Tuning . . . . .	114
6.7	Closed-loop simulation results . . . . .	115
6.7.1	Performance of CS1 and CS2 . . . . .	115
6.7.2	Performance of CS3 and CS4 . . . . .	117
6.8	Discussion . . . . .	117
6.8.1	Impact of feed disturbances & the $V_{min}$ diagram . . . . .	117
6.8.2	Temperature control . . . . .	124
6.8.3	Composition control . . . . .	124
6.9	Conclusions . . . . .	126
	References . . . . .	126
<b>7</b>	<b>Conclusions and further work</b>	<b>131</b>
7.1	Main Conclusions . . . . .	131
7.2	Further works . . . . .	132
	<b>Joint Declaration by Co-Workers</b>	<b>137</b>



# Chapter 1

## Introduction

### 1.1 Motivation

Distillation is a preferred technique for separating liquid mixtures in chemical industries. However, conventional distillation columns consumes a lot of energy and constitutes a big fraction of industrial energy consumption ([4]). Being the workhorse of separation in process industries, there is a huge incentive to reduce the energy usage in distillations. This can be accomplished by a variety of methods as listed in Chapter 2. Dividing-wall columns, offer one of the most practical and robust alternatives for improving energy efficiency as well as capital savings. There are more than 100 reported applications of dividing-wall columns in the industry. The recent improvements in the equipments associated with dividing-wall columns have led to a fresh impetus in the use of dividing-wall columns ([2]).

The focus of this thesis is to study control and operation of dividing-wall columns for three and four product separation. The open literature has abundance of simulation and experimental works reported on the three-product dividing-wall columns. The simulation study on three-product column reported here is complementary to some of those earlier works and at the same time, it highlights some of the limitations of old works with alternative solutions.

In contrast, little or no experimental works have been reported on dividing-wall columns for separation of quaternary mixtures. And therefore, we carried out experimental works to study steady state and start up operation for a four-product Kaibel column. A major hurdle in dividing-wall operations is the vapour split between the prefractionator and the main column. As, any energy saving potential can be lost if dividing-wall columns are operated far away from the optimal vapour split. This challenging issue is addressed

using an experiment study where we show for the first time the use of active manipulation of vapour split in dividing-wall columns.

Finally, we study operation of a four-product extended Petlyuk column, which may also be realised by a multiple partitioned column in a single shell ([1]). Such arrangements offer huge energy saving potential compared to the conventional arrangements.

## 1.2 Organization of thesis

Chapter 2 gives an introduction to different techniques of energy efficient distillation. In this thesis, we have used a graphical tool, the “ $V_{min}$  diagrams” developed by Halvorsen and Skogestad [3]. We therefore, describe the use of the “ $V_{min}$  diagrams” for estimation of minimum energy for conventional and thermally-coupled distillation. We also compare several directly coupled arrangements with conventional arrangement in terms of thermal efficiency and energy usage.

The next four chapters are dedicated to studying control properties of dividing-wall columns for three and four product separation. Each chapter gives an introduction to some of the recent and old trends on dividing-wall control studies. So there are some overlapping texts.

Chapter 3 deals with selecting control structures for three-product Petlyuk columns. We consider some decentralized PI control structures and propose some new strategies based on switching. We also give generalized recommendations for selecting composition based structures.

Chapter 4 presents experimental works on start-up and steady state operation of a four product Kaibel column. We use a four-point temperature control structure and test its performance against feed disturbances and set-point changes. We also present a method to fit a equilibrium-based model to steady state experimental data. We also compare our experimental results against some “optimal” operation scenarios.

Chapter 5 summarizes another experimental work. We show for the first time that the vapor split can be used as a degree of freedom during practical operation can be effectively used as a control degree of freedom on our experimental dividing-wall column.

In Chapter 6, a control study of a four-product extended Petlyuk column operating close to minimum energy is reported. Decentralized PI control structures are proposed and tested against a wide range of disturbances.

In Chapter 7, the main conclusions of this thesis are summarized along with some suggestions for further work.

## 1.3 List of Contributions

### 1. Chapter 3 <sup>1</sup>

**Dwivedi D.**, Halvorsen I.J., Skogestad S., Control structure selection for three-product Petlyuk (dividing-wall) column”, *Accepted for publication in Chemical Engineering and Processing: Process Intensification (2012)*, doi: “10.1016/j.cep.2012.11.006”.

### 2. Chapter 4 <sup>1</sup>

**Dwivedi D.**, Standberg J., Halvorsen I.J., Skogestad S., Steady state and dynamic operation of four-product dividing-wall (Kaibel) columns: Experimental Verification”, *Accepted for publications in Industrial & Engineering Chemistry Research (2012)*, doi: “10.1021/ie301432z”.

### 3. Chapter 5 <sup>1</sup>

**Dwivedi D.**, Standberg J., Halvorsen I.J., Preisig, H.A., Skogestad S., Active vapor split control for dividing-wall columns”, *Accepted for publication in Industrial & Engineering Chemistry Research (2012)*, doi: “10.1021/ie3014346”.

### 4. Chapter 6 <sup>1</sup>

**Dwivedi D.**, Halvorsen I.J., Skogestad S., “Control structure selection for four-product Petlyuk column”, *Accepted for publications in Chemical Engineering and Processing: Process Intensification (2012)*, doi: “10.1016/j.cep.2012.07.013”.

## Conferences

1. **Dwivedi D.**, Halvorsen I.J., Maryam Ghadrnan, Mohammad Shamsuzzoha and Skogestad S., “Basic Control of Complex Distillation Columns”, *Nordic Process Control Workshop, 2010*.
2. **Dwivedi D.**, Halvorsen I.J., Skogestad S., “Control Structure Design for Optimal Operation of 4-Product Thermally Coupled Columns”, *AIChE Spring Meeting, 2011*.
3. **Dwivedi D.**, Halvorsen I.J., Skogestad S., “Control Structure Design for 4-Product Petlyuk Column”, *European Congress of Chemical Engineering, Berlin, 2011*.

---

<sup>1</sup>Refer to the joint declaration at the end of the thesis for contributions of the co-authors.

4. **Dwivedi D.**, Halvorsen I.J., Skogestad S., “Dynamic behaviour and control of extended Petlyuk distillation arrangements”, *European Symposium on Computer Aided Process Engineering (ESCAPE)*, London, **2012**.
5. **Dwivedi D.**, Halvorsen I.J., Skogestad S., “Active Vapor Split Control for Fully Coupled Columns: Experimental Studies”, *AIChE Annual Meeting, Minneapolis*, **2012**.
6. Yelchuru R., Skogestad S., **Dwivedi D.**, “Optimal Measurement selection for controlled variables for Kaibel distillation column”, *AIChE Annual Meeting, Minneapolis*, **2012**.
7. **Dwivedi D.**, Halvorsen I.J., Skogestad S., “Active Vapor Split Adjustment for Energy Optimal Control of Dividing Wall Distillation Columns: Experimental Studies”, *Trondheim Gas Technology Conference*, **2012**.
8. **Dwivedi D.**, Halvorsen I.J., Skogestad S., “Regulatory Control of 4-product Kaibel column”, *Nordic Process Control Workshop*, **2012**.

## References

- [1] Dejanovic, I., Matijasevic, L., Halvorsen, I. J., Skogestad, S., Jansen, H., Kaibel, B., Olujic, Z., 2011. Designing four-product dividing wall columns for separation of a multicomponent aromatics mixture. *Chemical Engineering Research and Design* 89 (8), 1155 – 1167.
- [2] Dejanovic, I., Matijasevic, L., Olujic, Z., 2010. Dividing wall column—a breakthrough towards sustainable distilling. *Chemical Engineering and Processing: Process Intensification* 49 (6), 559–580.
- [3] Halvorsen, I. J., Skogestad, S., 2003. Minimum energy consumption in multicomponent distillation. 1. Vmin diagram for a two-product column. *Industrial & Engineering Chemistry Research* 42 (3), 596–604.
- [4] White, D. C., 2012. Optimize Energy use in Distillation. *Chemical Engineering Progress*, March, 35–41.

## Chapter 2

# Energy efficient distillation

This chapter gives a brief overview on the techniques for minimizing energy and capital costs in distillation. The methods in section 2.1 are for minimization energy in a single, two-product column. For a multicomponent separation, there are several alternatives including the sequence of column (Section 2.2) and the “direct coupling” (Section 2.3). The methods described in Section 2.1 are complementary and not competing with the methods described in Sections 2.2 and 2.3. For example, an optimum sequence of columns for a multicomponent separation is described in Section 2.2. A single column constituting this sequence can be operated more efficiently using the guidelines in Section 2.1.

### 2.1 Single Column

In a two-product distillation column with a single rectifying section and a single stripping section, some of the established methods to limit the energy consumption are by operating the column close to the specification of the products, by reducing direct heat losses by proper insulation, by choice of optimal pressure for operation, using sufficiently large number of stages for a required separation, introducing feed at the “optimum” stage to minimize mixing losses, by introducing multiple feeds (of different compositions) at their different “optimum” stage locations and, by introducing the feed at “correct” thermal state and vapor fraction. Use of intermediate (side) reboilers and condensers may reduce exergy losses and allow the use of inferior inventory for heating or cooling.

Another method is the heat pump assisted distillation column. Here, the heat of condensation from the overhead vapors can be extracted by some working fluid (external fluid or overhead vapor). The heated fluid is

compressed and used as heating medium in the reboiler. The fluid cooled in the reboiler can then be used as a coolant (if external fluid) in the condenser or can be used directly as liquid reflux (if working fluid is the overhead vapor) [8, 17].

A more radical method that combines the advantages of uniform heating and cooling by using diabatic stages and vapor recompression simultaneously is the “internally heat integrated column” or HIDiC [13, 14, 19].

## 2.2 Optimal Sequence of multiple columns

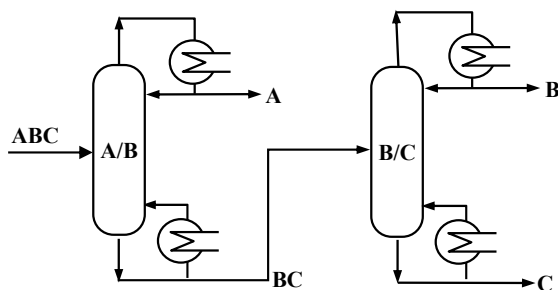


Figure 2.1: Direct sequence for three-product separation

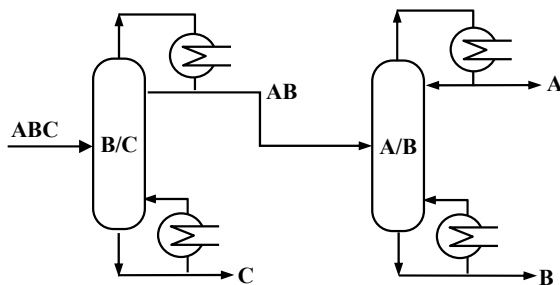


Figure 2.2: Indirect sequence for three-product separation

For separating a multicomponent feed using conventional column, the two most commonly used arrangements are the direct sequence (see, Figure 2.1) and the indirect sequence. In the direct sequence, the light components are removed first. In an indirect split sequence (see Figure 2.2) the heavy components are removed first. The number of columns using required using a direct or indirect sequence are  $N-1$  ( $N$ =number of components).



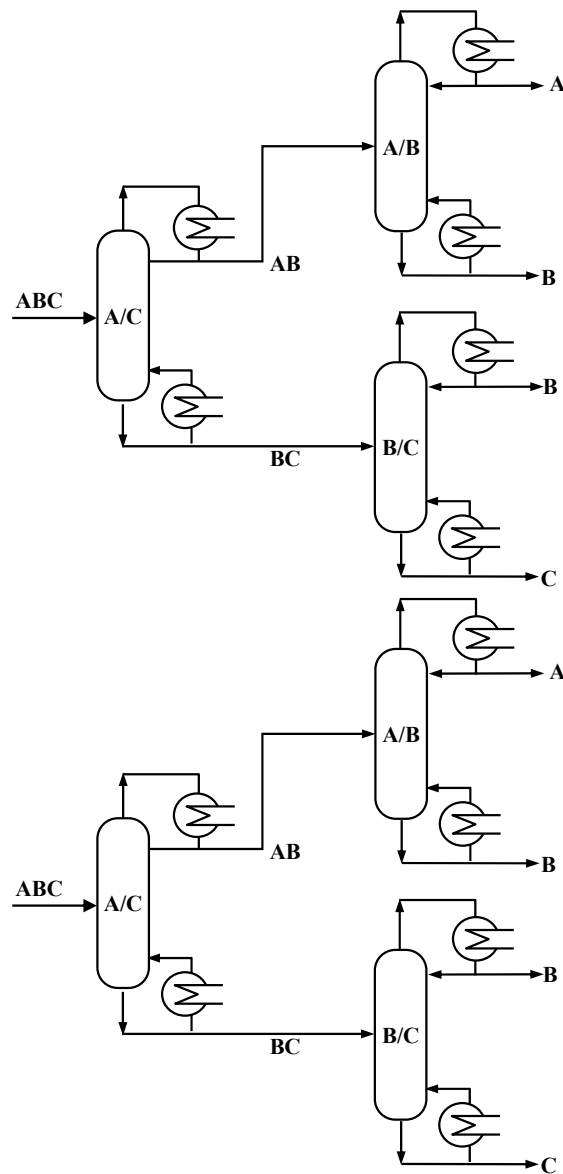


Figure 2.3: Three column sequence for three-product separation with easiest (A/C) separation in the first column

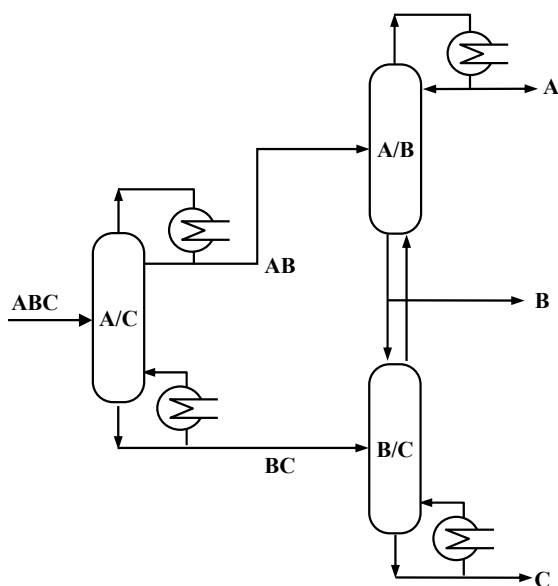


Figure 2.4: Prefractionator sequence for three-product separation with coupled main column

The scheme shown in Figure 2.3 uses three columns. The first column is designed to do only an easiest split i.e, between the lightest (A) and heaviest (B) components, which reduces mixing losses and is more advantageous than direct and indirect schemes in terms of energy consumption.

General heuristics for a good distillation sequence from energy point of view include doing the easiest split first, removing a major component early in the sequence, remove the most volatile component early, etc.[2]. For complex separation sequences, several works have also been done on devising more systematic methodologies [1, 3] to arrive at an optimal distillation sequence.

## 2.3 Thermal coupling

Thermal coupling of columns can reduce energy and/or capital requirements to perform a separation task and is classified further into indirect thermal coupling and direct thermal coupling.

### 2.3.1 Indirect Coupling

In an “indirect” coupling of distillation columns, heat from one column stream is used in another column. Two columns can be operated at different pressure levels so that the condenser of a column operating at higher pressure is at a higher temperature and can thus exchange heat with a reboiler of a column operating at lower pressure and hence lower temperature. Thus, the heating and cooling requirements can be met by the process streams thereby reducing load on the utilities.

Similarly, a column at higher condenser temperature due to its higher boiling components can be “indirectly” coupled with a reboiler of another column with lower boiling components.

### 2.3.2 Direct Coupling

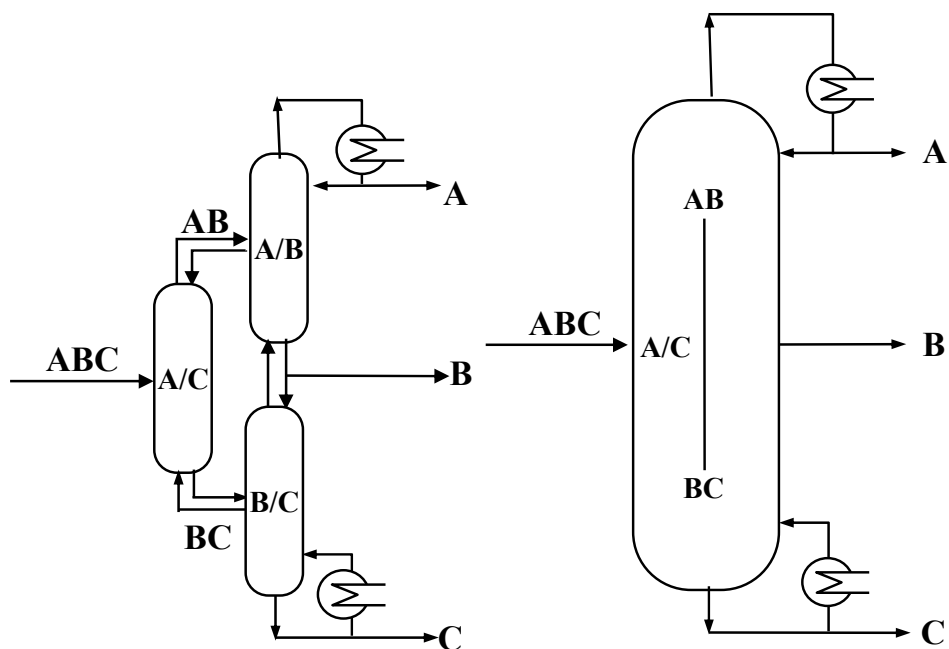
Directly (or fully) coupled columns involves coupling of material streams (both liquid and vapor) of two columns. In this way, a heat flux may be utilized for more than one separation thereby reducing energy usage [18]. The energy savings are also enhanced due to reduced mixing losses at the column ends because of fewer reboilers and condensers compared to conventional sequences. The energy and capital requirements in the three column arrangement shown in Figure 2.3 can be improved significantly simply by coupling the last two columns and removing one condenser and one reboiler as shown in Figure 2.4.

The direct coupling can be used to improve the energy and/or capital costs further using more complex arrangements like Petlyuk column and Kaibel column as discussed below.

### Petlyuk Column

Petlyuk et al. [16] proposed thermodynamically optimal methods for separating multicomponent mixtures. This laid the basis for what are known as Petlyuk columns. Petlyuk columns were also formally defined by Christiansen et al. [4] as “*the columns capable of separating multicomponent feed using a single reboiler and a single condenser, in which any degree of separation (purity) can be obtained by increasing the number of stages (provided the reflux is above a certain minimum value and the separation is thermodynamically feasible)*”. Each column is operated in such a way that only the easiest split between lightest and heaviest components is done.

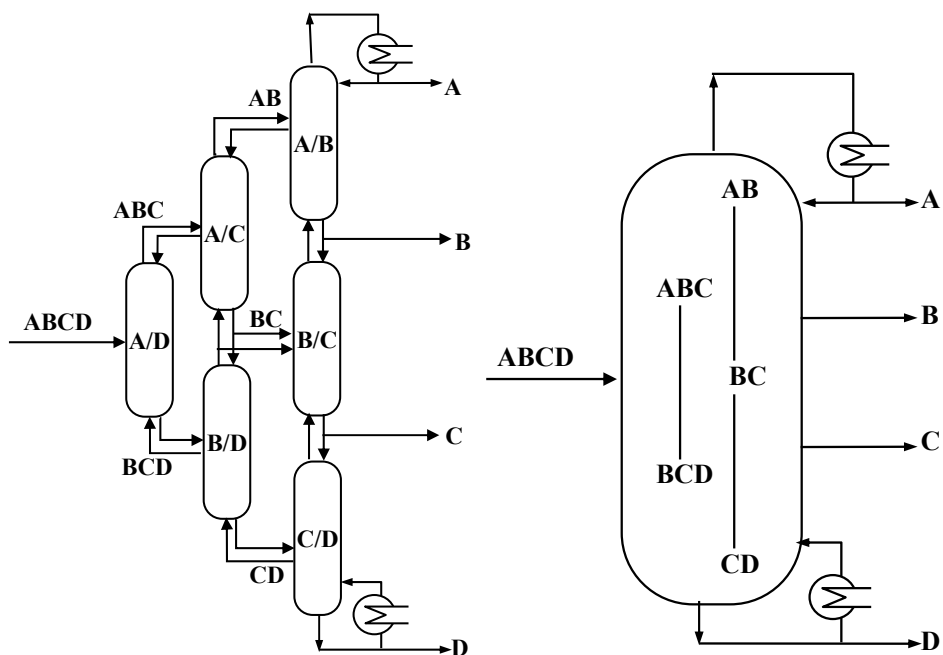
Figure 2.5a shows a three-product Petlyuk column. This can also be realized by using a dividing-wall in a single column shell as shown in Figure



(a) Implementation with *three* separate columns

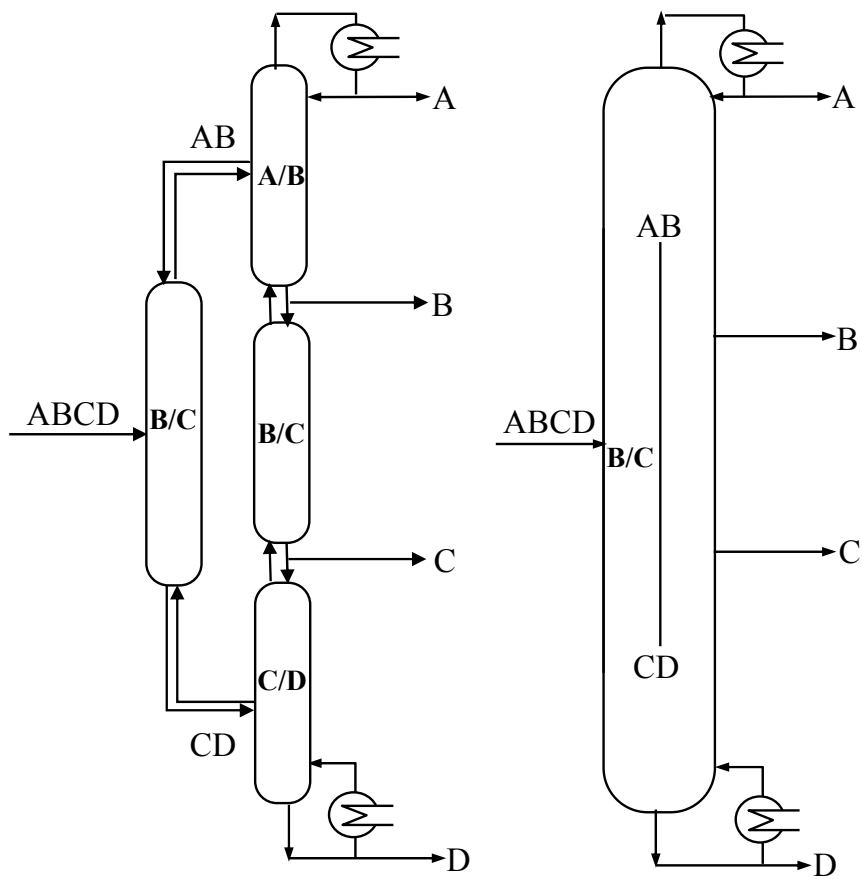
(b) Dividing-wall implementation with a side-product

Figure 2.5: Thermodynamically equivalent implementations of three-product Petlyuk column



(a) Implementation with *six* separate columns (b) Double-dividing-wall implementation with a two side-products

Figure 2.6: Thermodynamically equivalent implementations of four-product Petlyuk column



(a) Implementation with four separate column sections

(b) Dividing-wall implementation with two side products

Figure 2.7: Thermodynamically equivalent implementations of four-product Kaibel column

2.5b. Figure 2.6a shows a four-product Petlyuk column which can also be realized by using double vertical partitions 2.6b [5].

### Kaibel Column

Petlyuk arrangements do only the easiest split in any column and therefore in any column-section not more than one component is separated. This reduces the mixing losses and energy requirements but requires large number of columns and hence high capital costs. For example, for four product-separation, a Petlyuk arrangement shown in Figure 2.6, requires six columns to perform the separation task.

Petlyuk et al. [15] also proposed schemes for multicomponent separation with “minimum number of column sections”. Thermodynamically, for a four-product separation, this is equivalent to the scheme proposed later by Kaibel [12] with a vertical partition or dividing-wall (see, Figure 2.7b).

The four product Kaibel column (Figure 2.7) is less efficient than the Petlyuk arrangements (Figure 2.6), but requires fewer column sections and hence lesser capital cost.

## 2.4 $V_{min}$ diagrams

In this section, we introduce the “ $V_{min}$ ” diagram developed by Halvorsen and Skogestad [10] to estimate the minimum vapor requirements for sharp and non-sharp separation in conventional and thermally coupled distillation systems, is introduced. For separation of ideal multicomponent mixtures the Underwood equations [20] are adequate for generating the  $V_{min}$  diagrams. These  $V_{min}$  diagram may also be generated for non-ideal mixtures using more rigorous thermodynamic models [6].

Figure 2.8 shows the  $V_{min}$  diagram for an equimolar A-B-C mixture with a liquid feed. The  $y$ -axis shows the normalized minimum boilup ( $V/F$ ) and the  $x$ -axis shows the net product withdrawal ( $D/F$ ) in a conventional two-product column. For sharp separations, the peak points denoted by  $P_{AB}$ ,  $P_{AC}$ , and  $P_{BC}$  are of main interest. The peak  $P_{AB}$  gives the minimum vapor flow ( $V/F$ ), required for separating A from B-C. Note that the corresponding product split ( $x$ - coordinate)  $D/F = 0.33$ , since the feed is equimolar. Similarly point  $P_{AC}$  denotes the minimum vapor required to separate A and C, with component B distributing to both ends of the column.

Figure 2.9 shows the  $V_{min}$  diagram for an equimolar A-B-C-D mixture with a liquid feed. The peak  $P_{AB}$  gives the minimum vapor flow ( $V/F$ ),

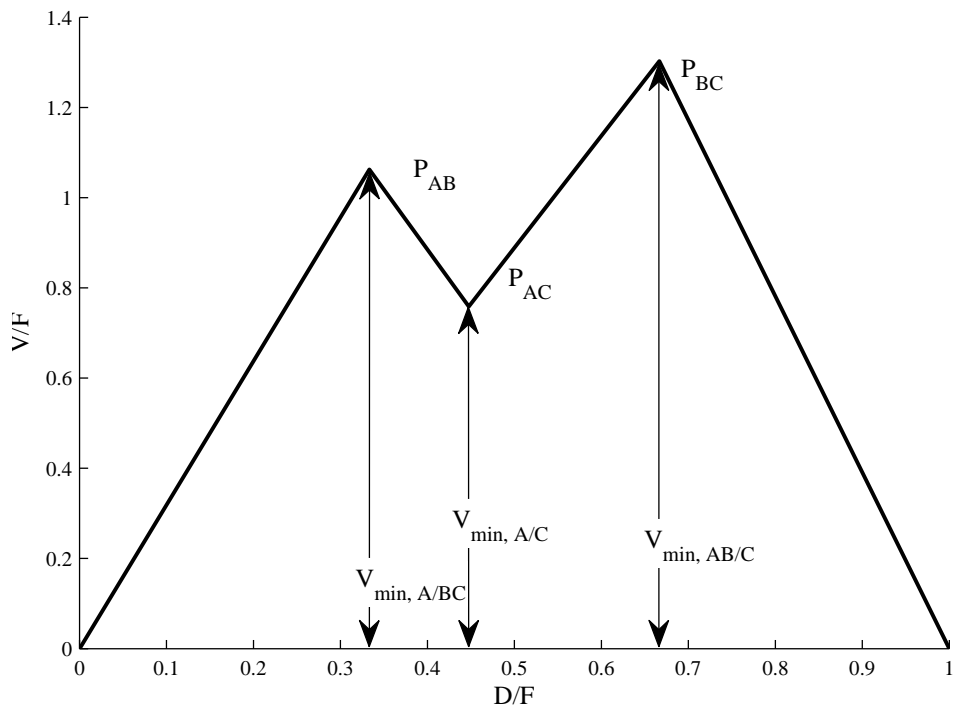


Figure 2.8:  $V_{min}$  diagram for an equimolar feed mixture of A, B and C.  
 Data: relative volatilities [A, B, C] = [4.2 2.1 1]  
 feed liquid fraction ( $q_F$ ) = 1



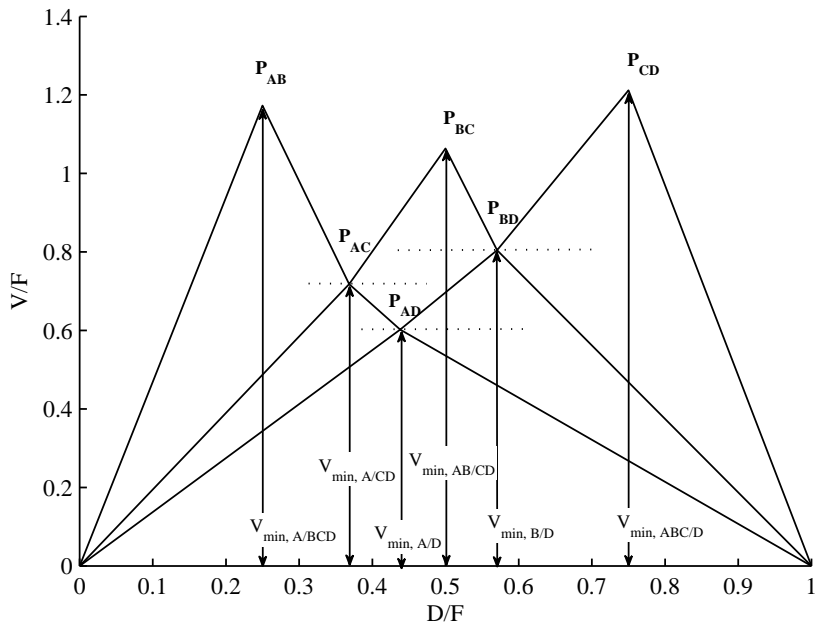


Figure 2.9:  $V_{min}$  diagram for an equimolar feed mixture of A, B, C & D  
 Data: relative volatilities [A, B, C, D]= [7.1 4.4 2.1 1]  
 feed liquid fraction ( $q_F$ ) =1

required for separating A from B-C-D. The corresponding product split ( $x$ -coordinate)  $D/F = 0.25$ , since the feed is equimolar. The point  $P_{AD}$  denotes the minimum vapor required to separate A and D, with components B & C distributing to both ends of the column.

## 2.5 Minimum energy and thermal efficiency for three-product separation using alternate configurations

### 2.5.1 Minimum energy in conventional arrangements

The  $V_{\min}$  diagrams like Figures 2.8 and 2.9 can be used to calculate the minimum energy requirement using alternate column configurations. For example, for a direct split configuration, the minimum energy is given by:

$$V_{min,direct} = (V_{AB} + F_{BC}/F \times V_{BC}) \quad (2.1)$$

where, for an equimolar separation,  $F_{BC}/F = 2/3$ .

### 2.5.2 Minimum energy in Petlyuk arrangements

Halvorsen and Skogestad [11], Fidkowski and Królikowski [7] showed that in a Petlyuk arrangement, the minimum energy required to separate a multicomponent feed is equal to the “most difficult binary separation”.

$$V_{min,Petlyuk} = \max(V_{AB}, V_{BC}, V_{CD}...) \quad (2.2)$$

Here,  $V_{AB}$ ,  $V_{BC}$  &  $V_{CD}$  are the minimum boilup required for sharp separation of A/BCD.., AB/CD.. and ABC/D.. in a conventional two-product distillation column with A-B-C-D.. feed.

Figure 2.8 shows the  $V_{min}$  diagram for three components. We observe that for the chosen components, the  $P_{BC}$  peak is the highest. This implies that the separation of B and C is the most difficult binary split in terms of energy usage. Thus, the minimum boilup required for sharp separation of this feed using Petlyuk arrangements is equal to the boilup required for this binary split (for example,  $=V_{\min,AB/C}$  in Figure 2.8).

### 2.5.3 Thermal efficiency in alternate configurations

So far, we have focussed on the minimum energy requirements of alternate configuration, as measured by minimum boilup requirements. In the fol-

Following section, we will focus on the thermal efficiency ( $\eta$ ). The thermal efficiency ( $\eta$ ) can be calculated as follows:

$$\begin{aligned} \eta &= \frac{1}{1 + \frac{\Delta S_{total}}{\Delta S}}, \text{ where} \\ \Delta S_{total} &= \Delta S + \Delta S_{sur} \\ \Delta S &= R \sum x_i \ln x_i \\ \Delta S_{sur} &= |Q_H| \left( -\frac{1}{T_H} + \frac{1}{T_C} \right) \text{ (liquid feed)} \\ Q_H &= H V_{min} \end{aligned} \tag{2.3}$$

and  $H \equiv$  Enthalpy of vaporization,  
 $T_H$  and  $T_C$  are temperature of reboiler and condenser, respectively,  
 $x_i$  mole fraction of components in feed;  $R$  is universal gas constant,  
 $S \equiv$  Entropy.  $V_{min} \equiv$  is the minimum boilup for each sub-column.

### 2.5.4 A Case Study

We use a case study for evaluating the minimum energy and thermal efficiency for sharp separation of an equimolar three component feed using alternate sequences. The relative volatilities are chosen similar to ethanol,  $n$ -propanol and  $n$ -butanol at atmospheric pressure. Similarly, the temperature of reboiler and condenser is corresponding to the normal boiling point of pure ethanol (78.1 [°C]),  $n$ -propanol (97.1 [°C]) and  $n$ -butanol (117.6 [°C]). The minimum energy is calculated using methods in (2.1) and (2.2) while thermal efficiency is calculated using method described in (2.3). The data used for calculation is given in Table 2.1.

In Table 2.1, we observe as expected, that the minimum boilup requirement is the least for the Petlyuk arrangement. As also observed by Fidkowski and Królikowski [7], Halvorsen [9], the thermodynamic efficiency of Petlyuk arrangement not as high as in the conventional arrangements. The reason for this that in the Petlyuk arrangements, all heat is added and removed at the highest and lowest temperatures respectively (that is, for sharp separation, at the boiling point of highest and least boiling components, respectively). Thus the energy used is least in case of Petlyuk arrangements while the second law thermal efficiency may be less compared to the conventional arrangements.

Table 2.1: Minimum energy and thermal efficiency of alternate configurations for three product separation.<sup>a</sup>

Column arrangement	Minimum Energy $V_{min}/F$	Thermodynamic efficiency $\eta = \frac{1}{1 + \frac{\Delta S_{total}}{\Delta S}}$
Direct sequence (Figure 2.1)	2.0006	0.6248
Indirect sequence (Figure 2.2)	1.9660	0.6103
3-column without coupled main column (Figure 2.3)	1.9241	0.7255
Prefractionator with coupled main column (Figure 2.4)	1.4789	0.6433
Petlyuk Arrangement (Figure 2.5)	1.3028	0.6090

<sup>a</sup> Data: Relative volatilities [A, B, C]=[4.2 2.1 1]; Feed liquid fraction = 1; Enthalpy of Vaporization, H = 40 kJ/kmol (for all components)

## 2.6 Conclusion

In this chapter, different methods of conventional and coupled distillation have been discussed. A short overview of the graphical tool, the  $V_{min}$  diagrams is also given. Using this tool, the minimum-boilup for sharp separation using conventional and directly coupled arrangements for a three-product separation are compared for an equimolar three-component feed as a case-study. The Petlyuk arrangement uses the least energy compared to conventional sequence of two product columns. However, in Petlyuk arrangements, the second-law thermal efficiency is less compared to conventional arrangements.

## References

- [1] Agrawal, R., 1996. Synthesis of distillation column configurations for a multicomponent separation. *Industrial & Engineering Chemistry Research* 35 (4), 1059–1071.
- [2] Biegler, L., Grossmann, I., Westerberg, A., 1997. Chapter 11, Systematic Methods of Chemical Process Design. Prentice Hall PTR.
- [3] Caballero, J. A., Grossmann, I. E., 2004. Design of distillation sequences: from conventional to fully thermally coupled distillation systems. *Computers & Chemical Engineering* 28 (11), 2307 – 2329.
- [4] Christiansen, A., Skogestad, S., Lien, K., 1997. Partitioned Petlyuk arrangements for quaternary separations. In: *Proc. symposium Distillation and Absorption 97*. R. Darton, Ed, pp. 745–756.
- [5] Dejanovic, I., Matijaevic, L., Halvorsen, I., Skogestad, S., Jansen, H., Kaibel, B., Olujic, ., 2011. Designing four-product dividing wall columns for separation of a multicomponent aromatics mixture. *Chemical Engineering Research and Design* 89 (8), 1155 – 1167.
- [6] Dejanovic, I., Matijasevic, L., Halvorsen, I. J., Skogestad, S., Jansen, H., Kaibel, B., Olujic, Z., 2011. Designing four-product dividing wall columns for separation of a multicomponent aromatics mixture. *Chemical Engineering Research and Design* 89 (8), 1155 – 1167.
- [7] Fidkowski, Z., Królikowski, L., 1987. Minimum energy requirements of thermally coupled distillation systems. *AIChE Journal* 33 (4), 643–653.
- [8] Fonyo, Z., Benko, N., 1998. Comparison of various heat pump assisted distillation configurations. *Chemical Engineering Research and Design* 76 (3), 348 – 360.
- [9] Halvorsen, I. J., 2001. Minimum energy requirements in complex distillation arrangements (Chapter 6). Ph.D. thesis, Norwegian University of Science and Technology, Department of Chemical Engineering, Trondheim, Norway.
- [10] Halvorsen, I. J., Skogestad, S., 2003. Minimum energy consumption in multicomponent distillation. 1. Vmin diagram for a two-product column. *Industrial & Engineering Chemistry Research* 42 (3), 596–604.

- 
- [11] Halvorsen, I. J., Skogestad, S., 2003. Minimum energy consumption in multicomponent distillation. 2. three-product Petlyuk arrangements. *Industrial & Engineering Chemistry Research* 42 (3), 605–615.
- [12] Kaibel, G., 1987. Distillation columns with vertical partitions. *Chemical Engineering & Technology* 10 (1), 92–98.
- [13] Naito, K., Nakaiwa, M., Huang, K., Endo, A., Aso, K., Nakanishi, T., Nakamura, T., Noda, H., Takamatsu, T., 2000. Operation of a bench-scale ideal heat integrated distillation column (HIDiC): an experimental study. *Computers & Chemical Engineering* 24 (27), 495 – 499.
- [14] Olujic, Z., Fakhri, F., De Rijke, A., De Graauw, J., Jansens, P., 2003. Internal heat integration - the key to an energy-conserving distillation column. *Journal of Chemical Technology and Biotechnology* 78 (2-3), 241–248.
- [15] Petlyuk, F., Platonov, V., Avetlyan, V., 1966. Optimum arrangements in the fractionating distillation of multicomponent mixtures. *Khimicheskaya Promyshlennost* 42 (11), 865–868.
- [16] Petlyuk, F., Platonov, V., Slavinskii, D., 1965. Thermodynamically optimal method for separating multicomponent mixtures. *International Chemical Engineering* 5 (3), 555–561.
- [17] Stichlmair, J., Fair, J., 1998. Chapter 7, Distillation - Principles and Practices. Wiley-VCH, New York.
- [18] Stupin, W., 1972. Thermally coupled distillation- a case history. *Chemical Engineering Progress* 68 (10).
- [19] Takamatsu, T., Lueprasitsakul, V., Nakaiwa, M., 1988. Modeling and design method for internal heat-integrated packed distillation column. *Journal of Chemical Engineering of Japan* 21 (6), 595–601.
- [20] Underwood, A. J. V., 1949. Fractional distillation of multicomponent mixtures. *Industrial & Engineering Chemistry* 41 (12), 2844–2847.

## Chapter 3

# Control structure selection for three-product Petlyuk (dividing-wall) column

### 3.1 Introduction

For three-product separations, the Petlyuk (Figure 3.1 [23]) or divided-wall arrangements [14] offer significant savings in both energy and capital costs, as also shown by Cahn and DiMiceli [5], Stupin [28]. The German company, BASF has more than 100 dividing-wall columns [7]. However, operation and control is challenging and this paper proposes some new control schemes which are workable for varying feed composition disturbances.

Halvorsen and Skogestad [11, 13] have developed a graphical tool, the “ $V_{min}$  diagrams”, to visualize the minimum energy requirement for sharp and non-sharp separations in conventional and thermally coupled columns. This tool can be used for designing such arrangements [7] and we will also demonstrate its use to give some insights into control and operation.

In terms of operation, several works have been published. Mutalib and Smith [20] reported simulation studies on the divided-wall columns. In their second work, Mutalib et al. [21] reported experimental studies conducted on a pilot plant and recommended a two point control of the system. Wolff and Skogestad [29] did a steady state study and operability analysis on a three-product Petlyuk column and conclude that the simultaneous specification of both impurities in the side-product is generally infeasible. Further, the liquid and vapor split ratios between pre-fractionator and the main column should be manipulated to get the optimal energy benefits. If the vapor split

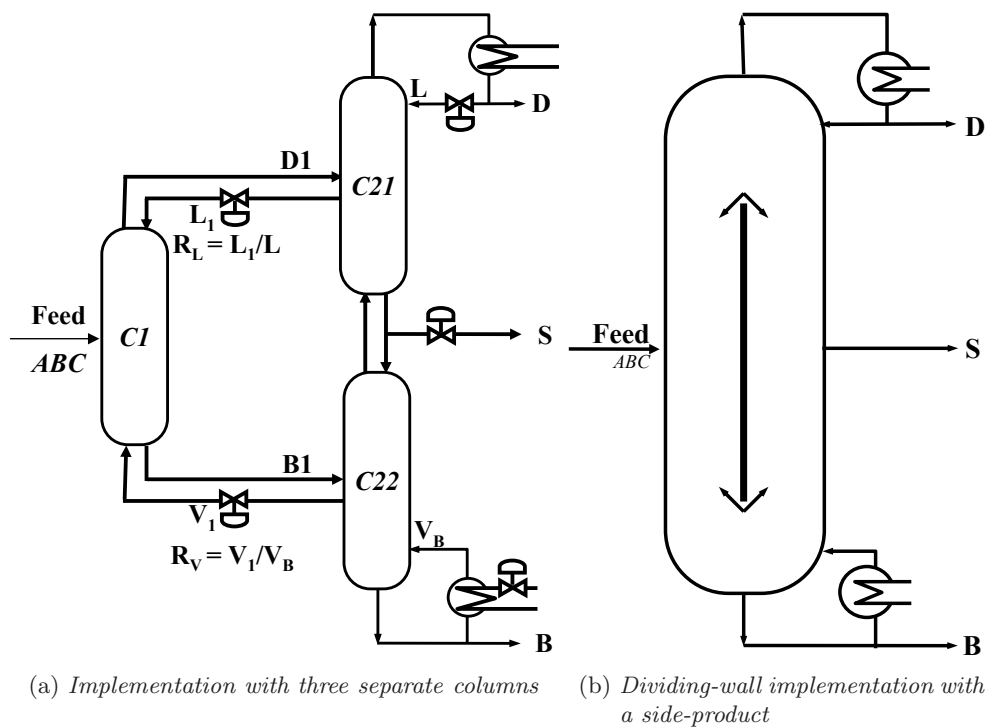


Figure 3.1: Thermodynamically equivalent implementations of three-product Petlyuk column



is not available as a degree of freedom, which is normally the case, one cannot control both ends of the prefractionator at the same time. Christiansen and Skogestad [6], Halvorsen and Skogestad [10] therefore proposed to use the liquid split to control the key impurity in the least pure end of the prefractionator. Ling and Luyben [18] explained that the liquid split valve ( $R_L$ ) must be manipulated and proposed a control structure with the use of four composition loops with the liquid split controlling the heavy key at the top stage of the prefractionator. In their second work, Ling and Luyben [19] studied the effectiveness of temperature control for BTX columns. Similar to Ling and Luyben [18], Kiss and Rewagad [15] and Rewagad and Kiss [24] suggested that control of the heavy key at the prefractionator top together with three composition loops in the main column may be sufficient to yield high-purity products and “implicitly” minimize the energy usage. Niggemann et al. [22] conducted simulation and experimental studies for separation of a mixture of fatty alcohols into three high-purity products. They reported that the heat transfer across the dividing wall can be a factor in design and operation. Lestak et al. [16] argued that in some cases the heat transfer across the dividing wall may decrease the overall energy consumptions. In non-beneficial regions however, the wall should be insulated. Some other works on the suitability of Model Predictive Control for dividing-wall columns have also been reported [1, 4, 24]. Ling et al. [17] suggested a control structure to avoid remixing of the intermediate component for optimal operation.

In this paper, we study the separation of a feed with components A (lightest), B and C (heaviest) in a Petlyuk column as shown in Figure 3.1. Note that the letter B is also used to denote the bottom product. To avoid confusion, we will use subscripts for components and superscripts for products. For example,  $x_A^D$  denotes the mole fraction of component A in product D.

With a given feed, the three-product Petlyuk column in Figure 3.1 has a total of five steady-state degrees of freedom, if we include an adjustable vapor split ( $R_V$ ). To obtain minimum energy operation, two of these degrees of freedom ( $R_L$  and  $R_V$ ) must be used to control the purity of the two “products” in the prefractionator (C1 in Figure 3.1), [10]. This leaves three degrees of freedom D, S and B in the main column (C21 and C22 in Figure 3.1), but we have four key impurities to control:

1. Heavy key or component B in product D ( $x_B^D$ )
2. Light key or component A in product S ( $x_A^S$ )
3. Heavy key or component C in product S ( $x_C^S$ )

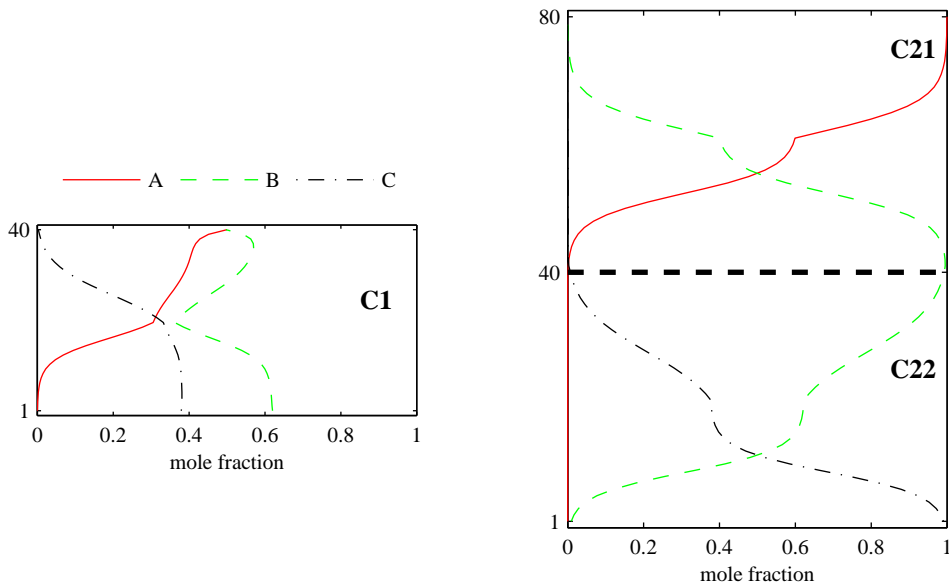


Figure 3.2: Nominal composition profiles of components: A (ethanol), B (propanol) and C (*n*-butanol) in sub-columns C1, C21 and C22

4. Light key or component B in product B ( $x_B^B$ )

In agreement with Wolff and Skogestad [29], we find that these four compositions can not be specified independently, but we find that there is a possibility to over-purify one product, with the other products at their specifications. The aim of this work is to find some simple single-loop (decentralized) PI control structures that are workable for large feed disturbances.

### 3.2 Case Study

The data for the case study are given in Table 3.1. The process is modelled in Matlab using the simplifying assumptions of constant relative volatility and constant internal molar flows in column sections. This may seem unrealistic but similar results are obtainable for real mixtures. The three hypothetical components A, B and C have relative volatilities similar to the mixture of ethanol, propanol and *n*-butanol. We assume constant pressure, negligible vapor holdup, a total condenser and equilibrium on all stages. We assume linearized liquid flow dynamics. Compared to the product purities given

in Table 3.1, we have a large number of stages in each sub-column. This implies that the required energy is close to the minimum energy using an infinite number of stages. The nominal composition profiles are shown in Figure 3.2.

Table 3.1: Input data and nominal conditions for the three-product Petlyuk column model

Relative volatilities [A, B, C]	[4.2 2.1 1]
Number of stages in C1	20+20
Number of stages in C21	20+20
Number of stages in C22	20+20
Nominal feed flow rate (F)	1 kmol/min
Nominal feed composition [A, B, C]	[33.3 33.3 33.3] (mol %)
Nominal liquid reflux (L)	1.0033 kmol/min
Nominal boilup (V)	1.3381 kmol/min
Nominal distillate flow rate (D)	0.3348 kmol/min
Nominal bottom flow rate (B)	0.3333 kmol/min
Nominal side-product (S)	0.3318 kmol/min
Nominal liquid split ( $R_L$ )	0.3465
Nominal vapor split ( $R_V$ )	0.5982
Nominal purity of distillate ( $x_A^D$ )	99.5 (mol %)
Nominal purity of side-product ( $x_B^S$ )	99.45 (mol %)
Nominal light impurity of side-product ( $x_A^S$ )	0.05 (mol %)
Nominal heavy impurity of side-product ( $x_C^S$ )	0.5 (mol %)
Nominal purity of bottom product ( $x_C^B$ )	99.5 (mol %)
Nominal heavy impurity of prefractionator top ( $x_C^{D1}$ )	0.29 (mol %)
Nominal light impurity of prefractionator bottoms ( $x_A^{B1}$ )	0.08 (mol %)

Figure 3.3 shows the  $V_{min}$  diagram for our A, B, C mixture with a liquid feed. The  $y$ -axis shows the normalized minimum boilup ( $V/F$ ) and the  $x$ -axis shows the net product withdrawal ( $D/F$ ) in a conventional two-product column. The red-solid line is for the nominal equimolar feed and the blue-dashed line is for a feed composition disturbance where the ratio of components A and B is changed from 1:1 to about 4:1.

For Petlyuk arrangements, the minimum energy requirement to separate a multi-component feed is equal to the “most difficult binary separation” [8, 12].

$$V_{min, Petlyuk} = \max(V_{AB}, V_{BC}) \quad (3.1)$$

Here,  $V_{AB}$  and  $V_{BC}$  are the vapor flows corresponding to the peaks  $P_{AB}$

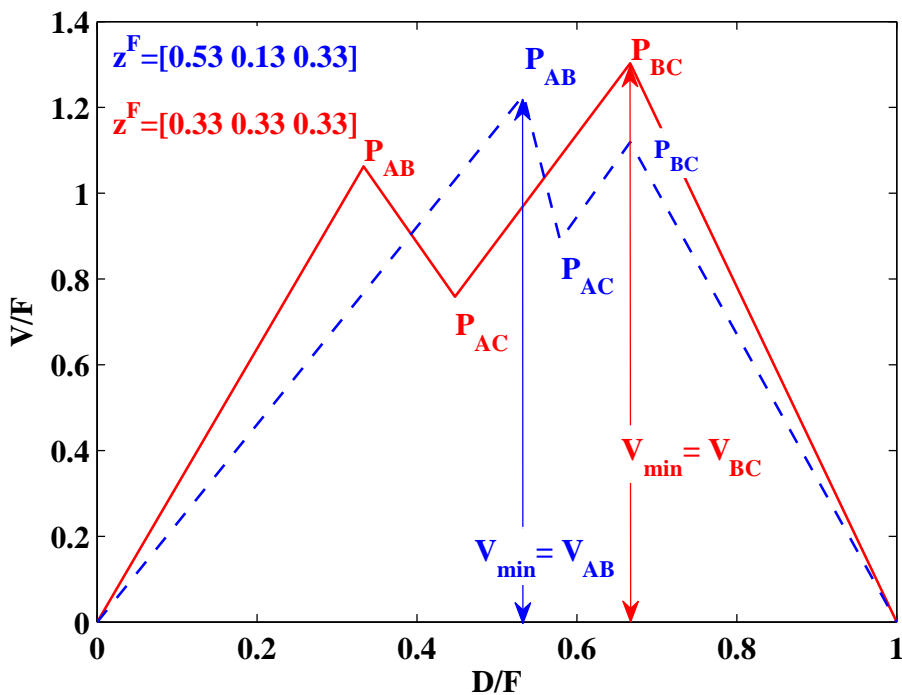


Figure 3.3:  $V_{min}$  diagrams for nominal equimolar feed (solid-red line) and for feed composition,  $z_5^F$  (mol%) = [53.33 13.33 33.33] (dashed-blue line). Relative volatilities,  $\alpha = [4.2 \ 2.1 \ 1]$  and feed liquid fraction,  $q_F = 1$ .

and  $P_{BC}$ , respectively, in Figure 3.3. For the nominal case with an equimolar feed, the  $P_{BC}$  peak is the highest. This implies that nominally, B/C is the most difficult binary split in terms of energy usage. However, for the feed composition disturbances, the A/B split becomes the most difficult split. Depending on whether A/B or B/C is the more difficult split, we will have excess energy in one of the sections (C21 or C22, respectively) of the main column. Therefore, there is a possibility to over-purify in one of these two sections with only minor penalty in terms of energy usage. When A/B is the more difficult split, we may choose to over-purify the bottom product or the heavy component (C) in the side-product, and when B/C is the more difficult split, we may choose to over-purify the top product or the light component (A) in the side-product.

### 3.3 Control Structures for three-product Petlyuk column

#### 3.3.1 Control Objectives

We assume that the operational objective for a given feed is to minimize the energy consumption subject to satisfying purity constraints on the three products. That is, the cost function to be minimized is:

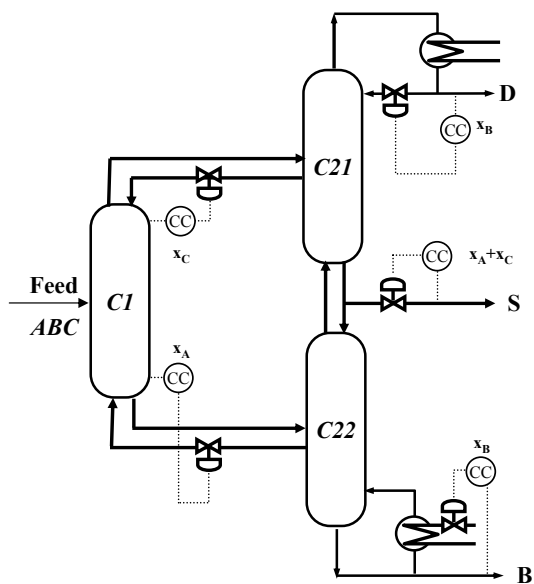
$$J = \text{energy } (V) \tag{3.2}$$

A more general cost function would be to take into account also the prices and amounts of products and of heat input and cooling, but this is not considered here. The purity constraints are assumed to be given in terms of the amount of key impurity in each product:

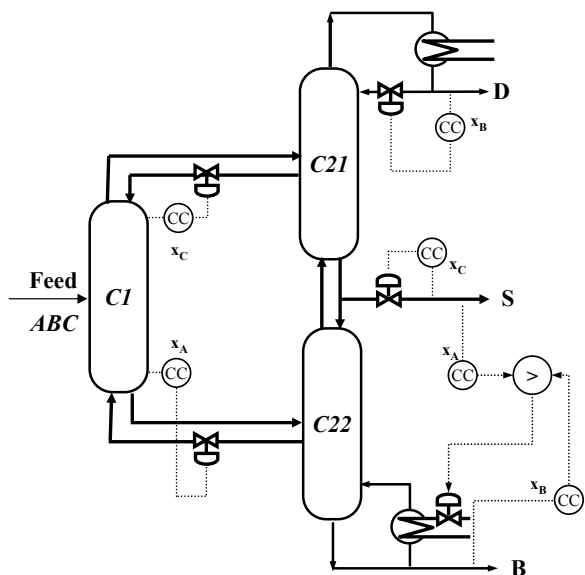
$$\begin{array}{ll}
 \text{Impurity in top product} & (D) : x_B^D \leq x_{B,s}^D \quad (= 0.5\%) \\
 \text{Light Impurity in side product} & (S) : x_A^S \leq x_{A,s}^S \quad (= 0.5\%) \\
 \text{Heavy Impurity in side product} & (S) : x_C^S \leq x_{C,s}^S \quad (= 0.5\%) \\
 \text{Impurity in bottom product} & (B) : x_B^B \leq x_{B,s}^B \quad (= 0.5\%)
 \end{array} \tag{3.3}$$

Note that the side-product contains the two impurities (A and C). The resulting minimum purity of the main component in each product is 99.5% for the distillate, 99.0% for the side-product and 99.5% for the bottom product.

We assume that these four constraints are always optimally active, meaning that the energy consumption ( $J=V$ ) is minimized by having equality for

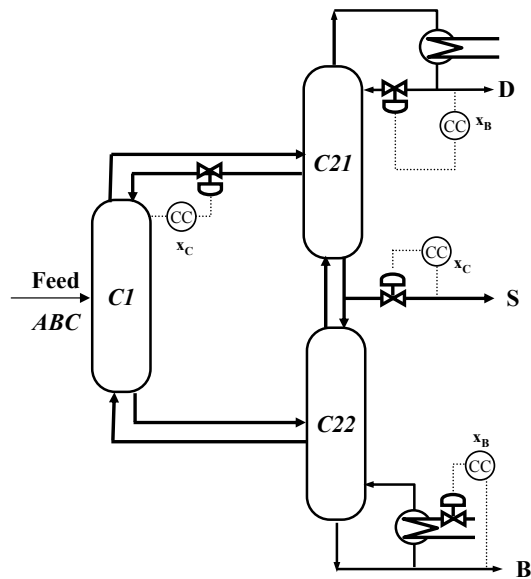


(a) CS1: control of  $x_A + x_C$  in sidestream (*Not recommended for dynamic reasons*).

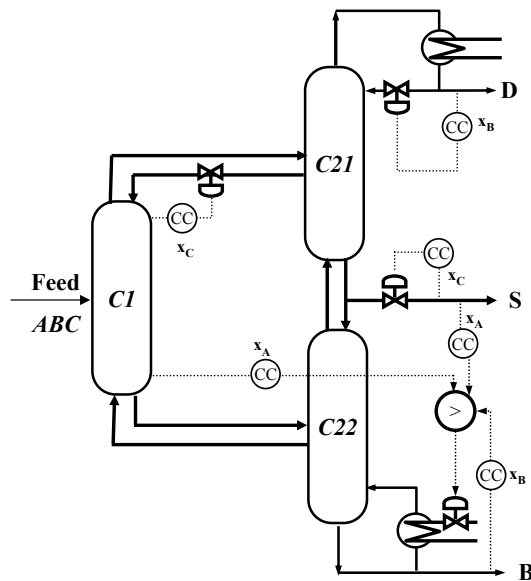


(b) CS2: control of  $x_C$  in sidestream and max-selector to avoid  $x_A$  in side stream (*Recommended for all feed compositions*).

Figure 3.4: Control Structures *with* active use of vapor split ( $R_V$ ).



(a) CS3: No control of  $x_A$  in sidestream and in bottom of prefractionator [18] (Recommended  $A/B$  is the easy split).



(b) CS4: Max-selector to avoid large  $x_A$  in sidestream and in bottom of prefractionator (Recommended for all feed compositions).

Figure 3.5: Control Structures *without* use of vapor split ( $R_V$ ).

the four specifications in (3.3).<sup>1</sup> However, as discussed by Wolff and Skogestad [29], they may be “holes” in the operating range making it difficult or impossible in practice to control all four compositions simultaneously. Instead of controlling four compositions, we therefore, consider two options for controlling three compositions:

1. *Option I*: Control the total impurity in the side stream  $x_A^S + x_C^S$  (as done in structure CS1, see Figure 3.4a).
2. *Option II*: Over-purify one of the products (as done in structure CS2, see Figure 3.4b). This will come at some loss in terms of energy (V) but as discussed in the previous section, the loss may be very small.

To satisfy three of the specifications in (3.3) using “*Option I*” or “*Option II*”, we need three degrees of freedom (e.g., L, S and V).<sup>2</sup> There are then two unconstrained degrees of freedom (e.g.,  $R_L$  and  $R_V$ ) left for minimizing the energy ( $J=V$ ) and these need to be translated to control objectives.

One may think that a good approach would be to set the energy input (boilup) V directly and try to minimize it, but this is not a workable solution as it may lead to infeasibility because the product specifications can not be met if V is set lower than its optimal (minimum) value. The concept of “self-optimizing control” [25] provides a general theory for obtaining good control objectives. In this paper, we assume that good self-optimizing variables are the two “product” compositions in the prefractionator (C1) [10]. This is reasonable because the prefractionator will then operate very close to its “preferred” split. Thus, we use the following controlled variables (specifications):

$$\begin{aligned}
 \text{Heavy key (C) in top “product” of prefractionator (D1)} & : x_C^{D1} = x_{C,s}^{D1} \\
 \text{Light key (A) in bottom “product” of prefractionator (B1)} & : x_A^{B1} = x_{A,s}^{B1}
 \end{aligned}
 \tag{3.4a}$$

---

<sup>1</sup>Alstad et al. [3] have shown that in some cases it may be possible to obtain some minor energy savings by over-purifying the top product (for the case when B/C is the difficult split) or the bottom product (for the case when A/B is the difficult split), because this simplifies the separation in the side-product by increasing the amount of component B in the side-product. However, the effect is small, and we here assume that all product purity specifications are optimally active.

<sup>2</sup>It may seem strange that the cost variable  $J=V$  is also a degree of freedom, but this is correct.



### 3.3.2 Setpoints for the controlled variables

The setpoints for the compositions in the main column are determined by the product specification as given in (3.4a). For the prefractionator, the setpoint values in (3.4a) should ideally be the optimal values that minimize the energy consumption ( $V$ ). The optimal value may vary depending on the feed composition and product purity specifications (for D, S and B), but since the prefractionator performs the “easy” A/C-split, we usually have enough stages to “over-purify” in the prefractionator, with only a slight penalty in terms of increased energy ( $V$ ). Some over-purification in prefractionator is also good from operational perspective, as we can then avoid the problem of infeasibility of purity specifications in the main column, in the event of disturbances. This is equivalent to the introducing a “back-off” from the self-optimizing variable as also described by Govatsmark and Skogestad [9].

In our case study, we use for in all simulations and control studies (and for the nominal point) the following specifications for the prefractionator:

$$\begin{aligned} x_{C,s}^{D1} &= 0.29\% \\ x_{A,s}^{B1} &= 0.08\% \end{aligned} \quad (3.4b)$$

How did we arrive at these values? This is quite a long story, but let us first repeat that the exact values are not critical because the A/C split performed in the prefractionator is relatively easy. We started by obtaining the optimal solution for the nominal feed composition: For the constraints in (3.3) and the objective (3.2) we found a minimum boilup ( $V$ ) of 1.3322 kmol/min with all the four impurity constraints in (3.3) optimally active. However, this “optimal” solution has some undesirable features. First, we find that the amount of component C over the top in the prefractionator is high (0.83%) given that we want less than 0.5% C in the side-product. Second, this “optimal” solution does not over-purify any of the products, in spite of the fact that we know from the  $V_{min}$  diagram in Figure 3.3 (where we see that A/B is the easier split at nominal feed conditions) that we can over-purify either the top product or the side product with almost no extra energy ( $V$ ). In some sense we can say that the “optimal” solution is going against the “natural” product distribution, which is to over-purify one of the products. Which product should we over-purify? This is mainly an operational issue, and we choose to over-purify A in the side stream. This makes control of the side stream easier, since we at least nominally need not consider the amount of A in the side-product. So we reduced the impurity of A in the side stream from its specification of 0.5% to 0.1%, and re-optimized the operation. The resulting boilup ( $V$ ) increased only marginally from 1.3322 kmol/min to 1.3325 kmol/min, so we can indeed over-purify

for free. The resulting optimal values for the "product" compositions in the prefractionator were:  $x_{C,opt}^{D1}=0.58\%$  and  $x_{A,opt}^{B1}=0.16\%$ . However, this is for the nominal feed composition, and to handle feed compositions changes, we choose divide these values by a factor 2 and ended up with the final specifications in (3.4b). Using the specifications in (3.4b), resulted in a slight further increase in boilup (V) from 1.3325 kmol/min to 1.3381 kmol/min, and it gave a further reduction of A-impurity in the side stream from 0.10% to 0.05%. The final nominal flows and purities are given in Table 3.1.

So far, we have assumed that the vapor split ( $R_V$ ) is a degree of freedom. Unfortunately, this is not the case with most (if not all) Petlyuk columns in operation. Thus, for practical columns, where  $R_V$  is not a degree of freedom, we generally need to use extra energy, and the result is that we will get over-purification (inequality) for yet one more of the purities in (3.3) and (3.4).

### 3.3.3 Control Structures

With this introduction to the control objectives and setpoints, we now consider four alternative control structures; CS1 and CS2 (Figure 3.4) are for the next-generation dividing-wall columns where the vapor split ( $R_V$ ) is available as a degree of freedom, whereas CS3 and CS4 (Figure 3.5) are for the more realistic case today where  $R_V$  is not a degree of freedom.

Note that in all cases, we use the standard "LV-configuration" where the distillate flow (D) is used for level control of the condenser and the bottoms flow (B) is used for level control of the reboiler, so that reflux (L) and boilup (V) remain as degree of freedom for composition control.

#### Control Structure 1 (CS1)

In this structure, we use "Option I" and control the sum of the impurities ( $x_A^S + x_C^S$ ) with the side-product (S). Since the vapor split ( $R_V$ ) is available for manipulation, we then have two degrees of freedom left and can control both "products" in the prefractionator (see 3.4a). This will guarantee operating the prefractionator at its preferred split [12]. For control loop pairings, we use the most obvious "close-by" manipulated variables as shown in 3.4a.

This scheme is workable at steady state but performs poorly for some feed disturbances. The reason is that the sign of the initial gain of the molar flow rate of side-product on the two key impurities is opposite. Depending upon the dominant impurity in the side-product, the input (S)-output ( $x_A^S + x_C^S$ ) relationship will change, making it very difficult to work under transient conditions. We will demonstrate using closed-loop simulations that

structure CS1 has poor dynamic response properties to feed composition disturbances and CS1 is therefore *not* recommended.

### Control Structure 2 (CS2)

In structure CS2, we use “*Option II*” where we overpurify one of the products. We use the side-product (S) to control the heavy key impurity ( $x_C^S$ ). This means that the amount of light component, A ( $x_A^S$ ) is left uncontrolled which is acceptable as long as it is over-purified. However, if  $x_A^S$  becomes large then we need to increase the vapor flow in section C21 and instead overpurify the bottom product. To achieve this we pair the boilup (V) with two composition controllers (both  $x_B^D$  and  $x_A^S$ ) and use a max-selector. This means that one of the two products (bottoms or side-product) will be over-purified for any disturbance. However, as explained earlier this will only slightly increase the energy usage (V).

### Control Structure 3 (CS3)

We also study two structures for the case when the vapor split is not available as a degree of freedom. Control structure CS3 in Figure 3.5a, has been suggested by Ling and Luyben [18] and a similar control structure was reported by Alstad [2, Chapter 9] and Kiss and Rewagad [15]. Since the vapor split is not available for control, the prefractionator column C1 can have only one-point control and the light component (A) at C1 bottoms is left uncontrolled. In the main column, the side-product is paired with the heavy key (C) while the light key (A) in side-product remains uncontrolled. This is acceptable as long as there is little light component A in the side-product (over-purified). As confirmed in the simulations, this structure fails if the feed composition is such that A/B split is the most difficult one.

### Control Structure 4 (CS4)

This is an improvement of CS3, which is workable also when A/B is the more difficult split. It is based on the same idea as structure CS2, but the boilup now also looks after the amount of A in the prefractionator C1 bottoms. To ensure sufficient vapor flow, we use a maximum-select controller and pair the boilup with the largest boilup resulting from controlling the following three impurities:

1. Component A in bottom of prefractionator ( $x_A^{B1}$ )
2. Component A in side-product ( $x_A^S$ )

3. Component B in bottom-product ( $x_B^B$ )

This implies that two of these compositions will be overpurified at any given time, and that the energy usage (V) may be large for some disturbances.

### 3.4 Closed loop simulation results

Table 3.2: Summary of closed-loop composition responses using different control structures (superscript numbers refer to corresponding Figure numbers)

Disturbance	CS1	CS2	CS3	CS4
Feed, +20 %	OK <sup>3.6a</sup>	OK <sup>3.7a</sup>	OK <sup>3.8a</sup>	OK <sup>3.9a</sup>
Feed, -20 %	OK <sup>3.6b</sup>	OK <sup>3.7b</sup>	OK <sup>3.8b</sup>	OK <sup>3.9b</sup>
$z_1^F$ (mol%) = [ <b>13.3 53.3 33.3</b> ]	Poor <sup>3.6c</sup>	OK <sup>3.7c</sup>	OK <sup>3.8c</sup>	OK <sup>3.9c</sup>
$z_2^F$ (mol%) = [ <b>13.3 33.3 53.3</b> ]	OK	OK	OK	OK
$z_3^F$ (mol%) = [ <b>33.3 53.3 13.3</b> ]	Poor <sup>3.6d</sup>	OK <sup>3.7d</sup>	OK <sup>3.8d</sup>	OK <sup>3.9d</sup>
$z_4^F$ (mol%) = [ <b>33.3 13.3 53.3</b> ]	Poor <sup>3.6e</sup>	OK <sup>3.7e</sup>	Fail <sup>3.8e</sup>	OK <sup>3.9e</sup>
$z_5^F$ (mol%) = [ <b>53.3 13.3 33.3</b> ]	OK <sup>3.6f</sup>	OK <sup>3.7f</sup>	Fail <sup>3.8f</sup>	OK <sup>3.9f</sup>
$z_6^F$ (mol%) = [ <b>53.3 33.3 13.3</b> ]	OK	OK	Fail	OK

<sup>a</sup> OK: Closed-loop stable and purities all products are either restored/ over-purified and the transient responses are not very severe

<sup>b</sup> Fail: Closed-loop stable but purity of side-product is not maintained ( $x_B^S$  dropped considerably)

<sup>c</sup> Poor: Although steady state purities may be restored, the transient response is poor and shows valve saturation

<sup>d</sup> Nominal feed rate:  $F=1$  kmol/min

Nominal feed composition,  $z_F$  (mol%) = [33.3 33.3 33.3]

The four control structures were simulated for the nominal case, for a  $\pm 20$  % feed rate change and for six feed composition disturbances of which four cases are shown in Figures 3.6 to 3.9. All the control structures could handle the feed rate disturbance of  $\pm 20$  % but for the feed composition disturbances, some responses using structures CS1 and CS3 were poor.

Nominally, the column is operated at a point where both splits A/B and B/C are “difficult” and none of the products are over-purified. However, for feed composition disturbances,  $z_1^F$ ,  $z_2^F$  and  $z_3^F$ , the B/C split is the most difficult one and for feed composition disturbances  $z_4^F$ ,  $z_5^F$  and  $z_6^F$ , the A/B split is more difficult. The results of the closed-loop simulations feed

Table 3.3: SIMC tuning parameter ( $\tau_C$ ) used in the four control structures <sup>a,b</sup>

Loop	CS1	CS2	CS3	CS4
R <sub>L</sub>	10 min	10 min	10 min	40 min
R <sub>V</sub>	40 min	40 min	–	–
L	20 min	10 min	10 min	40 min
S	80 min	40 min	40 min	10 min
V <sub>B</sub>	10 min	40 & 40 min <sup>a</sup>	40 min	40, 40 & 10 min <sup>b</sup>

<sup>a</sup>  $\tau_C$  for V<sub>B</sub> paired with B in reboiler &  $\tau_C$  for V<sub>B</sub> paired with A in side-product respectively

<sup>b</sup>  $\tau_C$  for V<sub>B</sub> paired with B in reboiler ,  $\tau_C$  for V<sub>B</sub> paired with A in side-product &  $\tau_C$  for V<sub>B</sub> paired with A in sub-column C1 bottoms respectively

rate and all six compositions are summarized in Table 3.2 and we see that structure CS3 fails when the A/B split is more difficult.

Simple decentralized proportional-integral (PI) controllers with SIMC tuning [25] were used. Step changes in the manipulated variables were made to identify the input-output steady state gain and effective time delay. The SIMC tuning parameter,  $\tau_C$  was selected to get a smooth response (see Table 3.3). Note that the tuning was straight forward. The energy loop involving the maximum-select controllers were detuned for a smooth response.

In addition, logarithmic transformations of compositions were used to reduce the effect of non-linearity [26, 27]. Therefore, the controlled composition variables are actually  $\ln x_i$ , where  $x_i$  is the key impurity being controlled.

### 3.4.1 Simulation of structure CS1

Figure 3.6 shows closed-loop responses using CS1 for a  $\pm 20\%$  feed rate changes and feed composition disturbances. We use a semi-log scale to plot the compositions of the key impurities in the main products D, S and B. The side-product has two key impurities, A and C. We observe that the closed-loop responses for feed disturbances,  $z_1^F$  and  $z_3^F$  (Figures 3.6c and 3.6d) show poor transient responses. After a long time (not shown in simulations), the impurities are restored to their steady-state values. However, this structure is not recommended, as during the transient conditions, the inputs saturate and there are very large changes in the product compositions.

### 3.4.2 Simulation of structure CS2

Control structure CS2 shows good dynamic responses for the  $\pm 20\%$  feed rate changes and the feed composition disturbances as shown in Figure 3.7. The steady state impurities of the products are better than the specifications (3.3). For feed compositions when the B/C split is more difficult (Figures 3.7c and 3.7d), the light impurity (A) in side-product is not controlled and is over-purified. For feed compositions when A/B is the more difficult split, the maximum-select controller pairs the boilup with the light key in side-product and the bottom product is over-purified (Figures 3.7e and 3.7f). Note that for these cases, both key impurities in the side-product are controlled simultaneously.

### 3.4.3 Simulation of structure CS3

We next consider the case when the vapor split ( $R_V$ ) is not a degree of freedom. Control structure CS3 does not attempt to control A in the side product and is workable for cases where B/C is the most difficult split (disturbances  $z_F^4$  and  $z_F^5$ , see Figures 3.8c and 3.8d). However, for disturbances when A/B is the more difficult split (Figures 3.8e and 3.8f), we have a “breakthrough” of A in the bottom of the prefractionator (see, for example, Figure 3.10) and the impurity constraint ( $x_A^S < 0.5\%$ ) is violated both dynamically and at steady-state.

### 3.4.4 Simulation of structure CS4

Figure 3.9 shows closed-loop responses using control structure CS4. The product purities of all products can be controlled within the constraints (3.3) at steady state in all cases. When A/B is the more difficult split, the boilup is not paired with the bottom light key and therefore the bottom product is over-purified (Figures 3.9e and 3.9f).

## 3.5 Analysis of energy usage

We have found in the simulations that control structures CS2 and CS4 give good composition control in all cases, but in addition we want the structures to achieve minimum energy usage, or at least close to minimum energy usage. We have plotted the energy usage (V) in all simulations, but to say how good it is we need to compare with the minimum energy usage for the various feed compositions. This is shown in Table 3.4 where we compare the steady-state energy usage for control structures CS2 and CS4 with the

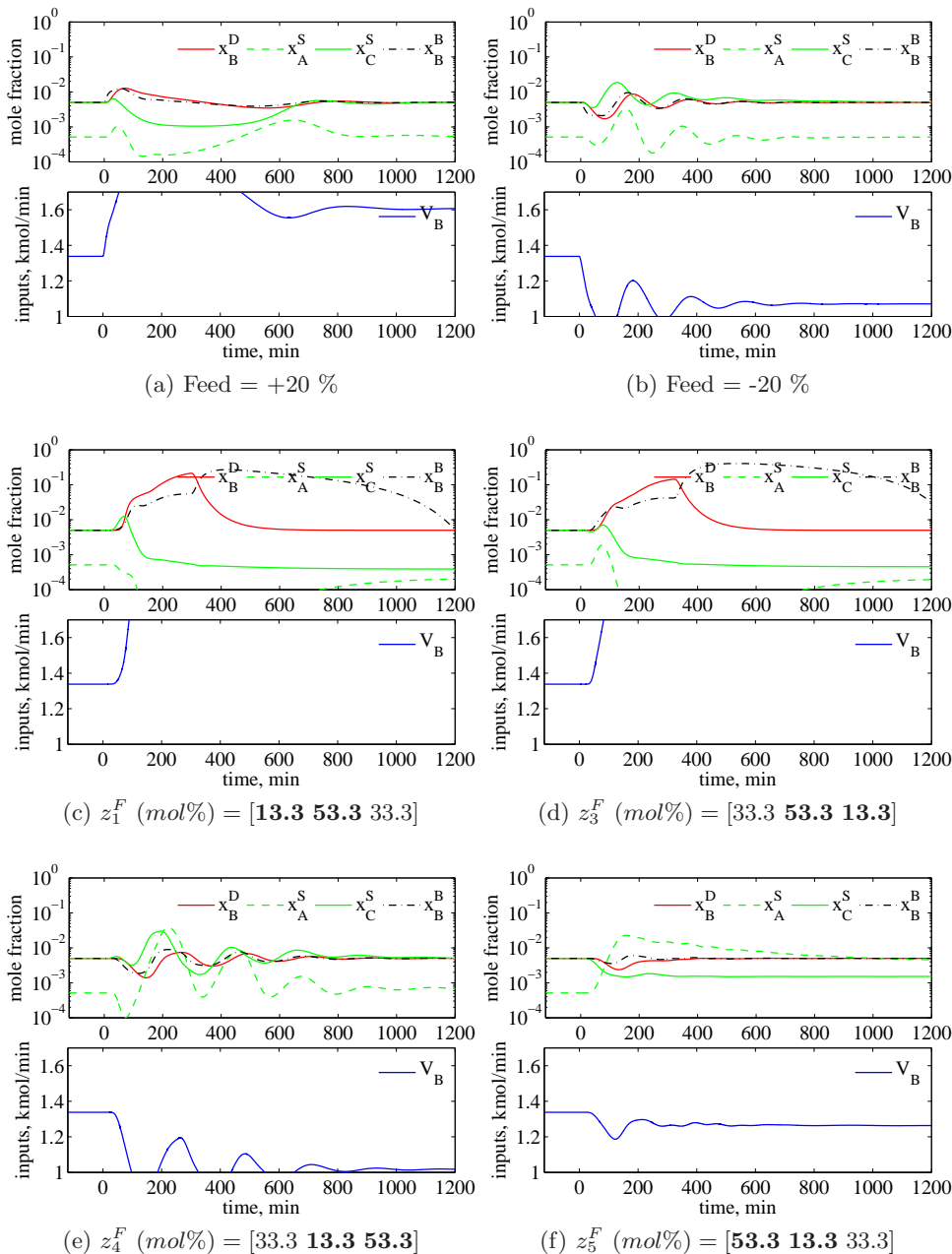


Figure 3.6: CS1: Closed-loop results for feed rate and composition disturbances (**Not acceptable** for feed composition disturbance  $z_1^F$ ,  $z_3^F$  and  $z_4^F$  as the transient response is poor).

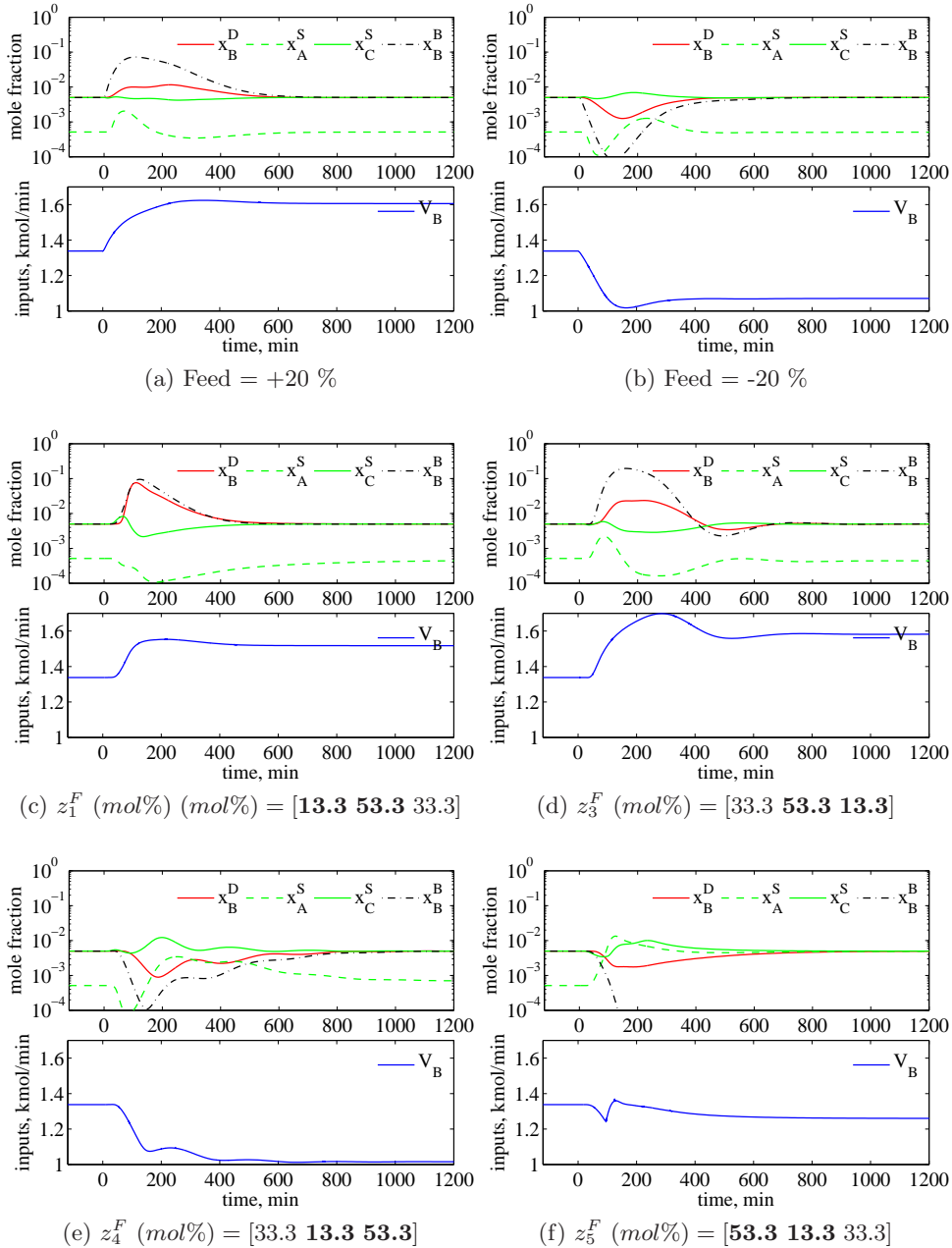


Figure 3.7: CS2: Closed-loop results for feed rate and composition disturbances (**Acceptable** for all disturbances).



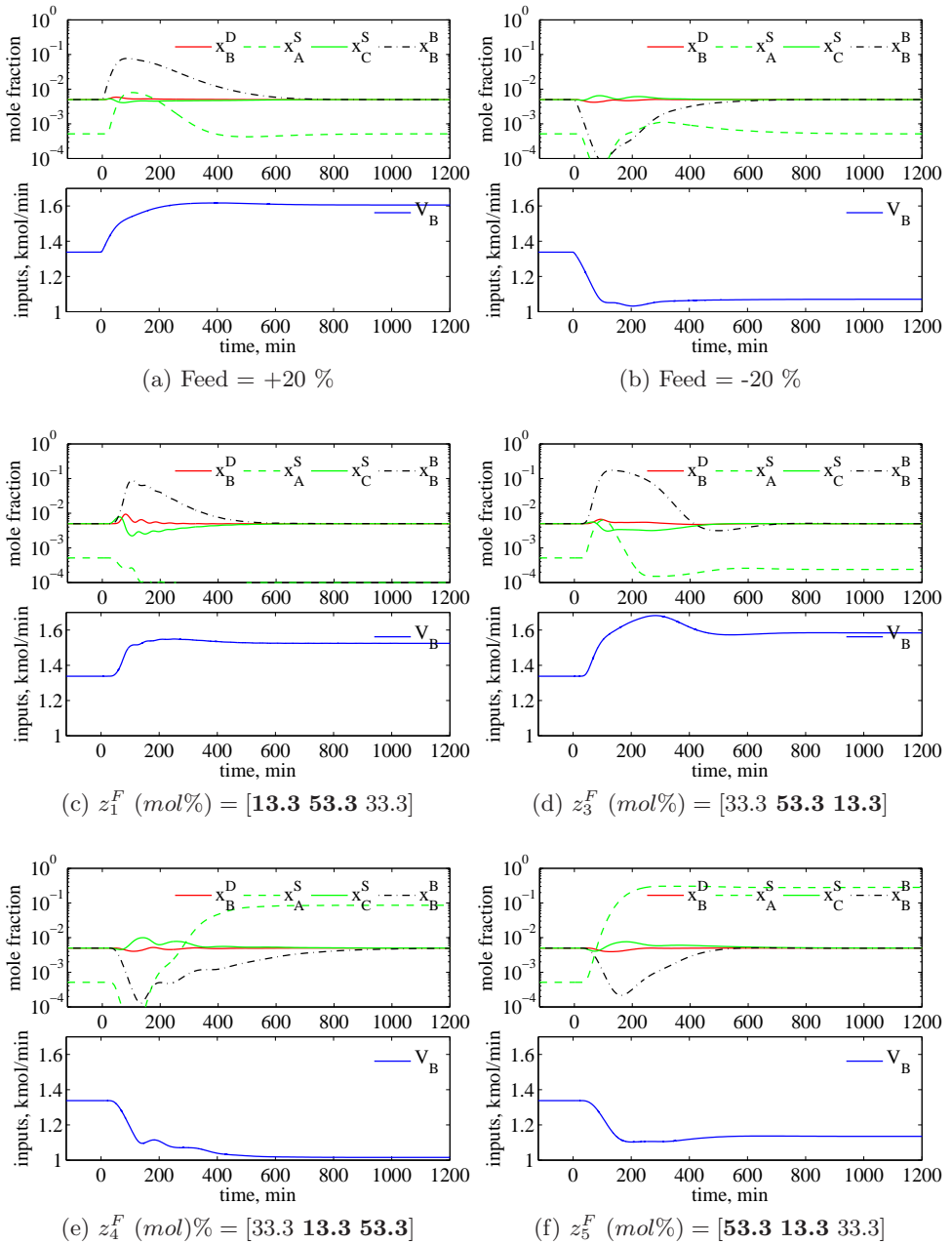


Figure 3.8: CS3: Closed-loop results for feed rate and composition disturbances (**Not Acceptable** for disturbances  $z_4^F$  and  $z_5^F$  as  $x_A^S$  goes out of bounds).

## Control structure selection for three-product Petlyuk (dividing-wall) column

40

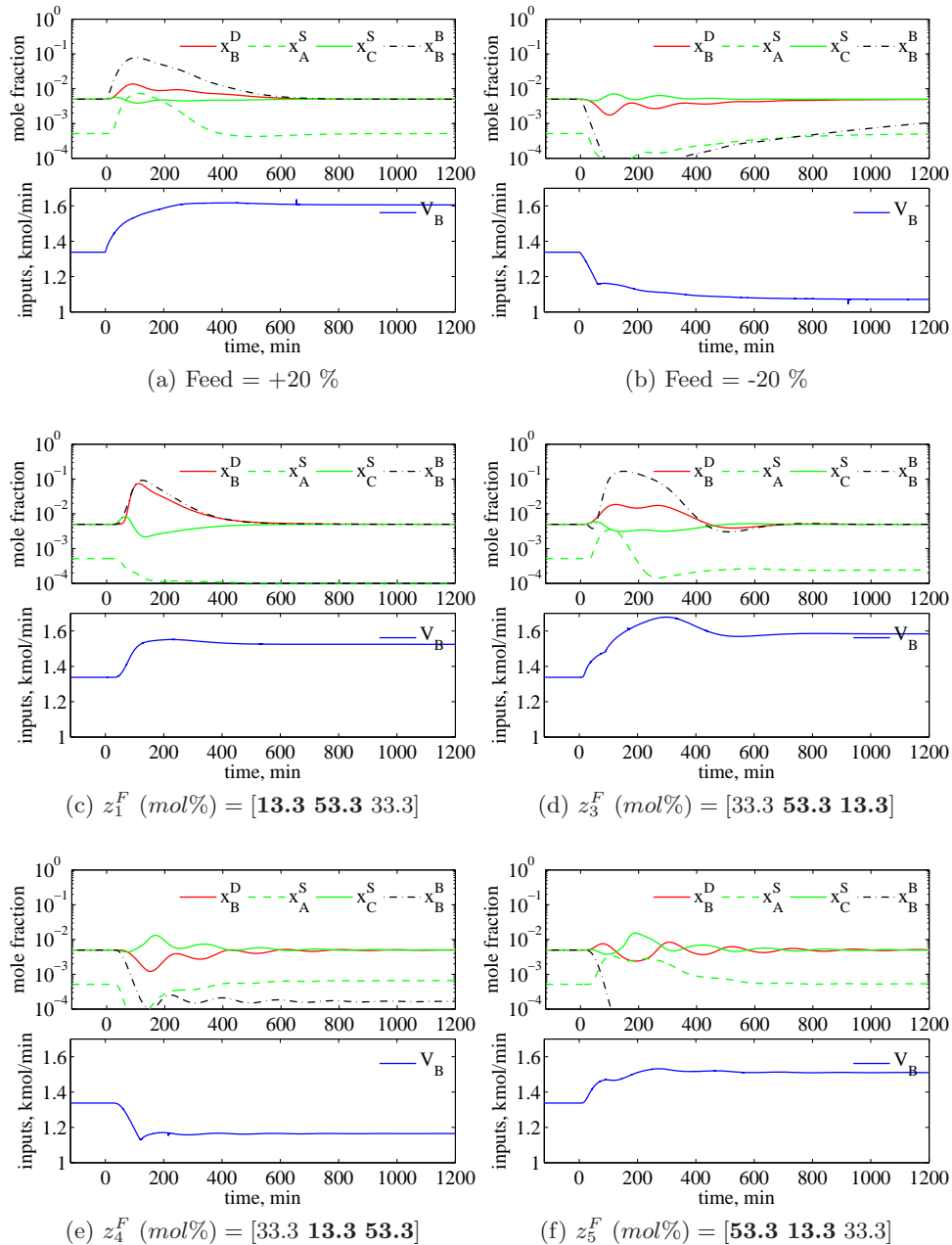


Figure 3.9: CS4: Closed-loop results for feed rate and composition disturbances (**Acceptable** for all disturbances).

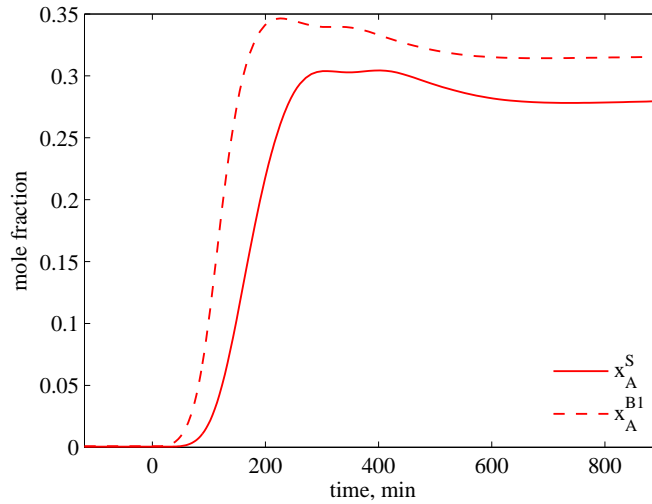


Figure 3.10: Failure of control structure CS3 for feed composition disturbance  $z_5^F$  (mol%) = [53.3 13.3 33.3] caused by breakthrough of component A in bottoms of prefractionator ( $x_A^{B1}$ ) resulting in contaminated side product ( $x_A^S$ ).

optimal for each case, that is, with and without the vapor split ( $R_V$ ) as a degree of freedom, respectively. The results show that control structure CS2 is close to the optimal for all feed compositions, with a maximum energy loss of 1.01 % for feed composition  $z_6^F$ . Control structure CS4 is also close to the optimal for all feed compositions, with a maximum energy loss of 2.27% for feed composition  $z_5^F$ . Note that the optimal energy usage is generally higher for structure CS4 than for CS2 (up to about 20 % for  $z_5^F$ ), but this is an inevitable loss caused by operating with a fixed vapor split ( $R_V$ ). The reason for the (albeit small) energy losses for control structures CS2 and CS4 is mainly because the prefractionator is not operating quite optimally, that is, the prefractionator setpoints in (3.4b) are not the optimal ones as explained earlier in Section 3.3.2. This is also why the energy usage is 0.42 % above the minimum even for the nominal feed composition.

## 3.6 Discussion

### 3.6.1 Change in difficult split

Figure 3.3 shows how the  $V_{min}$  diagram depends on the feed composition. As explained earlier, the minimum boilup for sharp separation is set by the

Table 3.4: Energy usage at steady state for control structures CS2 and CS4 as compared against optimum energy usage with and without the vapor split ( $R_V$ ) for different feed composition disturbances.

Disturbance	Boilup (V), kmol/min			
	with $R_V$		without $R_V$	
	optimal	CS2	optimal	CS4
$z_1^F$ (mol%) = [13.3 53.3 33.3]	1.5070	+0.7 %	1.5072	+1.2 %
$z_2^F$ (mol%) = [13.3 33.3 53.3]	1.2528	+0.33 %	1.2551	+0.37 %
$z_3^F$ (mol%) = [33.3 53.3 13.3]	1.5713	+0.68 %	1.5722	+0.76 %
$z_4^F$ (mol%) = [33.3 13.3 53.3]	1.0151	+0.06 %	1.1434	+1.88 %
$z_5^F$ (mol%) = [53.3 13.3 33.3]	1.2571	+0.23 %	1.4769	+2.27 %
$z_6^F$ (mol%) = [53.3 33.3 13.3]	1.4533	+1.01 %	1.6406	0.87 %
$z^F$ (mol%) = [33.3 33.3 33.3]	1.3325	+0.42 %	1.3325	+0.42 %

“most difficult binary split”, which are given in Figure 3.3 by the peaks  $P_{AB}$  and  $P_{BC}$ . For the nominal feed (red solid line), the peak  $P_{BC}$  is highest. This implies that the B/C split is more difficult. It is then acceptable to leave A uncontrolled in the side stream as in structure CS3. However, for a feed composition making A/B the more difficult split (blue dashed line in Figure 3.3), the boilup should be increased, for example, using a selector to avoid A in the bottoms of the main column section C21 (A/B split) and as well as bottom of the prefractionator (A/C split, see Figure 3.10).

The magnitude of feed composition disturbance in this study is large. However, simulations show that structure CS3 fails and there is a breakthrough of light impurity (A) in the side product also for smaller feed disturbances. The reason is that the nominal operating point is quite close to a region where A/B may become the more difficult split.

### 3.6.2 Multivariable Control (MPC)

In this work, we have studied performance of decentralized control schemes based on PI-controllers and max-selectors as this is the preferred solution in industry, whenever it is found to be workable. We found that its performance is acceptable, but tuning the controllers was difficult in some cases. Thus, this may be a case where multivariable control (e.g. MPC) should be considered to reduce interactions and improve performance.

One may think that the max- select controllers can easily be replaced by

a constrained multivariable controllers, like MPC. However, a more careful evaluation reveals that this is not so clear, because when we switch using the PI-controllers, we use controllers tuned in different operating regions, for example, with and without A in the side product. Thus, to get acceptable control with MPC, one probably would need to include model information from different operating regions, which may be difficult to handle in a conventional linear MPC framework. Possibly, this could be a case where non-linear MPC based on physical models may be the preferred solution.

### 3.6.3 Other control structures

In principle, there are many other possible control structures with selectors, in addition to CS2 and CS4, but these have not been studied. To see this, note that we are attempting to control *six* compositions, which include *two* for the two “products” in the prefractionator and *four* for the three products in the main column, see (3.3) and (3.4). However, we only have *five* degrees of freedom for the case when  $R_V$  is a manipulated variable, and *four* degrees of freedom for the case when  $R_V$  is fixed during operation, respectively. Thus, we have too few degrees of freedom to control all *six* compositions and to satisfy the *six* specifications we need to overpurify some products. For the case when  $R_V$  is fixed, we are lacking two degrees of freedom and we propose in control structure CS4 to always control *three* of the compositions, and to overpurify *two* of the remaining *three* compositions using a selector. However, it is not given which *three* compositions to include in the selector, and it is not given that boilup should be used in the selector. Specifically, for the split A/B we may choose to overpurify  $x_B^D$  (B in distillate) rather than  $x_A^S$  (A in sidestream), and for the split B/C we may choose to overpurify  $x_C^S$  (C in side stream) rather than  $x_B^B$  (B in bottom). Similarly, for the prefractionator, we may for the split A/C choose to overpurify  $x_C$  in the top rather than  $x_A$  in the bottom. Some of these alternatives may be worthwhile considering, in particular, if overpurification of some product is desirable, whenever possible. Nevertheless, of all these possible alternative structures, it seems that structure CS4 is a good choice, mainly because the boilup ( $V$ ) has a direct effect on the three compositions used by the selector, and because the three remaining manipulated variables have a direct effect on the three remaining compositions. Indeed, it was found to give good composition control with close to minimum energy usage for a wide range of feed composition changes.

### 3.7 Conclusions

In this work, we study decentralized control structures when the objective is to achieve desired purities for the three products with minimum use of energy ( $V$ ). For the case where the vapor split ( $R_V$ ) is a degree of freedom, we propose to use structure CS2 as shown in Figure 3.4a. It will generally lead to overpurification of either the side stream or bottom product, but this will cost very little in terms of extra energy usage. For the more realistic case where the vapor split is not a degree of freedom, the energy usage will be higher for some disturbances. This is inevitable, but otherwise the proposed structure CS4 (see Figure 3.5b) achieves the desired purities with use of minimum energy. The simpler structure CS3 may be used instead of CS4 for cases where the A/B split is relatively simple so that we always have low concentration of A (“overpurification”) in the side stream.

### References

- [1] Adrian, T., Schoenmakers, H., Boll, M., 2004. Model predictive control of integrated unit operations: Control of a divided wall column. *Chemical Engineering and Processing* 43 (3), 347–355.
- [2] Alstad, V., 2005. Studies on selection of controlled variables. Ph.D. thesis, Norwegian University of Science and Technology, Department of Chemical Engineering.
- [3] Alstad, V., Halvorsen, I. J., Skogestad, S., 2004. Optimal operation of a Petlyuk distillation column: Energy savings by over-fractionating. In: *Escape-14: Lisbon, Portugal, 2004*.
- [4] Buck, C., Hiller, C., Fieg, G., 2011. Applying model predictive control to dividing wall columns. *Chemical Engineering & Technology* 34 (5), 663–672.
- [5] Cahn, R. P., DiMiceli, A. G., 1962, US 3058893, United States Patent Office. Separation of multicomponent mixture in single tower.
- [6] Christiansen, A. C., Skogestad, S., 1997. Energy savings in complex distillation arrangements: importance of using the preferred separation. In: *AIChE Annual Meeting, Los Angeles, November 1997*, paper 199d.
- [7] Dejanovic, I., Matijasevic, L., Halvorsen, I. J., Skogestad, S., Jansen, H., Kaibel, B., Olujić, Z., 2011. Designing four-product dividing wall

- columns for separation of a multicomponent aromatics mixture. *Chemical Engineering Research and Design* 89 (8), 1155 – 1167.
- [8] Fidkowski, Z., Królikowski, L., 1987. Minimum energy requirements of thermally coupled distillation systems. *AIChE Journal* 33 (4), 643–653.
- [9] Govatsmark, M. S., Skogestad, S., 2005. Selection of controlled variables and robust setpoints. *Industrial & Engineering Chemistry Research* 44 (7), 2207–2217.
- [10] Halvorsen, I. J., Skogestad, S., 1999. Optimal operation of Petlyuk distillation: steady-state behavior. *Journal of Process Control* 9 (5), 407 – 424.
- [11] Halvorsen, I. J., Skogestad, S., 2003. Minimum energy consumption in multicomponent distillation. 1. Vmin diagram for a two-product column. *Industrial & Engineering Chemistry Research* 42 (3), 596–604.
- [12] Halvorsen, I. J., Skogestad, S., 2003. Minimum energy consumption in multicomponent distillation. 2. three-product Petlyuk arrangements. *Industrial & Engineering Chemistry Research* 42 (3), 605–615.
- [13] Halvorsen, I. J., Skogestad, S., 2003. Minimum energy consumption in multicomponent distillation. 3. more than three products and generalized Petlyuk arrangements. *Industrial & Engineering Chemistry Research* 42 (3), 616–629.
- [14] Kaibel, G., 1987. Distillation columns with vertical partitions. *Chemical Engineering & Technology* 10 (1), 92–98.
- [15] Kiss, A. A., Rewagad, R. R., 2011. Energy efficient control of a BTX dividing-wall column. *Computers & Chemical Engineering* 35 (12), 2896 – 2904.
- [16] Lestak, F., Smith, R., Dhile, V., 1994. Heat transfer across the wall of dividing wall columns. In: *Trans. Inst. Chem. Eng.* 1994, 72A, 639-644.
- [17] Ling, H., Cai, Z., Wu, H., Wang, J., Shen, B., 2011. Remixing control for divided-wall columns. *Industrial & Engineering Chemistry Research* 50 (22), 12694–12705.
- [18] Ling, H., Luyben, W. L., 2009. New control structure for divided-wall columns. *Industrial & Engineering Chemistry Research* 48 (13), 6034–6049.

- 
- [19] Ling, H., Luyben, W. L., 2010. Temperature control of the BTX divided-wall column. *Industrial & Engineering Chemistry Research* 49 (1), 189–203.
  - [20] Mutalib, M. I. A., Smith, R., 1998. Operation and control of dividing wall distillation columns: Part 1: Degrees of freedom and dynamic simulation. *Chemical Engineering Research and Design* 76 (3), 308–318.
  - [21] Mutalib, M. I. A., Zeglam, A. O., Smith, R., 1998. Operation and control of dividing wall distillation columns: Part 2: Simulation and pilot plant studies using temperature control. *Chemical Engineering Research and Design* 76 (3), 319–334.
  - [22] Niggemann, G., Hiller, C., Fieg, G., 2010. Experimental and theoretical studies of a dividing-wall column used for the recovery of high-purity products. *Industrial & Engineering Chemistry Research* 49 (14), 6566–6577.
  - [23] Petlyuk, F., Platonov, V., Slavinskii, D., 1965. Thermodynamically optimal method for separating multicomponent mixtures. *International Chemical Engineering* 5 (3), 555–561.
  - [24] Rewagad, R. R., Kiss, A. A., 2012. Dynamic optimization of a dividing-wall column using model predictive control. *Chemical Engineering Science* 68 (1), 132 – 142.
  - [25] Skogestad, S., 2003. Simple analytic rules for model reduction and pid controller tuning. *Journal of Process Control* 13 (4), 291–309.
  - [26] Skogestad, S., 2007. The do’s and dont’s of distillation column control. *Chemical Engineering Research and Design* 85 (1), 13 – 23.
  - [27] Skogestad, S., Morari, M., 1988. LV-control of a high-purity distillation column. *Chemical Engineering Science* 43 (1), 33 – 48.
  - [28] Stupin, W., 1972. Thermally coupled distillation- a case history. *Chemical Engineering Progress* 68 (10).
  - [29] Wolff, E. A., Skogestad, S., 1995. Operation of integrated three-product (Petlyuk) distillation columns. *Industrial & Engineering Chemistry Research* 34 (6), 2094–2103.



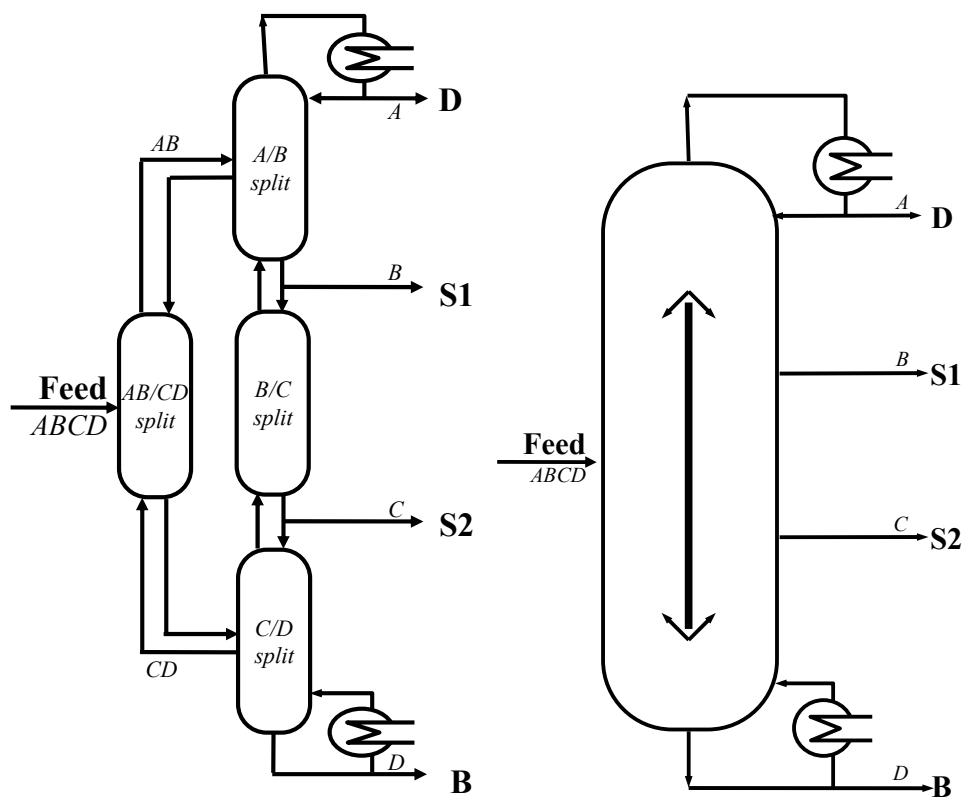
## Chapter 4

# Steady state and dynamic operation of four-product dividing-wall (Kaibel) columns: Experimental Verification

### 4.1 Introduction

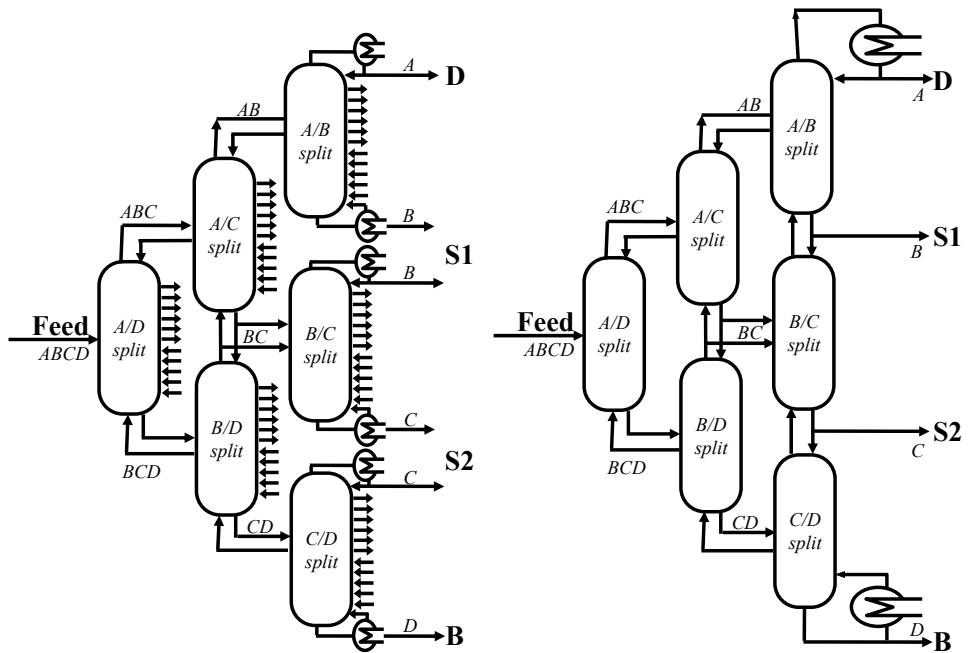
Distillation is a separation technique that uses heat energy to provide the separation work of “un-mixing” the feed mixture. In this paper, we study the integrated Kaibel distillation scheme for separation of four components as shown in Figure 4.1[10]. The main motivation for this scheme is combination of capital savings and energy savings compared to conventional distillation sequences for multicomponent separation. This scheme is not the best in terms of minimum separation work (exergy), mainly because it performs a difficult B/C split in the prefractionator and not the easiest (A/D) split.

An “ideal reversible” system with minimum exergy requires a more complex arrangement, infinite number of stages and heating and cooling on all stages. [5, 6, 21]. For four-product separation, Figure 4.2a shows the reversible scheme proposed by Petlyuk and Platonov [19]. The column sections are directly coupled and the easiest split is done first. Any mixing losses near the feed stage and at the ends can thus be avoided. Some of the features of reversible distillation are retained in an adiabatic “four-product



(a) Implementation with four separate column sections [20] (b) Dividing-wall implementation with two side products[10]

Figure 4.1: Thermodynamically equivalent implementations of four-product Kaibel column (studied in this paper)



(a) Four-product "reversible" Petlyuk column

(b) Four-product adiabatic Petlyuk column

Figure 4.2: "Reversible" and adiabatic arrangements of Four-product "extended" Petlyuk column (*not studied in this paper*)

extended Petlyuk column”, which has only one heater (reboiler) and one cooler (condenser) (See Figure 4.2b). In fact, the adiabatic scheme shown in Figure 4.2b is better than the reversible scheme in Figure 4.2a in terms of energy although it is inferior in terms of exergy. Compared to conventional two-product column sequences, the potential energy savings in an adiabatic “four-product extended Petlyuk arrangement” (Figure 4.2b) can be up to 50% [3]. The disadvantage of using the arrangements shown in Figure 4.2 is that, a large number of sections are required for a multicomponent separation. Petlyuk et al. [20] also proposed schemes for multicomponent separation with a minimum number of column sections. For a four-product separation, one of the schemes given by Petlyuk is same as the “Kaibel” scheme in figure 4.1a [9].

The four-product Kaibel column, in Figure 4.1, although less efficient than the Petlyuk arrangements in Figure 4.2, can still offer up to 30% energy saving compared to conventional sequences due to the directly coupled prefractionator [8]. Our experimental setup is similar to the scheme in Figure 4.1a, which does not have a vertical dividing-wall but the results are extendable to dividing-wall columns.

Numerous successful industrial implementations of three-product dividing-wall columns have been reported by the German company BASF [4, 18]. In the open literature, a thorough experimental study for operation of a three-product high purity distillation column was reported Niggemann et al.[17]. Earlier, start-up for a three-product column based on rigorous simulations was reported by Niggemann et al.[16]. Mutalib and Smith[14] reported a simulation study on a three-product dividing-wall column and concluded that a conventional proportional-integral (PI) control scheme can give good regulation. They also reported experimental studies done on a pilot plant column [15]. Ling and Luyben [13] performed a simulation study and proposed a four-point control structure for a three-product dividing-wall column. van Diggelen et al.[26] compared conventional PID controller with controllers obtained by  $H_\infty$  controller synthesis and  $\mu$ -synthesis. Ling et al.[12] proposed control structures considering remixing losses for an energy optimal operation. Several works have also been reported for the use of Model Predictive Control for divided wall columns [1, 2, 22].

There is one reported use of four-product Kaibel column in BASF and several patents from BASF as summarized by Dejanovic et al.[4]. Some simulation work has also been carried out on control and operation of four-product Kaibel columns. Strandberg and Skogestad[25] found in a simulation study that a four-point temperature control scheme with inventory control can stabilize the column and prevent “drift” of the composition

profiles during operation. Ghadrđan et al.[7] reported another simulation study on optimal steady state operating solutions for economic criterions like minimizing energy for fixed purity specifications. Kvernland et al.[11] studied a multivariable Model Predictive Controller on top of a regulatory layer with a four-point temperature control.

In the open literature, there are no experimental studies reported on operation and control of four-product directly coupled columns. In this paper we present experimental results for a four-product Kaibel column separating methanol, ethanol, 1-propanol and 1-butanol (with normal boiling points of 64.7 °C, 78.4 °C, 97.2 °C and 117.7 °C, respectively).

## 4.2 Experimental setup

Figure 4.3a shows a picture of our experimental column [24]. Although this is not a dividing-wall column, it is thermodynamically equivalent as illustrated in Figure 4.1. The height of the column is about 8 meters. The system is operated at atmospheric pressure and the column sections are packed with 6-mm glass Raschig rings. The column sections are numbered from 1 to 7 as shown in Figure 4.3a. Sections 1 and 2 constitute the prefractionator, while sections 3-7 form the main column. The internal diameter of vacuum jacket glass column-sections 1, 2, 4, 5 and 6 is 50 mm while that of column-sections 3 and 7 is 70 mm (column sections are numbered in Figure 4.3c). The height of packing in sections 1 and 2 is 1.1 m and 1.6 m, respectively, while in sections 3, 4, 5 it is 0.65 m. The height of packing in sections 6 and 7 is about 0.75 m and 0.9 m, respectively.

The reboiler is kettle type and the power to the reboiler is adjusted by varying the voltage to the heater elements through a thyristor. The condenser is mounted on top of the column and is water-cooled. The condensed vapor flows back to the column due to gravity; a part is taken out as top product and the rest forms the liquid reflux.

The liquid reflux split valve, top product valve and side product valve are swinging funnels (On/ Off) and are controlled by externally placed solenoids. The flow through the swinging funnel depends on the internal liquid flows in the respective column section. To implement the continuous output of the proportional-integrator (PI) controllers, the common technique of pulse width modulation (PWM) is used where the width (length of the pulse is the adjustable continuous variable) and the period (cycle time) is normally fixed. The cycle time of the On/ Off valves should be much shorter than the plant time constant and hence emulate continuous-pump like flow conditions. In our case, the valve switching function has a total

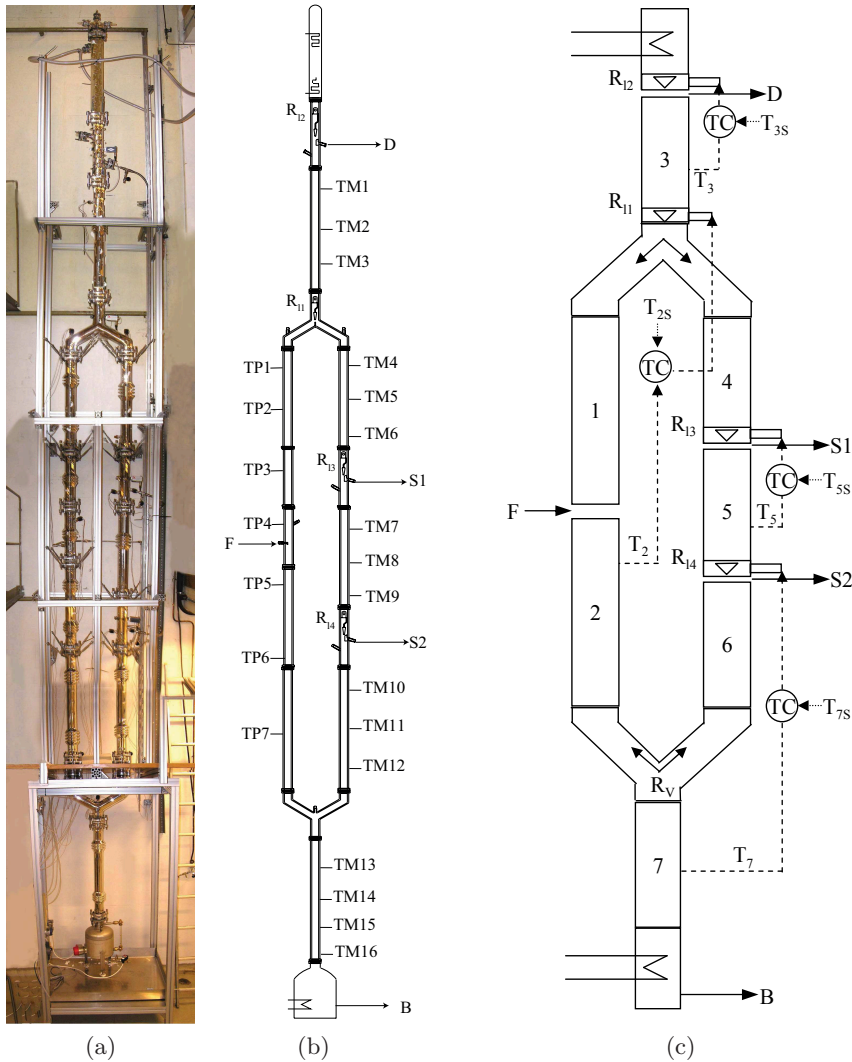


Figure 4.3: (a) Picture of the experimental column. [24]  
 (b) Schematic showing location of temperature sensors. [24]  
 (c) 4-point regulatory control structure used for operation  $T_2 = TP5$ ,  $T_3 = TM2$ ,  $T_5 = TM8$  &  $T_7 = TM14$ .

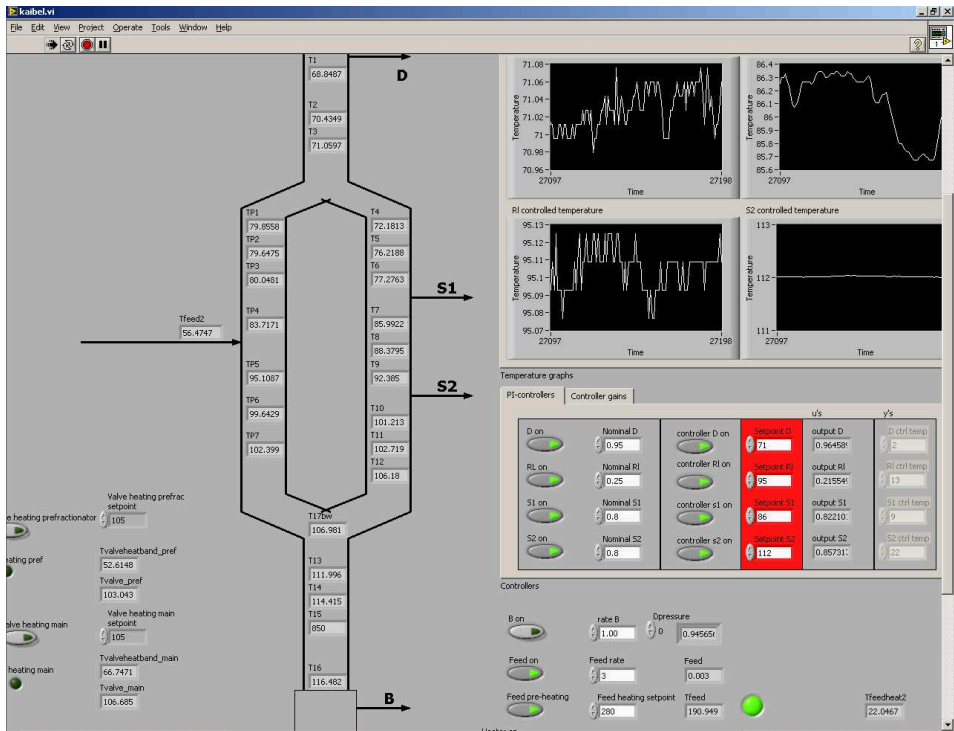


Figure 4.4: Screen-shot of operator interface during experimental run 12.

cycle time about 10 seconds and a resolution time for switching of 0.2 seconds. For example, if the controller output is 0.22, a valve position on one side of the funnel is 2.2 seconds and 7.8 seconds on the other. This gives an implemented accuracy of 4% when the valve position is 0.5, but much worse resolution when close to the fully open (0)/ close (1) position. To improve the resolution, we used an algorithm that allows also the total cycle time to change between 5 seconds and 15 seconds. This implementation reduces the rounding off errors and improves the resolution of the valve.

In our setup, it is also possible to adjust the vapor split ratio ( $R_V$ ) between the prefractionator and the main column using a valve, but in the reported experiments it has been kept constant as is common in industrial implementations. The vapor split between the prefractionator and the main column is then determined by the normal pressure drop offered by the packing in the column sections.

The liquid-level measurement in the reboiler was faulty and a level controller could not be installed. Therefore, the bottom product was allowed to accumulate during the experimental runs. With a large reboiler, the composition of the bottoms will then take a long time to reach steady state, but otherwise this should have little effect on the experimental results.

The control setup is implemented in Lab View<sup>TM</sup> on a standard PC. Figure 4.4 is a screen-shot from the computer interface (Lab View) during the experimental run 12, with a snapshot of temperatures as read by the probes in various sections. The dialog labelled “Temperature graphs” shows the four controlled temperatures for 100 seconds. Note that some of the temperature measurements have large measurement biases (for example, TP4 and T16) and their values are calibrated for later analysis and one probe (T15) is faulty.

### 4.3 Control Structure

As reported in the simulation study earlier by Strandberg and Skogestad[25], a 4-point temperature control structure can avoid “drift” of the composition profile in the various sections of a 4-product column. Temperature is a good indicator of composition and is easy to measure. Temperature control is fast and can keep the compositions (and split) in the column close to nominal value and hence preventing “drift” in the event of disturbances.

In Figure 4.3c, we show the control structure used in the experiments. In Table 4.1, we show in more detail the loop pairings. The four temperature control loops are named loop 1, 2, 3 and 4. In the footnote to Table 4.1, we also define the four corresponding liquid flow ratios  $R_{L1}$ ,  $R_{L2}$ ,  $R_{L3}$  and  $R_{L4}$



Table 4.1: Four-point temperature regulatory control structure <sup>a,b</sup>

Control loop	Manipulated Variable <sup>a</sup>	Controlled Variable <sup>b</sup>
Loop 1	Liquid split valve ( $R_{L1}$ )	Temperature in section 2 ( $T_2$ )
Loop 2	Distillate split valve ( $R_{L2}$ )	Temperature in section 3 ( $T_3$ )
Loop 3	Upper side product split valve ( $R_{L3}$ )	Temperature in section 5 ( $T_5$ )
Loop 4	Lower side product split valve ( $R_{L4}$ )	Temperature in section 7 ( $T_7$ )

<sup>a</sup> manipulated variables (controller outputs) are the swinging funnel ratios

$R_{L1}$ ,  $R_{L2}$ ,  $R_{L3}$  and  $R_{L4}$ :

$$R_{L1} = \frac{L_1}{L_3}, R_{L2} = \frac{L_3}{L_3+D}, R_{L3} = \frac{L_5}{L_5+S1}, R_{L4} = \frac{L_6}{L_6+S2}$$

Here,  $L_1$ ,  $L_3$ ,  $L_5$  and  $L_6$  are liquid flows in sections 1, 3, 5 and 6, respectively (see Figure 4.3)

$S1$  and  $S2$  are side product flow rates

<sup>b</sup> controlled variables are temperature sensors as shown in figures 4.3b and 4.3c:

$$T_2 = TP5, T_3 = TM3, T_5 = TM8 \text{ and } T_7 = TM14$$

which are set by the swinging funnels.

In control loop 1, the liquid split ratio ( $R_{L1}$ ) is used to control a sensitive temperature in the prefractionator ( $T_2 = TP5$ ). In loop 2, the distillate split ratio ( $R_{L2}$ ) controls a temperature in section 3 ( $T_3 = TM3$ ). In the loop 3, the upper side product split ratio ( $R_{L3}$ ) controls a sensitive temperature in section 5 ( $T_5 = TM8$ ). Finally, in control loop 4, the lower side product split ratio ( $R_{L4}$ ) is used to control a sensitive temperature in the bottom section ( $T_7 = TM14$ ).

The controllers are conventional proportional-integrator (PI) controllers. As the system is interactive, we used sequential tuning and loop 1 in the prefractionator was closed first. Next loops 2, 3 and 4 in the main column were closed. The tuning of the loops was done using the SIMC rules [23] with the tuning parameter,  $\tau_C$ , chosen to be 1 minute for loops 1 and 2 and 2 minutes for loops 3 and 4. The temperature setpoints for the loops were adjusted during start-up as explained below.

The remaining two degrees of freedom, the boilup ( $V$ ) and the vapor split ratio ( $R_V$ ), are not used for control in experiments, but may be in general available for some optimizing objective, like minimizing energy for a given specification.

Table 4.2: List of experiments <sup>a</sup>

Experiment	Description
Run 1	cold start-up
Run 2	-2 [°C] setpoint change in T <sub>2</sub> (prefractionator loop)
Run 3	±1 [°C] setpoint changes in T <sub>3</sub> (distillate product loop)
Run 4	±1 [°C] setpoint changes in T <sub>5</sub> (upper side product loop)
Run 5	±1 [°C] setpoint changes in T <sub>7</sub> (lower side product loop)
Run 6	simultaneous ±1 [°C] setpoints changes in all temperatures
Run 7	+20 % disturbance in feed rate
Run 8	steady state run with constant setpoints: T <sub>2</sub> = 80.6 °C T <sub>3</sub> = 69 °C T <sub>5</sub> = 82 °C T <sub>7</sub> = 110.2 °C
Run 9	steady state run with constant setpoints: T <sub>2</sub> = 88°C T <sub>3</sub> = 69°C T <sub>5</sub> = 88°C T <sub>7</sub> = 113°C
Run 10	steady state run with constant setpoints: T <sub>2</sub> = 91°C T <sub>3</sub> = 69.5°C T <sub>5</sub> = 92°C T <sub>7</sub> = 113°C
Run 11	steady state run with constant setpoints: T <sub>2</sub> = 91.5°C T <sub>3</sub> = 72°C T <sub>5</sub> = 92°C T <sub>7</sub> = 112°C
Run 12	steady state run with constant setpoints: T <sub>2</sub> = 95°C T <sub>3</sub> = 71°C T <sub>5</sub> = 86°C T <sub>7</sub> = 112°C
Run 13	total reflux experiment for calculating number of theoretical stages

<sup>a</sup> Feed rate for all runs (except run 7) = 3 LPH  
Reboiler duty for all runs = 2 kW

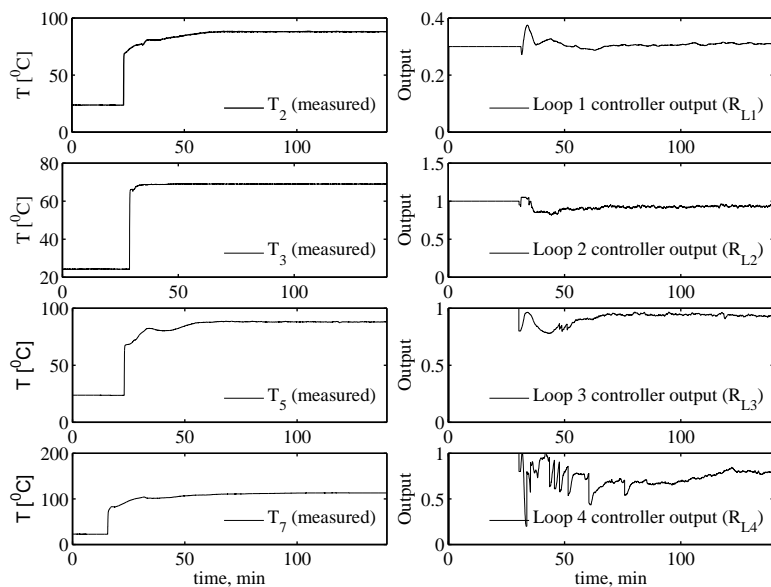
## 4.4 Experiments

Various experiments were conducted for studying the start-up operation, to test the 4-point control structure for setpoint changes, disturbance handling and to study steady state operation. Table 4.2 shows a list of the 13 experiments reported in this paper.

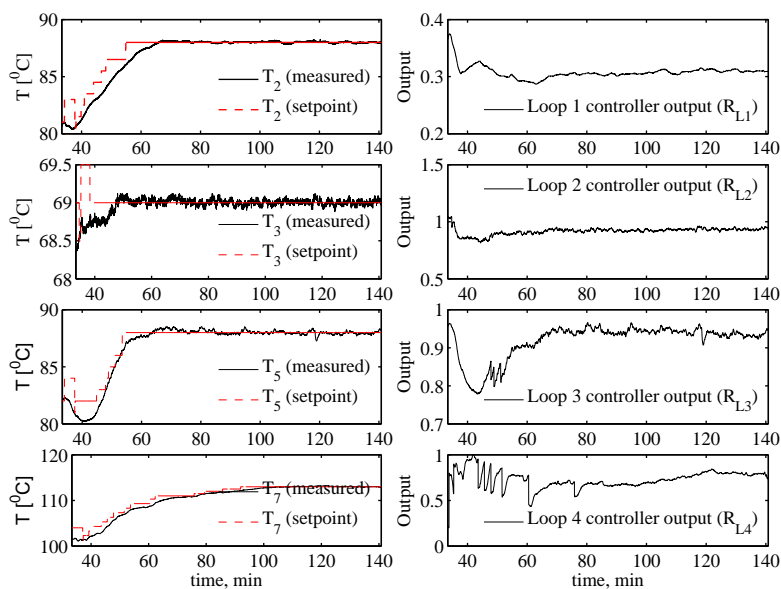
### 4.4.1 Start-up

Figure 4.5a shows the results from a typical cold start-up of the pilot plant (Experimental run 1). The following start-up policy was used:

After turning on the reboiler (at time = 0), the column is heated up in total reflux mode (D=0, S1=0, S2=0, F=0). Initially, the output of control loop 1 (R<sub>L1</sub>) is fixed at a reasonable value (manual mode). In our case, it was fixed at R<sub>L1</sub> = 0.3 which implies that 30% of the reflux is directed to the prefractionator and 70 % to the main column. The output of R<sub>L2</sub>, R<sub>L3</sub>



(a) Cold Start-up: Entire run



(b) Cold Start-up (Zoomed in from 35 min to 140 min)

Figure 4.5: Experimental Run 1: Cold Start-up

and  $R_{L4}$  of control loops 2, 3 and 4 were initially fixed at 1 (no product withdrawal). At about 30 minutes, the feed to the column is turned on. Shortly after, the controllers (loops 1, 2, 3 and 4) are turned on (AUTO mode). With control loops 2, 3 and 4 turned on, we begin to draw the three products D, S1 and S2. The initial temperature setpoints are the values from the total reflux mode, and the setpoints are then adjusted in closed-loop mode to get good separation in the column. The temperature setpoint for the prefractionator ( $T_{2s}$ ) is adjusted to get a large temperature change across the prefractionator column. This corresponds to a sharp split between the intermediate components (ethanol and propanol). The setpoints for the remaining loops ( $T_{3s}$ ,  $T_{5s}$  and  $T_{7s}$ ) are for the main column which performs binary splits, and these are adjusted in an attempt to get the temperatures of the four product close to the normal boiling point of their corresponding main components. Off-line analysis of the products (reported later) shows that this start-up procedure resulted in good quality products, in spite of the fact that we used only temperature loops. Of course, if online composition measurements are available, these should be used to adjust the temperature setpoints.

Figure 4.5b shows a zoomed-in plot of Figure 4.5a for the time period from 35 min to 140 min. In the experiments, the feed flow rate was held constant at 3 liters/hour and the reboiler duty was set constant at 2 kW. We conclude from the experiment (Figures 4.5a and 4.5b) that the start-up procedure works well and leads to stable operation.

#### 4.4.2 Closed-loop operation

In the following experiments (runs 2-7), the four temperatures setpoints are changed in closed-loop, to drive the system to various new steady states. The composition of the feed mixtures is also varied.

In Figure 4.6 (run 2), we show results for a temperature setpoint change of  $-2$  °C to control loop 1. This setpoint change can be handled well and the steady state is reached in about 25 minutes. There is an initial delay of about 1 minute as the location of the temperature is far from the valve. As a consequence, it takes a while for the change in the liquid reflux to affect the controlled temperature. This loop has interactions with loops 3 and 4, as  $T_5$  (measured) and  $T_7$  (measured) show some deviation from their setpoints due to action of  $R_{L1}$ .

Figure 4.7 (run 3) shows a setpoint change of  $\pm 1$  °C change in the loop 2. Again, this setpoint change is handled well. However, there is significant interaction with all the other loops. This is because a change in distillate

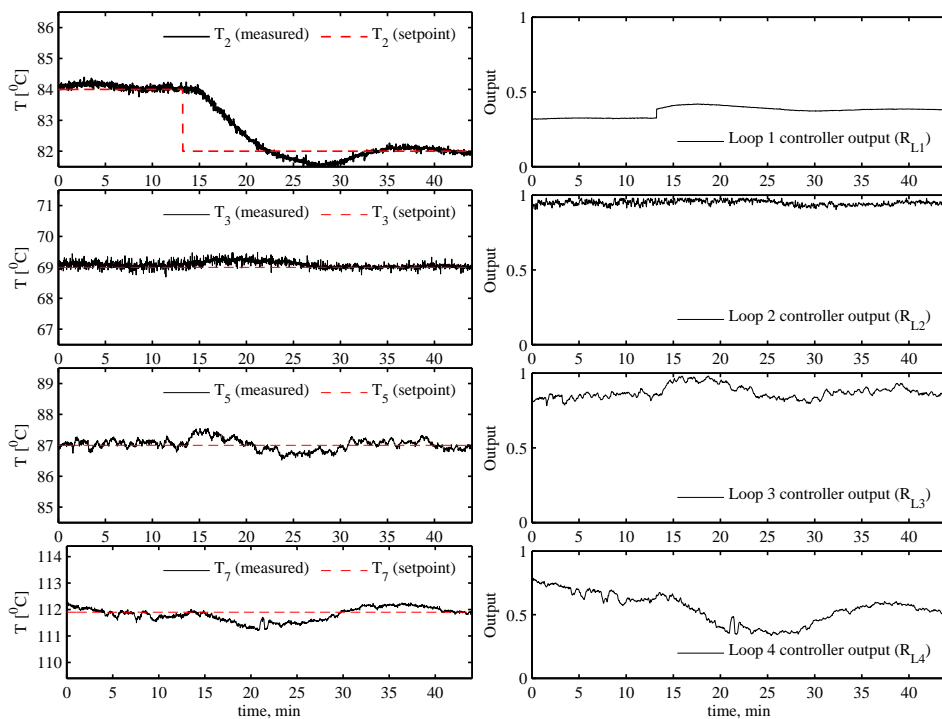


Figure 4.6: Experimental Run 2:  $-2[^{\circ}\text{C}]$  setpoint change in prefractionator temperature,  $T_2$  (control loop 1)

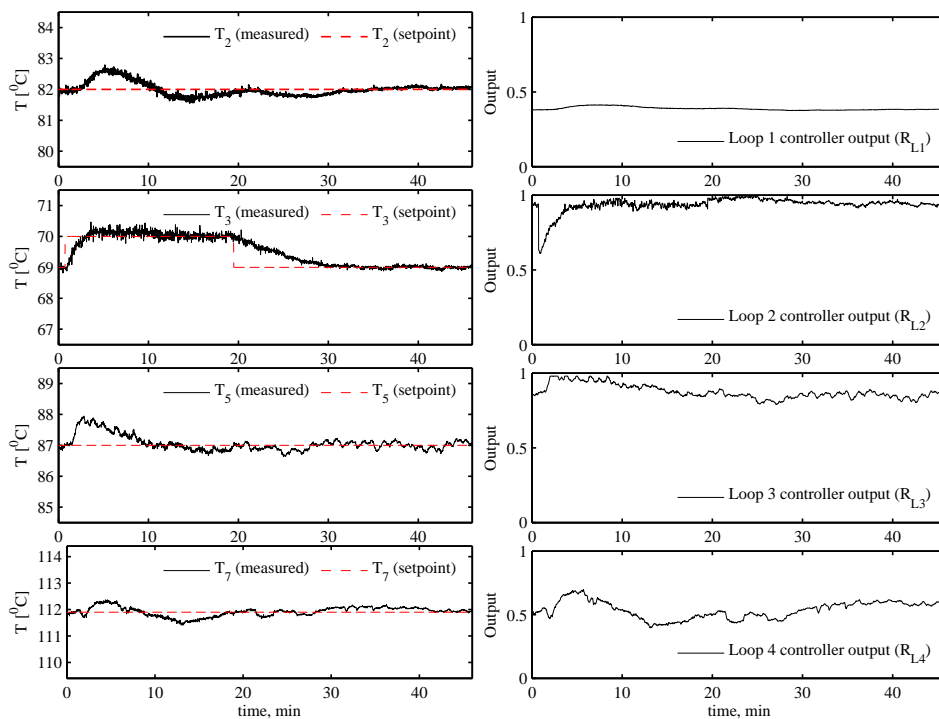


Figure 4.7: Experimental Run 3:  $\pm 1$  [°C] setpoint change in top section temperature,  $T_3$  (control loop 2)

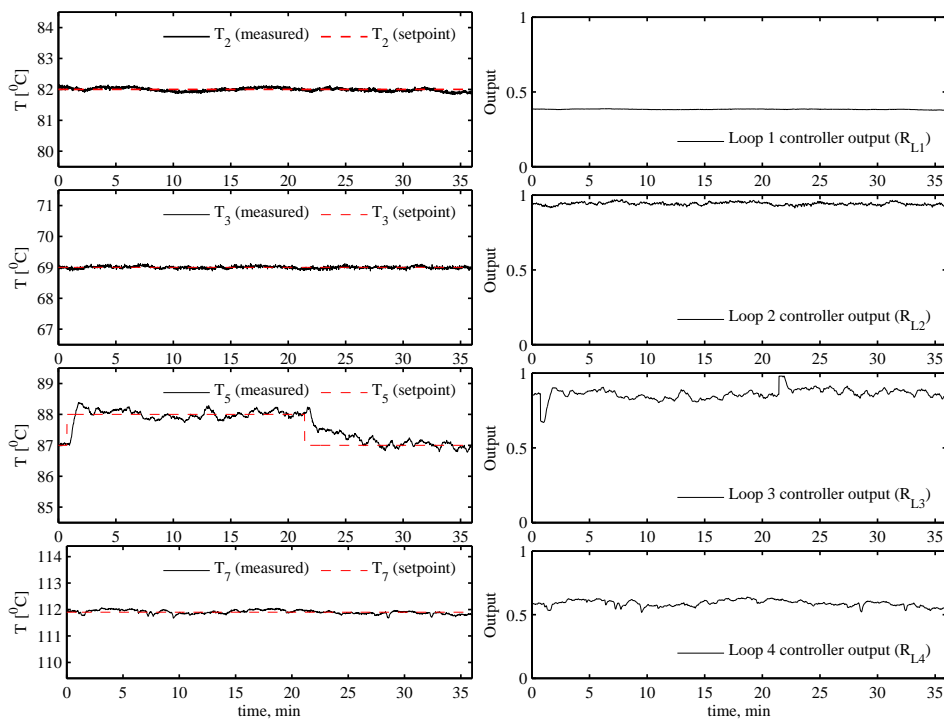


Figure 4.8: Experimental Run 4:  $\pm 1$   $^{\circ}\text{C}$  setpoint change in middle section temperature,  $T_5$  (control loop 3)

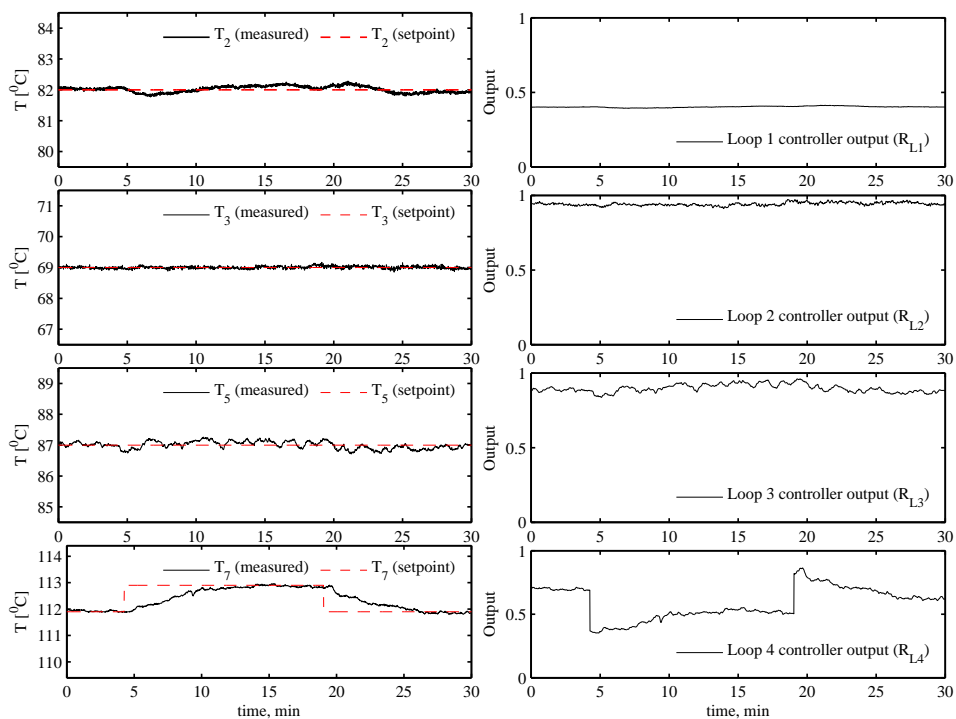


Figure 4.9: Experimental Run 5:  $\pm 1$  [ $^{\circ}\text{C}$ ] setpoint change in bottom section temperature  $T_7$  (control loop 4)



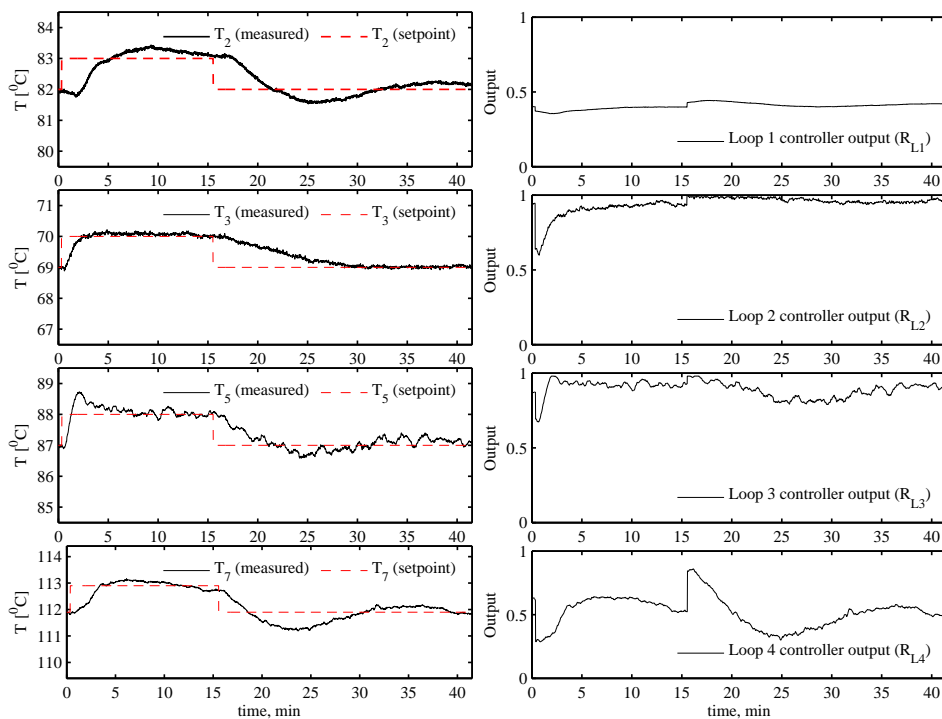


Figure 4.10: Experimental Run 6: Simultaneous change in all four temperature setpoints

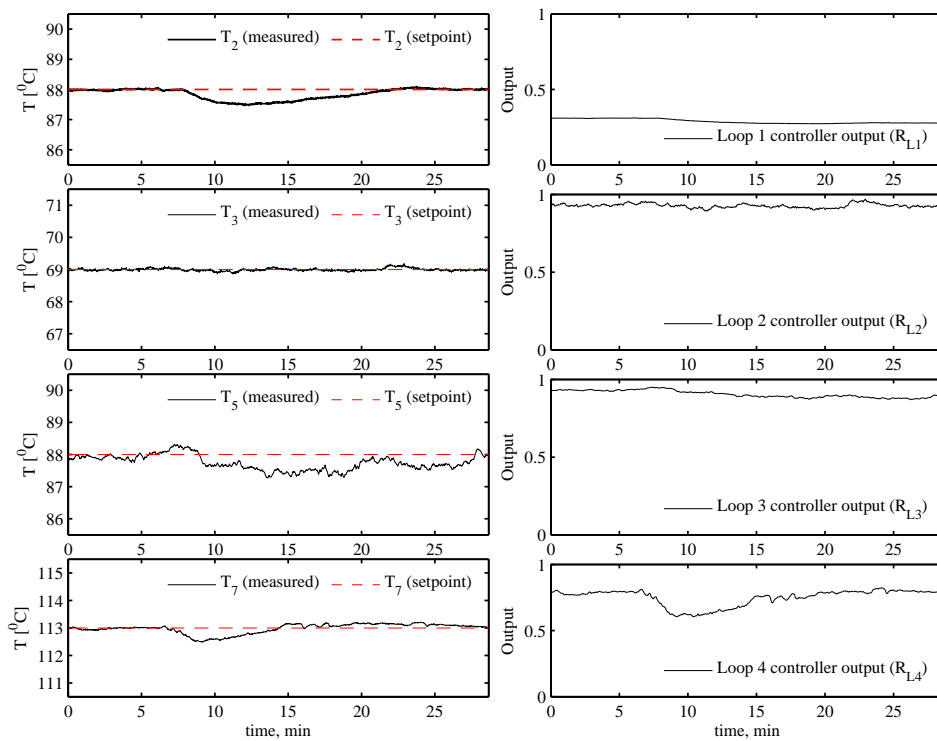


Figure 4.11: Experimental Run 7: +20 % feed rate disturbance (at  $t=5$  min)

## 4.5. Steady state experiments and comparison with simulation 65

flow affects directly the molar difference between the boilup (V) and liquid reflux (L) in the entire column.

Figures 4.8 and 4.9 (runs 4 and 5) plot show similar setpoint changes in loops 3 and 4, respectively, and these changes are handled well without interactions with other loops. Figure 4.10 (run 6) shows simultaneous changes in the setpoint for all the four loops, which are also handled reasonably well.

Finally, Figure 4.11 (run 7) shows the response for an increase in feed rate from 3 liters/hr to 3.6 liters/hr (+20%). This disturbance can also be handled well and the controlled-temperatures are brought back to their setpoints in about 30 minutes.

## 4.5 Steady state experiments and comparison with simulations

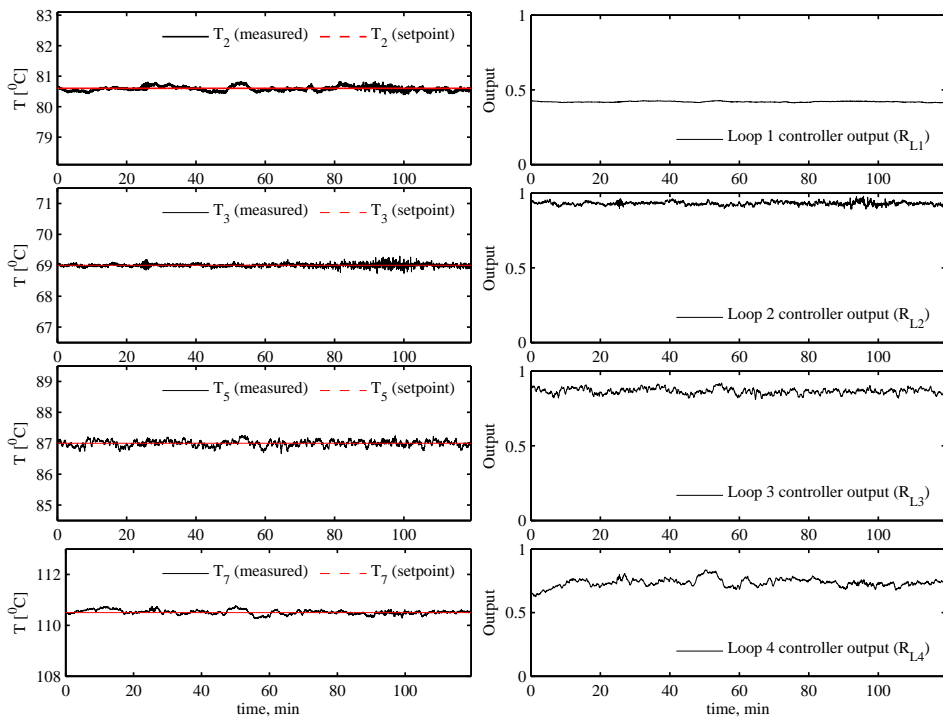


Figure 4.12: Experimental Run 8: steady state operation ( $T_{2S} = 80.6$  °C,  $T_{3S} = 69$  °C,  $T_{5S} = 82$  °C &  $T_{7S} = 110.2$  °C)

In order to study the steady-state behavior, experimental runs 8-12 were

carried out with constant temperature setpoints. For runs 9-12, samples of the feed and products were collected and analyzed using High-performance liquid chromatography (HPLC). Figure 4.12 (run 8) shows a typical response when the column is “steady” for a period of 2 hours, with all the four temperature loops closed. All the four temperatures can be maintained at their respective setpoints. The steady-state results for run 9-12 are summarized in Table 4.3 (compositions) and Table 4.4 (controller outputs  $\equiv$  plant inputs).

We now want to compare the steady-state experimental results with a standard equilibrium stage distillation model. The vapor-liquid equilibria is modelled using the Wilson model for the liquid phase and the vapor is assumed to be ideal. We use the constant molar overflow assumption, which is reasonable for our mixture (See Appendix for details of the dynamic model, but note that, we have compared only the steady state experiments with the model).

To match the experimental steady state data, we can adjust the following degrees of freedom in the model:

1. theoretical number of stages (we use a fixed value for all experiments)
2. boilup ( $V/F$ )
3. feed composition
4. liquid split ratio ( $R_{L1}$ )
5. vapor split ratio ( $R_V$ )
6. distillate product split ratio ( $R_{L2}$ )
7. upper side product split ratio ( $R_{L3}$ )
8. lower side product split ratio ( $R_{L4}$ )

The degrees of freedom are adjusted for each experiment, except for the theoretical number of stages in the sections. The number of theoretical stages was based on experimental estimation of height equivalent of a theoretical plate (HETP). For the estimation of HETP, a total reflux experiment (run 13) was performed with only two components, namely methanol and ethanol. The liquid split ratio ( $R_{L1}$ ) was used to control temperature difference ( $\Delta T = T_2 - T_5$ ) between the prefractionator (section 2) and the main column (section 5). The temperatures ( $T_2 \equiv TP5, T_5 \equiv TM8$ ) chosen were approximately at the same height (and of packing) from the reboiler. The setpoint of this controller was then set to *zero* so that the compositions

## 4.5. Steady state experiments and comparison with simulation 67

---

should be the same on both sides. The system was allowed to stabilize and samples were taken at the location of side products (S1 and S2) for analysis. Figure 4.13 shows the stable run during this experiment with the controlled-variable ( $\Delta T$ ) and controller output. The molar composition of methanol was about 75 % and 21 % in samples S1 and S2, respectively. The graphical McCabe Thiele method and Fenske equation both give the number of theoretical stages to be about 4. The height of packing between the sample points is 0.65 meters and, the HETP for our packing was thus estimated to be about 16 cm. The value of HETP = 16 cm was used to find the number of stages in each section which gives 17 (7+10) theoretical stages for the prefractionator and 22 (4+4+4+4+5+reboiler) for the main column.

Based on the power input of 2 kW to the reboiler, we can obtain the boilup (V/F) for use in the model. The feed composition is available from HPLC measurements. Finally, the liquid split ratio ( $R_{L1}$ ) was obtained directly from the experiments.

With the first *four* degrees of freedom determined (i.e., theoretical number of stages, boilup, feed composition and liquid split ratio), we are left with *four* more degrees of freedom (vapor split ratio  $R_V$ , distillate product split ratio  $R_{L2}$ , upper side product split ratio  $R_{L3}$  and lower side product split ratio  $R_{L4}$ ), which are adjusted to match the following experimental values from the steady state runs:

1. mole fraction of methanol in the top product (D)
2. mole fraction of ethanol in the upper side product (S1)
3. mole fraction of propanol in lower side product (S2)
4. a temperature in section 2 (TP5) of the prefractionator

This procedure for data fitting is used for experimental runs 9-12. Table 4.3 compares the product composition from experiments and simulations and Table 4.4 gives the corresponding values of the four degrees of freedom. Since the mole fractions of the main components in the top product (D), upper side product (S1) and lower side product (S2) are matched directly, there is an exact match of these compositions. But additionally, the key impurities in the side products (S1 & S2), which were not matched individually, show a very good fit. For example, in experimental run 9, the mole fraction of methanol in S1 from the experiment is 31.8%, while from the simulation it is 34.2%. The key impurities (propanol and n-butanol) of the lower side product (S2) also show a good fit. From Table 4.4, we see

that the simulated values of the four degrees of freedom ( $R_{L1}$ ,  $R_{L2}$ ,  $R_{L3}$  and  $R_{L4}$ ) which were obtained by matching the compositions, agree well with the experimental values.

Figure 4.14 compares the temperatures from the model (lines) and the experiments (points). The  $y$ -axis in Figure 4.14 shows the theoretical stages in the model, numbered from top (1) to bottom (22). The  $x$ -axis shows the corresponding temperatures. The locations of temperature probes in the experimental setup with respect to the theoretical stages in the model are not precise and were not adjusted, but nevertheless we find that the match is good.

In summary, we have a very good agreement between the experimental steady-state data and the equilibrium stage model.

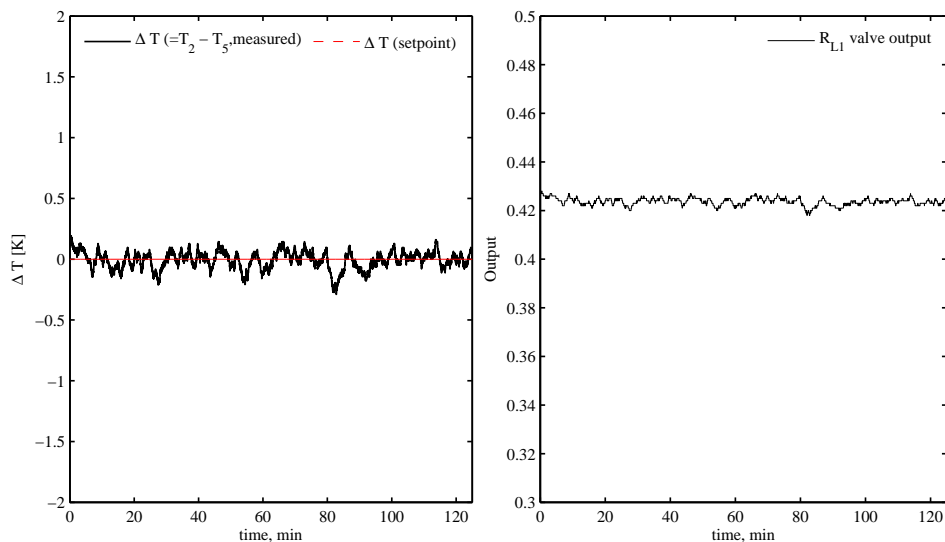


Figure 4.13: Experimental Run 13: total reflux conditions for determining the HETP.

## 4.6 Discussion

### 4.6.1 Practical issues related to operation

The operation of the experimental column had some problems. Early on, the column was very difficult to operate and stabilize with little material reaching the top of the column [24]. On the intuition that suggested that this was due to insufficient boilup, the reason turned out to be vapor leaking from

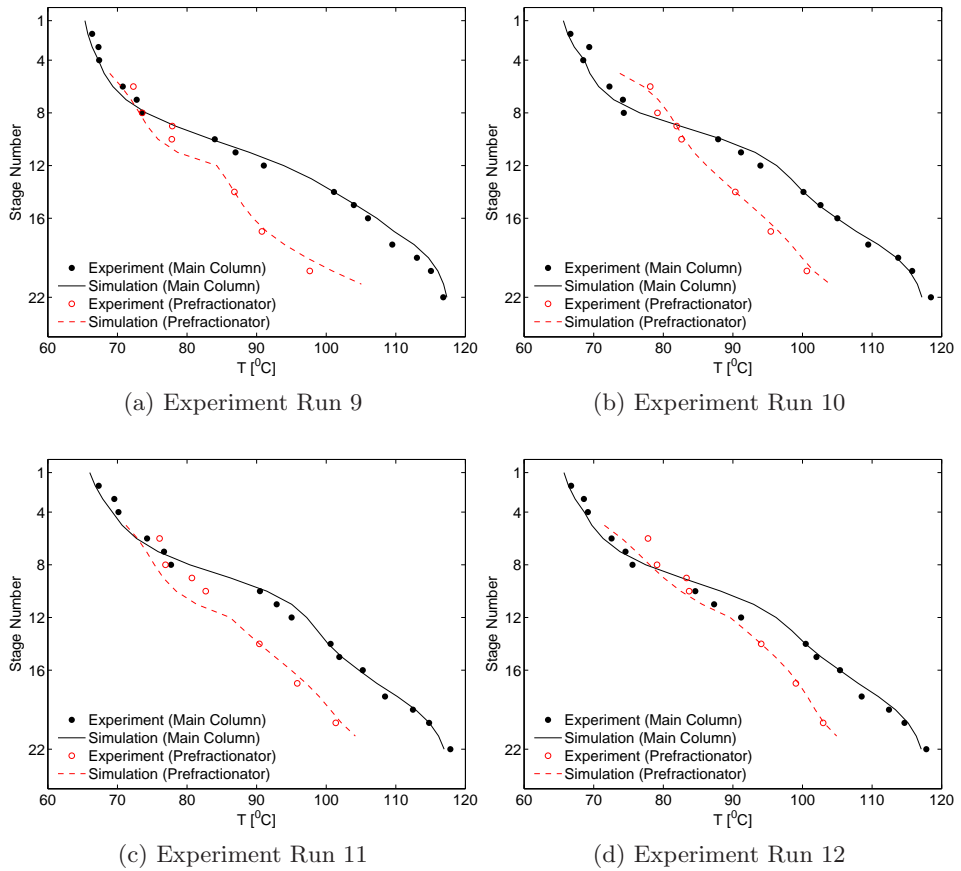


Figure 4.14: Steady state experimental and simulated temperature profiles in experiments 9-12

the product valves on the side streams. To resolve this issue, we installed an additional small manual valve and a solenoid valve (in series) downstream of the swinging funnels, just outside the column. The opening of the manual valve was adjusted to ensure that there was always a liquid hold up in the glass downcomer under the swinging funnel. The additional solenoid valves and the swinging funnel open and close simultaneously during the cycle. Alternatively, an externally placed liquid seal in the product withdrawal line would have stopped any vapor from “leaking” by providing a hydraulic head to counter the small positive pressure in the column.

#### 4.6.2 Plant-model mismatch

As mentioned, the equilibrium stage model fits well with the experiments. The mole fraction of butanol in the bottoms product was, however, smaller than that in the model in all the runs. One reason for this may be that we have no bottom product (B), meaning that the bottom product accumulates in the reboiler, and therefore it will take a very long time to reach the steady compositions in the reboiler.

The experimental data also had some uncertainties. The experimental results for example in Figure 4.12, show some noise in the temperatures. This can be just instrument noise or process noise due to the use of swinging funnels and not continuous valves with pumps. The composition measurements with HPLC also have some measurement error. There were some biases in temperature probes. These were calibrated using their measurements in cold column conditions. Some probes showed up to 3 °C of error from the room temperature and their measurements were accordingly corrected.

Another source of error can be the column pressure drop, which was neglected in the model. The total pressure drop under normal operation of the column was about 16 *cm* of water or about 0.016 bar (measured using a U-tube manometer).

#### 4.6.3 Optimal operation

From the experimental data and the model in Table 4.3, the purities of top and bottom products are relatively high (up to about 96% and 95 %), while the purities of the side products are low (about 55% and 89 %). Is this the best one can achieve? To answer this question, we used the model to compare the four experimental steady-state runs to operations under two “optimal” modes.



In mode I, for a given boilup and with the purity of top product ( $x_{MeOH}^D$ ) and bottom product ( $x_{BuOH}^B$ ) specified, the objective is to maximize the sum of the purities of the side products. In mode II, also for a given boilup, the objective is to maximize the sum of purities of all the products.

The two optimization problems (mode I and mode II) are defined in more detail in Table 4.5 and the results are given in Table 4.6. Table 4.6 compares the product purities in the four experimental runs with the “optimal” values in modes I and II. In mode I, where the top and bottom purities are fixed, we find that some minor improvement can be made in the side stream purities. The largest difference is in experimental run 11, where the S1 purity can be improved from 51.5 % to 65.4 %. On the other hand, in runs 10, 11 and 12, the S2 purity is actually better in the experiment.

In mode II, even though there was an improvement on the sum of the purities of four products, the purity of the end products (D and B) decreased from the base case. The purity of the upper side products (S1) increased in all the scenarios while the purity of lower side product (S2) decreased in experimental runs 11 and 12.

From the results in Table 4.6, we conclude that the experimental results are close to “optimal” operations, as described by mode I or mode II. This shows that the temperature setpoint adjustment procedure described in the start-up procedure works well.

## 4.7 Conclusions

The experimental studies verify that stable operation of the four product Kaibel column can be achieved with the 4-point temperature control scheme shown in Figure 4.3c. The control structure gave good servo performance for setpoint changes as well as good regulation for a +20 % feed disturbance. The same control structure was adopted during the cold start-up of the column and with the proposed procedure for adjusting the temperature setpoints, it was possible to use only temperature measurements to approach the desired steady-state composition, that is, without needing on-line composition measurements.

An equilibrium stage model was fitted to the experiments. The fitted model gave good match with the experiments. This suggests that equilibrium staged models can be used to study the operation and design of such columns.

### 4.7.1 Acknowledgement

Ms. Kathinka Qvenild Lystad, Engineer, SINTEF Materials and Chemistry, assisted with the analysis of samples using HPLC.

## Appendix

### 4.7.2 Model Details

The Kaibel column under study is modelled in Matlab using seven column sections [24]. The model is available at the home page of the corresponding author, S. Skogestad. We assume constant pressure, equilibrium on all stages, a total condenser, constant molar flows and linearized liquid dynamics. The model equations for a column sections are:

1. Total material balance on stage 'i'

$$\frac{d}{dt}M_i = L_{i+1} - L_i + V_{i-1} - V_i$$

where,  $M_i$  is molar holdup on stage 'i'; tray numbering is from bottom to top.

$L_i$  is liquid molar flow and  $V_i$  is total molar vapor flow from a stage 'i'

2. component balance on stage 'i' for a component 'j'

$$\frac{d}{dt}(x_{j, i} M_i) = L_{i+1} x_{j, i+1} + V_{i-1} y_{j, i-1} - L_i x_{j, i} - V_i y_{j, i}$$

where,  $x_{j, i}$  is mole fraction of component 'j' in liquid phase on stage 'i'

3. Vapor-Liquid Equilibria

Ideal vapor phase is assumed and the Wilson model is used for the liquid phase activity coefficients ( $\gamma_i$ ). The VLE is describe by the following equations:

$$P y_j = x_j \gamma_j P_j^S$$

where, P is the total pressure and saturation vapor pressures ( $P^S$ ) is given by Antoine equation

$$\log P_j^S = A_j - \frac{B_j}{T_i + C_j}$$

where A, B and C are Antoine constants and  $T_i$  is absolute temperature of a stage 'i'.

#### 4. Constant molar flow in a section

$$V_{i-1} = V_i = V_{i+1}$$

This assumption holds well since the four components have similar heats of vaporization (35.3, 38.5, 41.8 and 43.1 *kJ/kmol*) at their normal boiling points.

#### 5. Linearized flow dynamics

$$L_i = L_{0,i} + (M_i - M_{0,i})/\tau + V_{i-1} - V_{0,i-1}$$

$L_0$ ,  $V_0$  and  $M_0$  are nominal values for molar liquid flows, molar liquid flows and molar hold up, respectively at time,  $t=0$ ;  $\tau = 0.063$  *min*.

## References

- [1] Adrian, T., Schoenmakers, H., Boll, M., 2004. Model predictive control of integrated unit operations: Control of a divided wall column. *Chemical Engineering and Processing* 43 (3), 347–355.
- [2] Buck, C., Hiller, C., Fieg, G., 2011. Applying model predictive control to dividing wall columns. *Chemical Engineering & Technology* 34 (5), 663–672.
- [3] Dejanovic, I., Matijaevic, L., Halvorsen, I., Skogestad, S., Jansen, H., Kaibel, B., Olujić, ., 2011. Designing four-product dividing wall columns for separation of a multicomponent aromatics mixture. *Chemical Engineering Research and Design* 89 (8), 1155 – 1167.
- [4] Dejanovic, I., Matijašević, L., Olujić, Z., 2010. Dividing wall column, a breakthrough towards sustainable distilling. *Chemical Engineering and Processing: Process Intensification* 49 (6), 559 – 580.
- [5] Fonyó, Z., 1974. Thermodynamic analysis of rectification. i. reversible model of rectification. *International Chemical Engineering* 14 (1), 18–26.

- [6] Fonyó, Z., 1974. Thermodynamic analysis of rectification. ii. finite cascade models. *International Chemical Engineering* 14 (2), 203–210.
- [7] Ghadrzan, M., Halvorsen, I. J., Skogestad, S., 2011. Optimal operation of Kaibel distillation columns. *Chemical Engineering Research and Design* 89 (8), 1382 – 1391, special Issue on Distillation & Absorption.
- [8] Halvorsen, I. J., Skogestad, S., 2003. Minimum energy consumption in multicomponent distillation. 3. more than three products and generalized Petlyuk arrangements. *Industrial & Engineering Chemistry Research* 42 (3), 616–629.
- [9] Kaibel, G., 1984. A distillation column for fractionating multicomponent feed (German Title: Destillationskolonne zur destillativen Zerlegung eines aus mehreren Fraktionen bestehenden Zulaufproduktes), European Patent EP 0 122 367 A2, 1984 (1984); Priority data DE 3302525 (1983).
- [10] Kaibel, G., 1987. Distillation columns with vertical partitions. *Chemical Engineering & Technology* 10 (1), 92–98.
- [11] Kvernland, M., Halvorsen, I. J., Skogestad, S., 2010. Model predictive control of a Kaibel distillation column. *Proceedings of the 9th International Symposium on DYCOPS 2010*, 539–544.
- [12] Ling, H., Cai, Z., Wu, H., Wang, J., Shen, B., 2011. Remixing control for divided-wall columns. *Industrial & Engineering Chemistry Research* 50 (22), 12694–12705.
- [13] Ling, H., Luyben, W. L., 2009. New control structure for divided-wall columns. *Industrial & Engineering Chemistry Research* 48 (13), 6034–6049.
- [14] Mutalib, M. I. A., Smith, R., 1998. Operation and control of dividing wall distillation columns: Part 1: Degrees of freedom and dynamic simulation. *Chemical Engineering Research and Design* 76 (3), 308–318.
- [15] Mutalib, M. I. A., Zeglam, A. O., Smith, R., 1998. Operation and control of dividing wall distillation columns: Part 2: Simulation and pilot plant studies using temperature control. *Chemical Engineering Research and Design* 76 (3), 319–334.

- [16] Niggemann, G., Gruetzmann, S., Fieg, G., 2006. Distillation startup of fully thermally coupled distillation columns: theoretical examination Proceedings of the 8th Distillation & Absorption, IChemE Symp. Series; Vol. 152, 800–808.
- [17] Niggemann, G., Hiller, C., Fieg, G., 2010. Experimental and theoretical studies of a dividing-wall column used for the recovery of high-purity products. *Industrial & Engineering Chemistry Research* 49 (14), 6566–6577.
- [18] Olujić, Z., Jdecke, M., Shilkin, A., Schuch, G., Kaibel, B., 2009. Equipment improvement trends in distillation. *Chemical Engineering and Processing: Process Intensification* 48 (6), 1089–1104.
- [19] Petlyuk, F., Platonov, V., 1964. Thermodynamically reversible multi-component distillation. *Khimicheskaya Promyshlennost* (10), 723–726 (In Russian).
- [20] Petlyuk, F., Platonov, V., Avetlyan, V., 1966. Optimum arrangements in the fractionating distillation of multicomponent mixtures. *Khimicheskaya Promyshlennost* 42 (11), 865–868.
- [21] Petlyuk, F., Platonov, V., Slavinskii, D., 1965. Thermodynamically optimal method for separating multicomponent mixtures. *International Chemical Engineering* 5 (3), 555–561.
- [22] Rewagad, R. R., Kiss, A. A., 2012. Dynamic optimization of a dividing-wall column using model predictive control. *Chemical Engineering Science* 68 (1), 132 – 142.
- [23] Skogestad, S., 2003. Simple analytic rules for model reduction and pid controller tuning. *Journal of Process Control* 13 (4), 291–309.
- [24] Strandberg, J., 2011. Optimal operation of dividing wall columns. Ph.D. thesis, Norwegian University of Science and Technology, Department of Chemical Engineering, Trondheim, Norway.
- [25] Strandberg, J., Skogestad, S., 2006. Stabilizing control of an integrated 4-product Kaibel column. Proceedings of IFAC International Symposium on Advanced Control of Chemical Processes (ADCHEM 2006), Gramado, Brazil 2, 623–628.
- [26] van Diggelen, R. C., Kiss, A. A., Heemink, A. W., 2010. Comparison of control strategies for dividing-wall columns. *Industrial & Engineering Chemistry Research* 49 (1), 288–307.

Table 4.3: Steady state experimental and simulated compositions (in mol %) for runs 9-12

Experiment Run 9									
	Feed	D		S1		S2		B	
comp	exp & sim	exp	sim	exp	sim	exp	sim	exp	sim
methanol	<b>21.4</b>	<b>96.6</b>	<b>96.6</b>	31.8	34.2	0	1.3	0	0
ethanol	<b>15.4</b>	3.4	3.4	<b>55.4</b>	<b>55.4</b>	16.8	15.4	0	0
propanol	<b>21.4</b>	0	0	12.7	10.3	<b>75.0</b>	<b>75.0</b>	7.4	1.8
butanol	<b>41.7</b>	0	0	0	0	8.2	8.3	92.6	98.2
Experiment Run 10									
	Feed	D		S1		S2		B	
comp	exp & sim	exp	sim	exp	sim	exp	sim	exp	sim
methanol	<b>20.4</b>	<b>94.9</b>	<b>94.9</b>	29.9	27.4	0	0.6	0	0
ethanol	<b>27.4</b>	5.1	5.1	<b>51.2</b>	<b>51.2</b>	5.9	6.6	0	0
propanol	<b>28.5</b>	0	0	18.9	21.3	<b>87.5</b>	<b>87.5</b>	4.6	2.43
butanol	<b>23.7</b>	0	0	0	0	6.6	5.3	95.4	97.6
Experiment Run 11									
	Feed	D		S1		S2		B	
comp	exp & sim	exp	sim	exp	sim	exp	sim	exp	sim
methanol	<b>20.4</b>	<b>92.7</b>	<b>92.7</b>	17.3	14.8	0	0.2	0	0
ethanol	<b>17.6</b>	7.3	7.3	<b>51.5</b>	<b>51.5</b>	5.4	4.6	0	0
propanol	<b>26.7</b>	0	0	31.2	33.5	<b>89.6</b>	<b>89.6</b>	6.7	3.1
butanol	<b>35.3</b>	0	0	0	0.1	4.9	5.6	93.3	96.9
Experiment Run 12									
	Feed	D		S1		S2		B	
comp	exp & sim	exp	sim	exp	sim	exp	sim	exp	sim
methanol	<b>16.3</b>	<b>94.4</b>	<b>94.4</b>	26.3	22.3	0	0.5	0	0
ethanol	<b>19.0</b>	5.6	5.6	<b>56.3</b>	<b>56.3</b>	10.1	7.3	0	0
propanol	<b>28.3</b>	0	0	17.3	21.3	<b>86.3</b>	<b>86.3</b>	6.4	2.7
butanol	<b>36.4</b>	0	0	0	0	3.5	5.8	93.6	97.2

Table 4.4: Degree of freedom in the four experiments 9-12

Degree of freedom	Run 9		Run 10		Run 11		Run 12	
	exp	sim	exp	sim	exp	sim	exp	sim
R <sub>L1</sub>	<b>0.31</b>	<b>0.31</b>	<b>0.15</b>	<b>0.15</b>	<b>0.25</b>	<b>0.25</b>	<b>0.22</b>	<b>0.22</b>
R <sub>L2</sub>	0.93	0.95	0.98	0.98	0.93	0.95	0.96	0.97
R <sub>L3</sub>	0.94	0.90	0.72	0.81	0.81	0.86	0.83	0.88
R <sub>L4</sub>	0.75	0.87	0.83	0.91	0.90	0.91	0.86	0.88
R <sub>V</sub>	-	0.39	-	0.30	-	0.35	-	0.32

Table 4.5: Operation under two optimal modes <sup>a</sup>

	Mode I	Mode II
Objective	$J = x_{EtOH}^{S1} + x_{PrOH}^{S2}$	$J = x_{MeOH}^D + x_{EtOH}^{S1} + x_{PrOH}^{S2} + x_{BuOH}^B$
Degrees of freedom	Liquid split ratio, R <sub>L1</sub> Distillate split ratio, R <sub>L2</sub> Upper side product split ratio, R <sub>L3</sub> Lower side product split ratio, R <sub>L4</sub> Vapor split ratio, R <sub>V</sub>	R <sub>L1</sub> R <sub>L2</sub> R <sub>L3</sub> R <sub>L4</sub> R <sub>V</sub>
Constraints	boilup = nominal feed rate = nominal feed composition = nominal feed liquid fraction = nominal $x_{MeOH}^D = \text{nominal}$ $x_{BuOH}^B = \text{nominal}$	boilup = nominal feed rate = nominal feed composition = nominal feed liquid fraction = nominal

<sup>a</sup> Remaining degrees of freedom are used for liquid and vapor inventory control, hence are not available as degrees of freedom for optimization. The bottoms rate and distillate flow are consumed for level control of reboiler and condenser, respectively; Condenser duty is consumed for pressure control

Table 4.6: Comparison of experiments 9-12 with optimal operation in mode I (maximize sum of the purities of side products) and mode II (maximize sum of the purities of all the products).

Experiment Run 9												
comp	D			S1			S2			B		
	exp	mode		exp	mode		exp	mode		exp	mode	
		I	II		I	II		I	II		I	II
methan.	96.6	96.6	89.7	34.2	28.9	13.0	1.3	0.7	0.4	0.0	0.0	0.0
ethanol	3.4	3.4	10.2	55.4	52.9	71.2	15.4	10.1	13.4	0.0	0.0	0.0
propanol	0.0	0.0	0.0	10.3	18.1	15.9	75.0	80.8	82.2	1.8	1.8	3.5
butanol	0.0	0.0	0.0	0.0	0.1	0.0	8.3	8.4	4.0	98.2	98.2	96.5
Experiment Run 10												
comp	D			S1			S2			B		
	exp	mode		exp	mode		exp	mode		exp	mode	
		I	II		I	II		I	II		I	II
methan.	94.9	94.9	94.6	27.4	29.2	27.1	0.6	0.7	0.6	0.0	0.0	0.0
ethanol	5.1	5.1	5.3	51.2	53.6	53.6	6.7	8.6	7.7	0.0	0.0	0.0
propanol	0.0	0.0	0.0	21.4	17.1	19.2	87.5	85.5	88.0	2.4	2.4	3.5
butanol	0.0	0.0	0.0	0.1	0.1	0.0	5.3	5.1	3.6	97.6	97.6	96.5
Experiment Run 11												
comp	D			S1			S2			B		
	exp	mode		exp	mode		exp	mode		exp	mode	
		I	II		I	II		I	II		I	II
methan.	92.7	92.7	92.9	15.3	18.3	18.8	0.2	0.5	0.5	0.0	0.0	0.0
ethanol	7.3	7.3	7.1	51.5	65.4	64.2	4.4	11.7	10.9	0.0	0.0	0.0
propanol	0.0	0.0	0.0	33.0	16.2	16.9	89.6	83.2	84.7	3.2	3.2	3.8
butanol	0.0	0.0	0.0	0.1	0.0	0.0	5.7	4.6	3.9	96.8	96.8	96.2
Experiment Run 12												
comp	D			S1			S2			B		
	exp	mode		exp	mode		exp	mode		exp	mode	
		I	II		I	II		I	II		I	II
methan.	94.4	94.4	90.1	22.3	23.3	14.5	0.5	0.7	0.4	0.0	0.0	0.0
ethanol	5.6	5.6	9.9	56.3	60.3	69.8	7.3	10.4	11.9	0.0	0.0	0.0
propanol	0.0	0.0	0.0	21.3	16.4	15.6	86.3	83.6	83.6	2.8	2.8	4.0
butanol	0.0	0.0	0.0	0.1	0.0	0.0	5.9	5.4	4.0	97.2	97.2	96.0



## Chapter 5

# Active vapor split control for dividing-wall columns

### 5.1 Introduction

Dividing-wall distillation columns such as Petlyuk arrangements and the Kaibel column, shown in Figure 5.1 offer large capital and energy saving potentials compared to conventional schemes [6, 7, 14]. Their control and operations, however, remains a challenge. For three-product separation, the energy savings can be up to 30 % using a standard dividing-wall (Petlyuk) column with a single side stream (Figure 5.1a). The Kaibel column with two side streams (Figure 5.1b) can give up to 40 % energy savings for four-product separation. However, the energy saving potential can be lost if the column is operated away from the optimum vapor split ratio (see, Figure 5.2). Thus, the flexibility in operation of such systems at minimum energy over a large range of feed conditions or product specifications, can be restricted by the absence of an active vapor split during operation.

Dividing-wall column have been successfully implemented industrially, mainly at BASF [2]. In the academic community, several works have been reported on operation and control of three-product Petlyuk columns [8–13, 15]. However, all earlier works exclude the use of vapor split as a degree of freedom. Therefore, Agrawal and Fidkowski [1] suggested as an alternative to use a vapor side draw. Another alternative is to use the feed enthalpy as a degree of freedom, where the vapor fraction or degree of sub-cooling in the feed is varied to achieve optimum operation [5]. However, these solutions usually come with a penalty on energy requirement. The vapor split however, comes with no sub-optimal operation with respect to energy requirement. Therefore, in this work, we consider the vapor split which is

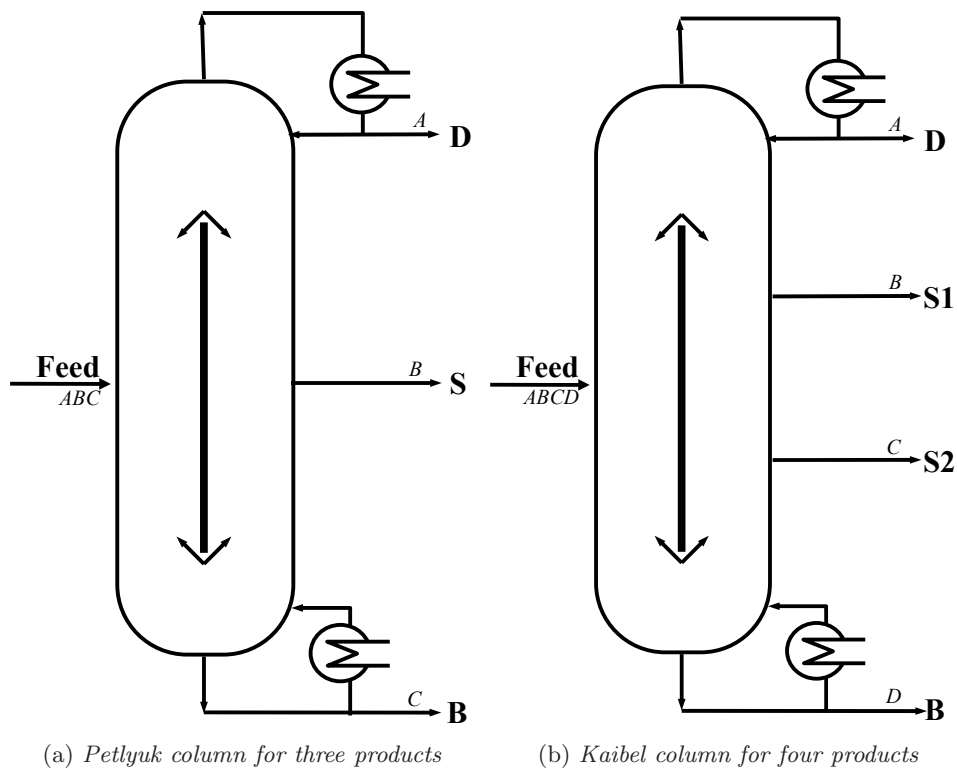
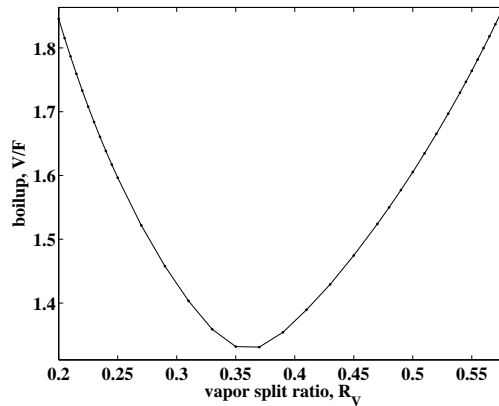


Figure 5.1: Dividing-wall columns with prefractionator section to the left of the dividing wall and “main” column section to the right.

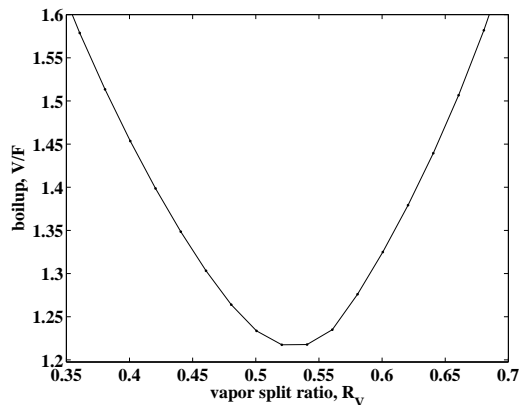


(a) *Three-product Petlyuk column: Boilup (V/F) vs Vapor Split Ratio ( $R_V$ )*

Data: Equimolar feed of methanol, ethanol and propanol with zero vapor fraction  
 Purities (mol %): 97.6 % (D), 97.3 % (S); 99.6 % (B)

Stages: 40 in prefractionator and 80 in main column (including top and bottom sections).

Liquid split ( $R_L$ ) has been optimized for each value of Vapor split ( $R_V$ )



(b) *Four-product Kaibel column: Boilup (V/F) vs Vapor Split Ratio ( $R_V$ )*

Data: Equimolar feed of methanol, ethanol, propanol and *n*-butanol with 50 % vapor fraction

Purities (mol %): 98.9 % (D); 98.0 % (S1); 98.0 % (S2); 99.8 % (B)

Stages: 40 in prefractionator and 100 in main column

Liquid split ( $R_L$ ) has been optimized for each value of Vapor split ( $R_V$ )

Figure 5.2: Effect of vapor split ratio ( $R_V$ ) on boilup (V/F) for fixed purity specifications in dividing-wall columns. ( $R_V \equiv$  fraction of vapor boilup that is sent to prefractionator from the main column)

always a potential degree of freedom.

To motivate the need for active vapor split in dividing-wall columns further, we first consider some simulation results. Halvorsen and Skogestad [5] studied steady state optimal operation of three product Petlyuk column. They reported that there may be a narrow operating window with respect to various degrees of freedom for operation of such system at minimum energy. The control system should carefully designed to operate within this range to ensure operation at minimum energy. Further, this operating window may change in presence of various disturbances such as feed composition and feed vapor fraction.

We confirm these results with a simulation study on a three-product Petlyuk column separating equimolar saturated liquid feed of methanol, ethanol and propanol (Figure 5.2a). The Wilson model is used for the vapor-liquid equilibria and we assume constant molar overflow. For the given purity specifications, the boilup is minimum ( $V/F=1.33$ ) for a vapor split ratio ( $R_V$ ) of 0.37. In Figure 5.2a, we plot the minimum boilup ( $V/F$ ) required as the vapor split ratio is fixed at values different from its optimum value of 0.37. By “minimum”, we mean that the liquid split ( $R_L$ ) has been adjusted so that the boilup is minimized for each  $R_V$ .

A similar simulation study for a four-product Kaibel column is shown in Figure 5.2b. We study an equimolar feed of methanol, ethanol, propanol and *n*-butanol with 50 % vapor fraction. Again the Wilson model is used for the vapor-liquid equilibria and we assume constant molar overflow. The boilup ( $V/F$ ) is minimum for an optimum vapor split ratio of 0.52 and again increases in both directions. In summary, the simulation results in Figure 5.2 shows that the energy usage (boil-up,  $V/F$ ) is sensitive to the value of  $R_V$ , and this motivates the need for introducing the vapor split ( $R_V$ ) as a degree of freedom during operation. Ghadrhan et al. [4] concluded similarly that there is a narrow operating window for energy optimal operation of a four-product dividing-wall column with respect to vapor split for a given purity specification.

In this work we demonstrate the use of direct active manipulation of the vapor split using an experimental four-product Kaibel arrangement (Figure 5.3). The experimental column consists of separate sections Figure 5.3a, but it is thermodynamically equivalent to a single-shell dividing-wall implementation (Figure 5.1b) as proposed by Kaibel[7]. Use of dividing-wall is usually the preferred solution at industrial scale because of lower capital costs. The schemes in Figure 5.3 are thermodynamically equivalent if the heat exchange across the wall is negligible and most industrial practitioners disregard this effect.

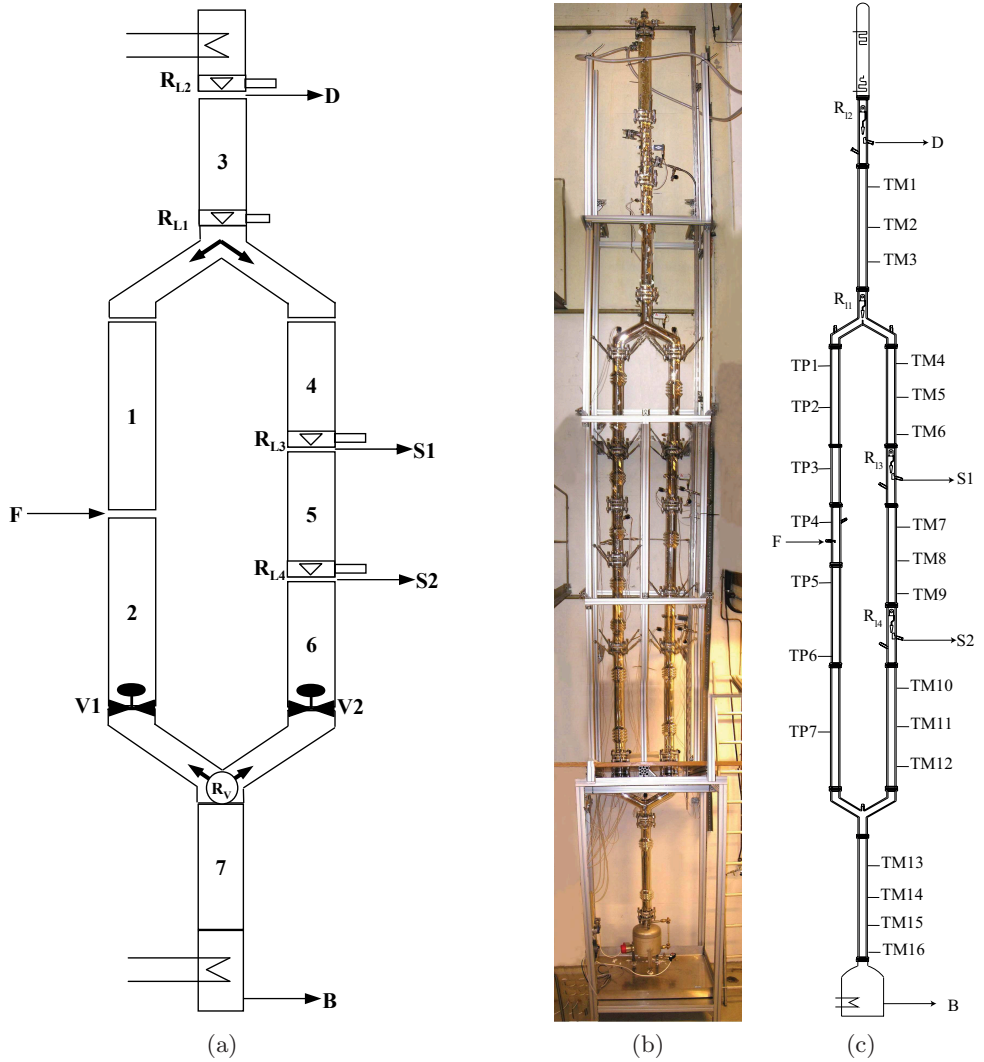
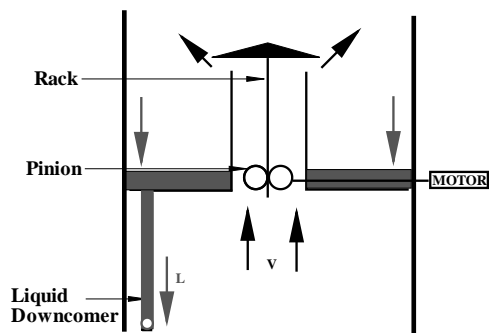


Figure 5.3: (a) Schematic of four-product Kaibel column with adjustable vapor split ratio ( $R_V$ )  
 (b) Picture of the experimental column [17]  
 (c) Location of temperature sensors. [17]



(a) Schematic of the vapor split valve



(b) Picture of the vapor split valves

Figure 5.4: Vapor split valves used for the experiments [17]

## 5.2 Experimental Setup

Figure 5.3 shows a schematic of our experimental column which is thermodynamically equivalent to the dividing-wall arrangement for separation of a feed into four products (D, S1, S2 and B) of desired purity. In Figure 5.3a, the column subsections are numbered for easy reference; Sections 1 and 2 constitute the prefractionator while section 3 to 7 constitute the main column.

In Figure 5.3b, we show a picture of the experimental column [17]. The height of the column is 8 meters and it operates under atmospheric pressure. The column subsections are packed with 6-mm glass Raschig rings. The column sections have packed sections with temperature probes and their locations are shown in Figure 5.3c.

The reboiler is of the kettle type and its power is controlled by voltage to the heater elements through a thyristor. The water-cooled condenser is mounted on top of the column. The condensate returns to the column due to gravity; a part is taken out as top product and the rest forms the liquid reflux. The control setup is implemented in Lab View<sup>TM</sup> on a standard PC.

The liquid reflux split valve  $R_{L1}$  and the valves for the products, D, S1 and S2;  $R_{L2}$ ,  $R_{L3}$  and  $R_{L4}$ , respectively are all swinging funnels. These are controlled by externally placed solenoids. Since these are ON/OFF valves, a continuous output of the PI controller is implemented using pulse width modulation.

The two vapor split valves are made in stainless steel and are operated by externally placed electrical motors using rack and pinion assembly. Figure 5.4a shows a schematic of the valves. There are two such valves, one below section 2 and one below section 6 (denoted V1 and V2 in Figure 5.3a), but they should be operated such that one of them is always fully open. The vapor flow rate through the valve is manipulated by opening and closing a cap that sits on a steel valve seat. There is a liquid downcomer which is needed to allow the liquid to flow against the pressure drop over the valve. The downcomer is designed to ensure that the vapor passes only through the clearance between the cap at the seat.

The circular pinion of each valve is powered by a step motor. The full span of the valve is divided into 150 small steps. In the current setting, the free cross section in the valve is somewhat too large, which results in very small required movements. As will be shown in the section below, the valve can affect the flows only in the first 10 steps. Whilst the performance of the valve could be significantly improved, having such a poor resolution provides an excellent case for demonstrating the effect of feedback, which

we document below.

## 5.3 Experiment

### 5.3.1 Vapor Split valve behavior

The first experiment was designed to test the behavior of the vapor split valves. This was done under total reflux conditions (no feed or products) and with constant liquid split ( $R_{L1}$ ) using only two chemical components, namely methanol and ethanol. After charging the reboiler, the heating was started with a fixed duty of 1.9 kW.

After reaching steady state operation, step changes were made to vapor valve V1 while valve V2 was fully open. The results are shown in Figure 5.5, where we show the effect of these changes on one prefractionator temperature ( $T_2 \equiv TP5$ ) and one main column temperature ( $T_5 \equiv TM7$ ). Any change in the vapor flow rate resulting from changes by the vapor split valve should lead to changes in these two temperatures. The output of the liquid split valve is manually fixed during this run.

When we close valve V1 from 15 steps to 10 steps at around 3 minutes, temperature  $T_2$  starts decreasing gradually while  $T_5$  starts increasing. This indicates, as expected, that less vapor is being sent to the prefractionator, while more vapor is being directed to section 6. At around 7 minutes, V1 is further closed by 5 steps. This gives a more noticeable change in the vapor flows and is clearly indicated by about 1 K drop in  $T_2$  and about 0.6 K temperature increase in  $T_5$ . This change is reversed when valve V1 is opened from 5 steps to 15 at about 13 minutes. A series of changes between 10 steps to 15 steps shows insignificant changes in the two temperatures. At around 33 minutes, V1 is closed from 8 steps to 3 steps. This leads to sharp changes in temperatures  $T_2$  and  $T_5$ . At 37 minutes, the valve V1 is opened from 3 steps to 50 steps. Since the vapor dynamics are very fast, the initial response on the temperatures is very quick, but the steady-state is restored more slowly .

We can conclude from this experiment that only the first 10 steps of the 150 steps are really effective, so the resolution is poor and the valve opening is too large. Nevertheless, we will see that the valve is acceptable for control purposes.

### 5.3.2 Total Reflux experiments

To study the suitability of the valve for feedback control, we performed a set of experiments under total reflux conditions using only two components,



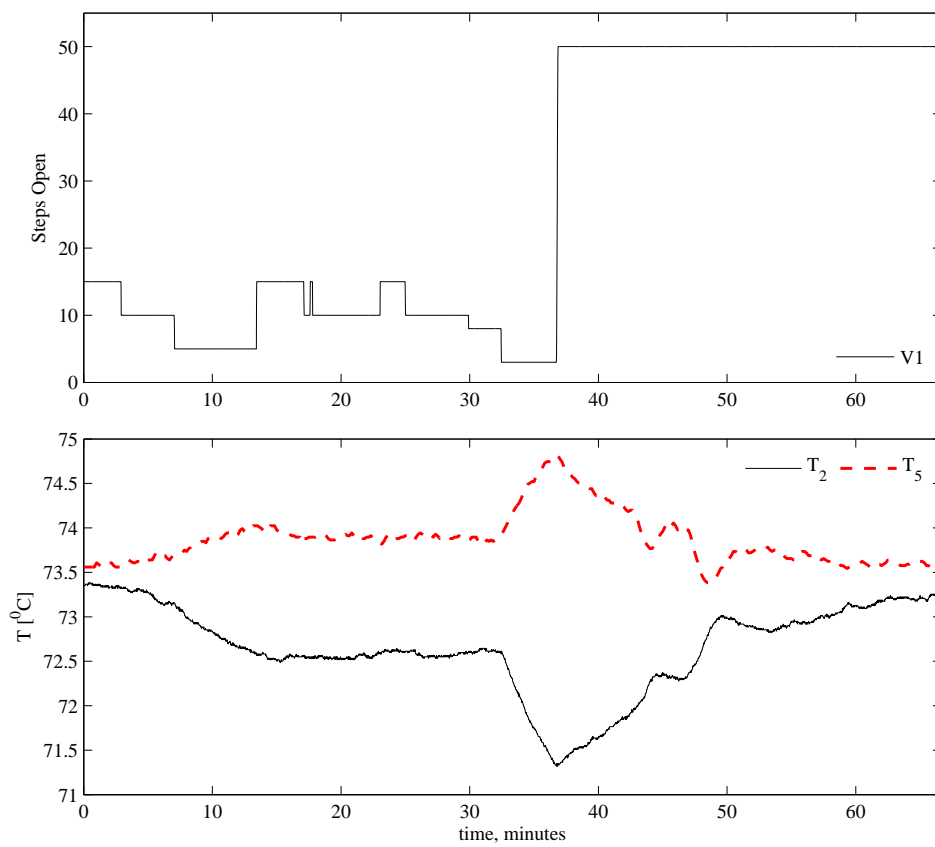


Figure 5.5: Experimental Run: Effect of changing the prefractionator vapor split valve, V1 with valve V2 fully open on prefractionator ( $T_2$ ) and main column ( $T_5$ ) temperatures.

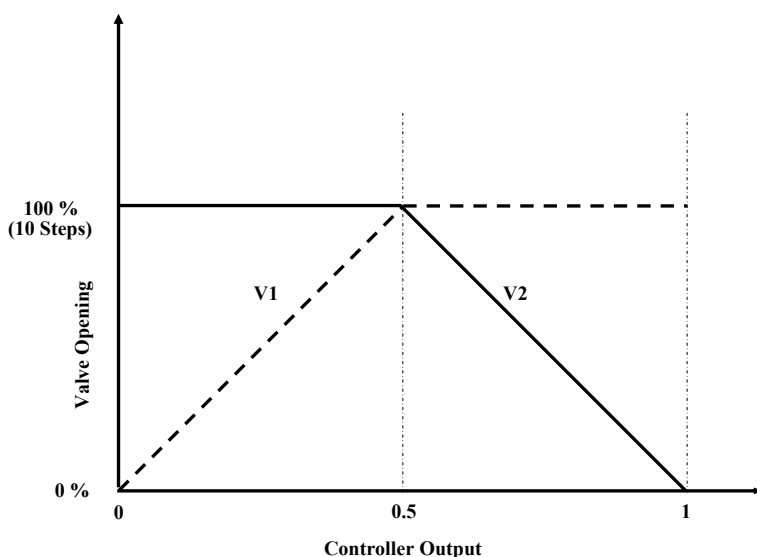


Figure 5.6: Split range logic (SRC) used for the vapor split controller

namely methanol and ethanol, with a fixed duty of 1.9 kW.

To minimize pressure drop, one of the valves should always be open. To ensure this, the valves are controlled using a split range logic as shown in Figure 5.6. For a controller output of 0, valve V1 is closed and valve V2 is fully open, while for a controller output of 0.5, both valves are fully open. Notice that we assume that 10 steps corresponds to a fully open valve.

The vapor split valves are used to control the temperature difference between the prefractionator and the main column,  $\Delta T = T_2 - T_5$  as shown in Figure 5.7. The proportional-integral (PI) controller is tuned using the SIMC rules [16] with the tuning parameter selected to be  $\tau_C = 2$  minutes.

Figure 5.8 shows a series of setpoint changes for  $\Delta T$ . We plot the controlled variable ( $\Delta T$ ) and the controller output ( $R_V$  in the range 0 to 1), which through the split range logic changes the valves (V1 and V2). The figure also shows the two individual temperatures ( $T_2$  and  $T_5$ ), the two valve opening step values (V1 and V2) and the values for the liquid split ratio ( $R_L$  and reboiler duty ( $Q$ )). Note that at any time at least one of the valves V1 or V2 is fully open.

For first 20 minutes the setpoint is unchanged at 0 K and the temperatures are steady. At 23 minutes, the setpoint for  $\Delta T$  is increased to 4 K, which requires increase in the vapor flow to the prefractionator. This setpoint is reached in about 7 minutes without any overshoots. This is followed by a series of setpoint changes which can be tracked as well. At about 100

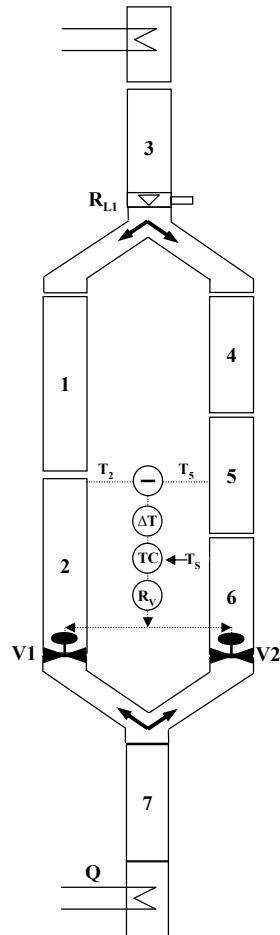


Figure 5.7: Control Structure used for total reflux experiments. Vapor split ( $R_V$ ) is used to control temperature difference between sections 2 and 5 ( $\Delta T = T_2 - T_5$ ;  $T_2 \equiv TP5$  and  $T_5 \equiv TM8$  in Figure 5.3c).

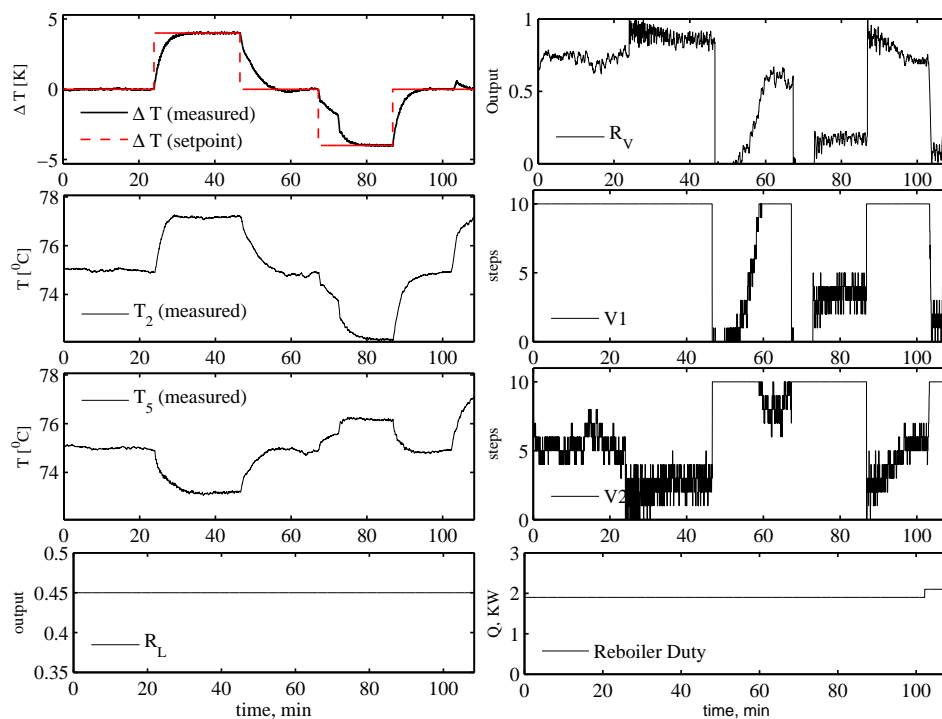


Figure 5.8: Initial experimental run 1: Total reflux operation. Vapor split ( $R_V$ ) is used to control  $\Delta T$  across the wall.

minutes, a disturbance is introduced by increasing the reboiler duty by 0.2 kW. This is shown by an increased difference in temperature by about 0.6 K. But the controller can bring the controlled variable back to the setpoint of 0 K. In summary, we see from Figure 5.8 that the vapor split valves are fully acceptable for closed-loop operation.

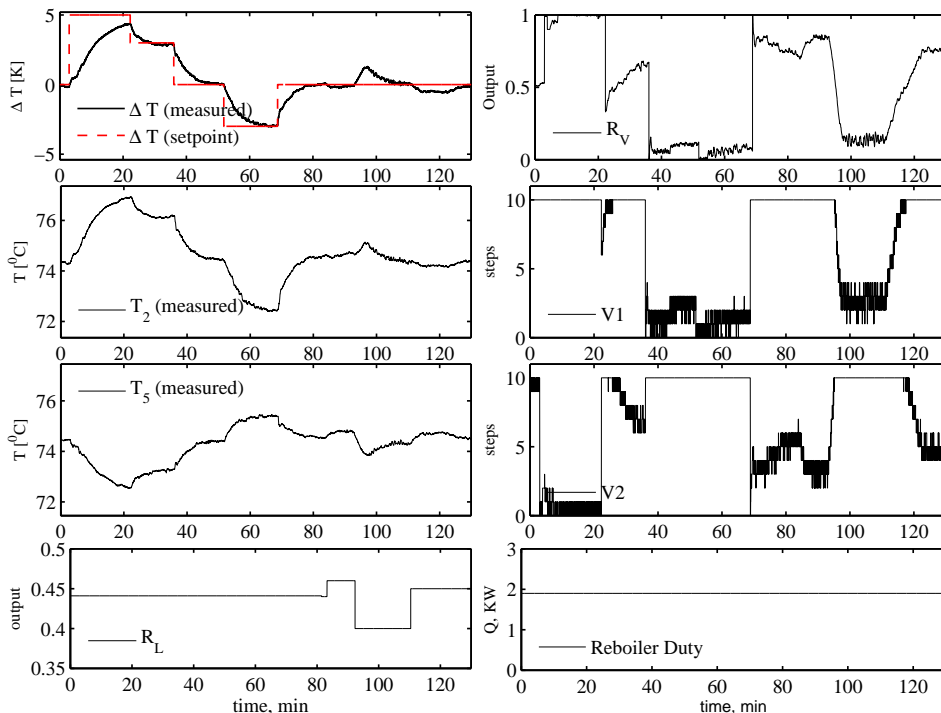


Figure 5.9: Initial experimental run 2: total reflux operation

Figure 5.9 shows another experiment under more difficult conditions. With a large setpoint change for  $\Delta T$  of +5 K at about 3 minutes, the output of the controller saturates and the setpoint can not be reached. The reason is probably that the valve V2 is nearly fully closed. However, when the setpoint is reduced, it can be reached. During last 30 minutes of the run, we also give disturbances by changing the output of the liquid split valve between 0.4 to 0.46. These disturbances can also be handled by the vapor split valve.

Based on these experiments, we conclude that even with rough manipulation of the vapor flow, yields good temperature control when implemented in an appropriate feedback loop.

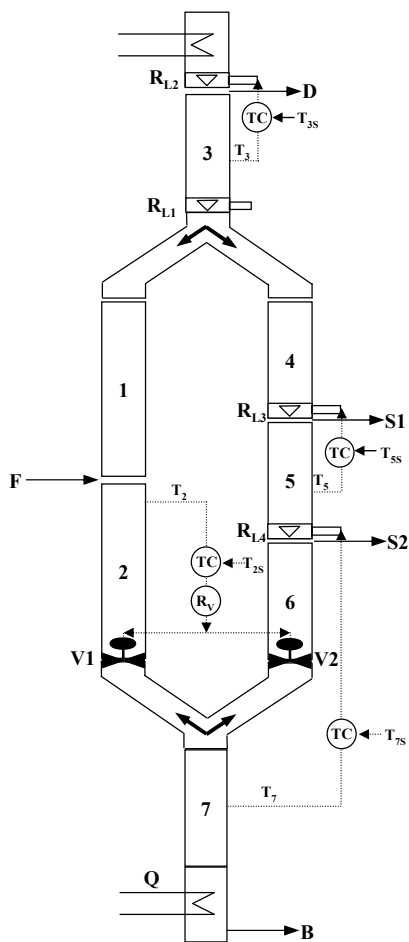


Figure 5.10: 4-point temperature control structure for continuous operation of Kaibel column using active vapor split ( $R_V$ ) for control of prefractionator temperature ( $R_{L,1}$  is kept constant, but could have been used for control for example, of a temperature in top section of prefractionator).

## 5.3.3 4-Product Kaibel Column experiments

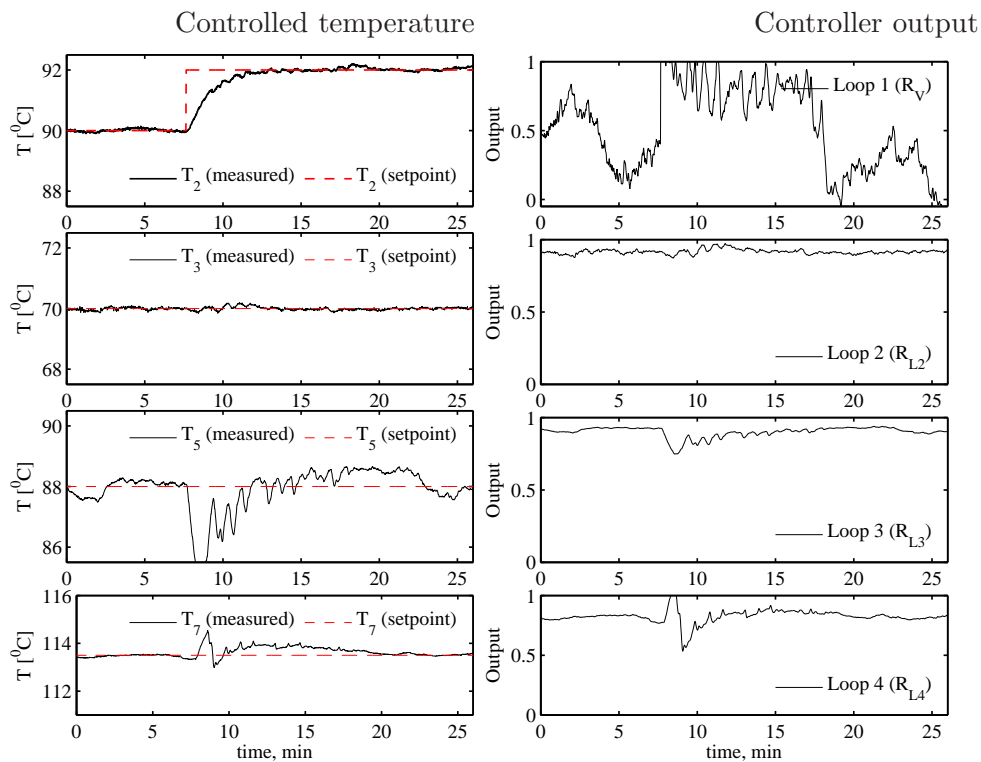


Figure 5.11: Main experimental run 3: Continuous operation of Kaibel column using 4-point temperature control with active vapor split ( $R_V$ ).

The following experiment demonstrates that the vapor split also can be used in practice for continuous operation. Strandberg and Skogestad[18] found in a simulation study that a 4-point temperature control scheme with one temperature controlled in the prefractionator can stabilize the column and as well as prevent “drift” of the composition profiles during operation. Correspondingly, in our previous experimental work [3], we used the liquid split ( $R_{L1}$ ) to control a temperature in prefractionator (with a constant vapor split  $R_V$ ).

Here, we show that the temperature in prefractionator can be controlled equally well using the vapor split  $R_V$  (with a constant liquid split,  $R_{L1}$ ). Figure 5.10 shows the control structure where a sensitive temperature in prefractionator section 2 ( $T_2$ ) is controlled using the vapor split valve. In

addition, one temperature in each of sections 3, 5 and 7 are controlled by the distillate split valve ( $R_{L2}$ ), upper side product split valve ( $R_{L3}$ ) and lower side product split valve ( $R_{L4}$ ), respectively. The details of the loop pairing is given in Table 5.1. The additional degree of freedom, i.e., the liquid split is not used in this stabilizing layer and is available for optimizing objective such as to reduce energy for a required purity specification.

Table 5.1: Four-point temperature regulatory control structure for Kaibel column <sup>a,b,c,d</sup>

Control loop	Manipulated Variable	Controlled Variable
Loop 1	Vapor split valve ( $R_V$ )	Temperature in section 2 ( $T_2$ )
Loop 2	Distillate split valve ( $R_{L2}$ )	Temperature in section 3 ( $T_3$ )
Loop 3	Upper side product split valve ( $R_{L3}$ )	Temperature in section 5 ( $T_5$ )
Loop 4	Lower side product split valve ( $R_{L4}$ )	Temperature in section 7 ( $T_7$ )

<sup>a</sup> The ratio  $R_{L1}$  is fixed and is not used in the control structure.

<sup>b</sup> Controlled variables are temperatures as shown in Figure 5.3c:  $T_2 = TP5$ ,  $T_3 = TM3$ ,  $T_5 = TM8$  and  $T_7 = TM14$ .

<sup>c</sup> Definitions of swinging funnel ratios:

$$R_{L1} = \frac{L_1}{L_3}, R_{L2} = \frac{L_3}{L_3+D}, R_{L3} = \frac{L_5}{L_5+S1}, R_{L4} = \frac{L_6}{L_6+S2}$$

where,  $L_1$ ,  $L_3$ ,  $L_5$  and  $L_6$  are liquid flows in sections 1, 3, 5 and 6, respectively.  $S1$  and  $S2$  are side product flow rates (see, Figure 5.3).

$$R_V = \frac{V_2}{V_7} = \frac{V_2}{V_2+V_6}$$

where,  $V_2$ ,  $V_6$  and  $V_7$  are vapor flows in sections 2, 6 and 7, respectively (see, Figure 5.3).

An experimental run is shown in Figure 5.11. At about 8 minutes, the setpoint for the temperature  $T_2$  controlled by the vapor split valve (Loop 1) is changed from 90°C to 92°C. This setpoint change can be handled well and the temperature settles in less than 5 minutes. The other temperature loops show some deviation due to interactions, however, all the temperatures are brought back to their setpoints in about 20 minutes.

There is a large scope for improving the vapor split valve and suggesting alternative designs. Nevertheless, even with our prototype valve with poor resolution, experimental results show that the vapor split can be manipulated effectively in feedback mode to achieve more energy efficient operation of dividing-wall columns.



## 5.4 Discussion

### 5.4.1 Feedback implementation of vapor split

We here argue in favor of feedback control using vapor split valves to set “optimum vapor split” between prefractionator and the main column in dividing-wall columns. There are two advantages of using the vapor split valve for using vapor split valve in feedback loop. First, the vapor split valve is a very fast handle since the vapor dynamics are much faster than the liquid. Further, there is no need to precisely measure the vapor split, the feedback action can “drive” the vapor split to its optimum value by tracking some controlled-variable like a composition or a temperature (Figure 5.10).

The additional degree of freedom, i.e., the liquid split, which can be adjusted more easily manually, can be used to reduce energy usage for a required purity specification or to improve the purities for a given energy usage.

Finally, note that vapor split remains as a degree of freedom when we introduce the feedback temperature controller, as it can be set to any value by adjusting the temperature setpoint.

### 5.4.2 Use of two vapor valves

In this work, two vapor valves are used to implement the active vapor split control. The use of two valves are needed to get the full range of changes in the vapor split. Another advantage of using two vapor valves is that for a given vapor split ratio, there may be several combinations of the openings of the two vapor valves. Of all such combinations, the proposed solution shall offer minimum pressure drop. This is because, with a split-range logic shown in Figure 5.6, one of the valves is always fully open while the other is operated (opening less than 100%) as shown in the experimental runs (see, Figures 5.9, 5.8).

## 5.5 Conclusions

The experimental results show for the first time that the vapor split can be used as a degree of freedom during practical operation of integrated columns, such as, Petlyuk, Kaibel and dividing-wall columns. Only with the vapor split available as a degree of freedom can the optimal operation be achieved. In particular, vapor split valve was found to be useful for closed-loop temperature or composition control, where deficiencies and inaccuracy in the vapor valves are corrected for by use of the feedback as shown in Figures

5.9, 5.8 and 5.11. The vapor split, which is difficult to set freely because of deficiency in the valve, is translated to a setpoint for temperature or composition, which is then a degree of freedom and can be set freely. The vapor split valve used in this study is clearly not optimally designed, but results with an improved valve may not be very different, because temperature control is already satisfactory.

### 5.5.1 Acknowledgement

Mr Jon Anta Buljo Hansen, Master Student (Cybernetics), Norwegian University of Science and Technology, assisted with the modifications of the column and Lab View implementation.

## References

- [1] Agrawal, R., Fidkowski, Z. T., 1998. More operable arrangements of fully thermally coupled distillation columns. *AIChE Journal* 44 (11), 2565–2568.
- [2] Dejanovic, I., Matijasevic, L., Olujic, Z., 2010. Dividing wall column—a breakthrough towards sustainable distilling. *Chemical Engineering and Processing: Process Intensification* 49 (6), 559–580.
- [3] Dwivedi, D., Halvorsen, I., Skogestad, S., 107f, *AIChE Spring Meeting*, 2011. Control structure design for optimal operation of thermally coupled columns. In: *Heritage Distillation Symposium*. Dr James Fair. topical Conference at the 2011 *AIChE Spring Meeting*.
- [4] Ghadrđan, M., Halvorsen, I. J., Skogestad, S., 2011. Optimal operation of Kaibel distillation columns. *Chem. Eng. Res. Des.* 89 (8), 1382 – 1391.
- [5] Halvorsen, I. J., Skogestad, S., 1999. Optimal operation of Petlyuk distillation: steady-state behavior. *Journal of Process Control* 9 (5), 407 – 424.
- [6] Halvorsen, I. J., Skogestad, S., 2003. Minimum energy consumption in multicomponent distillation. 2. three-product Petlyuk arrangements. *Industrial & Engineering Chemistry Research* 42 (3), 605–615.
- [7] Kaibel, G., 1987. Distillation columns with vertical partitions. *Chemical Engineering & Technology* 10 (1), 92–98.

- 
- [8] Kiss, A. A., Bildea, C. S., 2011. A control perspective on process intensification in dividing-wall columns. *Chemical Engineering and Processing: Process Intensification* 50 (3), 281 – 292.
- [9] Ling, H., Cai, Z., Wu, H., Wang, J., Shen, B., 2011. Remixing control for divided-wall columns. *Industrial & Engineering Chemistry Research* 50 (22), 12694–12705.
- [10] Ling, H., Luyben, W. L., 2010. Temperature control of the btx divided-wall column. *Industrial & Engineering Chemistry Research* 49 (1), 189–203.
- [11] Mutalib, M. I. A., Smith, R., 1998. Operation and control of dividing wall distillation columns: Part 1: Degrees of freedom and dynamic simulation. *Chemical Engineering Research and Design* 76 (3), 308–318.
- [12] Mutalib, M. I. A., Zeglam, A. O., Smith, R., 1998. Operation and control of dividing wall distillation columns: Part 2: Simulation and pilot plant studies using temperature control. *Chemical Engineering Research and Design* 76 (3), 319–334.
- [13] Niggemann, G., Hiller, C., Fieg, G., 2010. Experimental and theoretical studies of a dividing-wall column used for the recovery of high-purity products. *Industrial & Engineering Chemistry Research* 49 (14), 6566–6577.
- [14] Petlyuk, F., Platonov, V., Slavinskii, D., 1965. Thermodynamically optimal method for separating multicomponent mixtures. *International Chemical Engineering* 5 (3), 555–561.
- [15] Rewagad, R. R., Kiss, A. A., 2012. Dynamic optimization of a dividing-wall column using model predictive control. *Chemical Engineering Science* 68 (1), 132 – 142.
- [16] Skogestad, S., 2003. Simple analytic rules for model reduction and pid controller tuning. *Journal of Process Control* 13 (4), 291–309.
- [17] Strandberg, J., 2011. Optimal operation of dividing wall columns. Ph.D. thesis, Norwegian University of Science and Technology, Department of Chemical Engineering, Trondheim, Norway.
- [18] Strandberg, J., Skogestad, S., 2006. Stabilizing Control of an Integrated 4-Product Kaibel Column. Vol. 2. IFAC, pp. 623–628.



## Chapter 6

# Control structure selection for four-product Petlyuk column

### 6.1 Introduction

Significant energy losses in conventional distillation sequences result from internal remixing. This can be reduced greatly by direct material coupling and by doing easiest split first. Petlyuk et al. [28] proposed such a scheme to separate feed into three products, using a prefractionator. The prefractionator is designed and operated to do the easiest split first. A similar scheme was shown in a patent by Cahn et al. [5]. Stupin [34] claimed significant energy and capital saving using thermally coupled arrangement with a prefractionator. Such prefractionator arrangements can also be implemented in a single column shell using a dividing wall [18]. The German company BASF reports more than 100 industrial installations [9] of divided wall columns for separation of a feed into three products.

The idea of Petlyuk to separate a mixture to three products can be extended to separate a feed mixture into four products in a “four-product extended Petlyuk column”. Such systems may offer further energy savings [17]. While several control studies have been reported on three-product divided wall columns and four-product Kaibel columns, there are no control studies reported on four-product extended Petlyuk columns.

Wolff and Skogestad [37] did a steady state study and operability analysis on a three-product Petlyuk column and conclude that the simultaneous specification of both impurities in the side product may be infeasible. Fur-

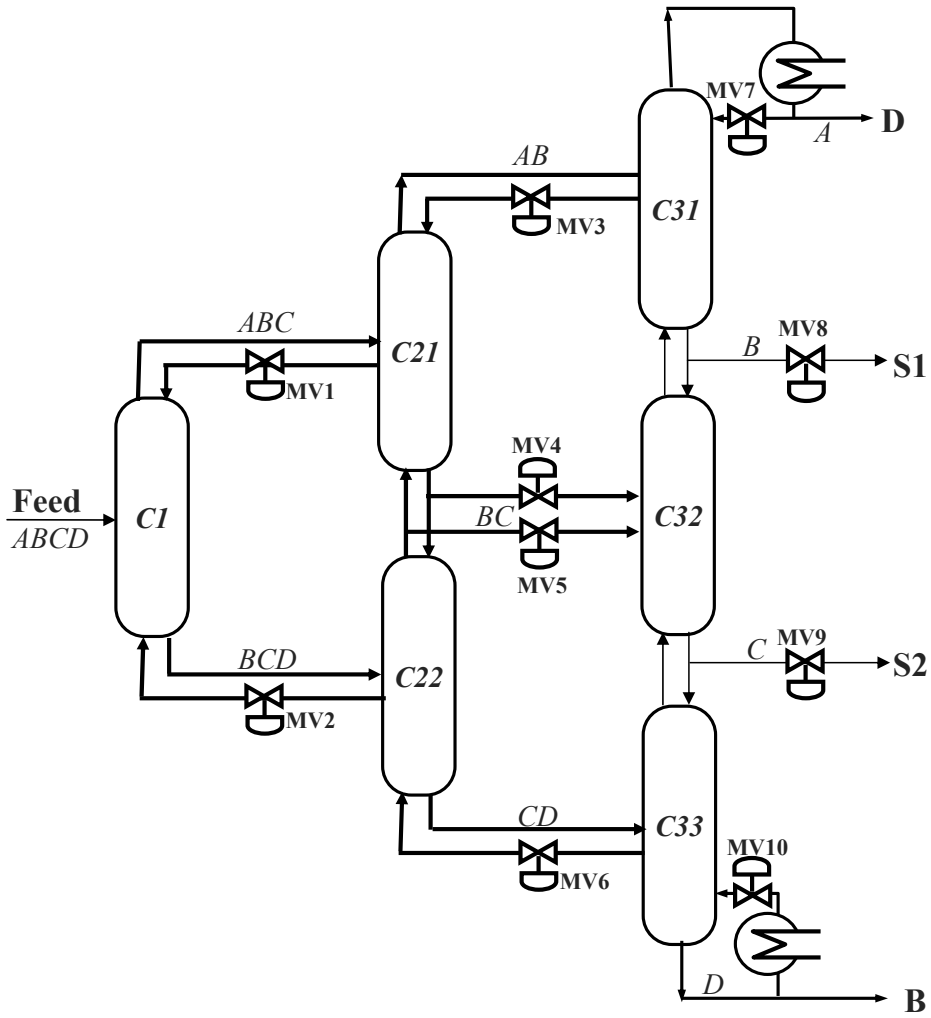


Figure 6.1: Four-product extended Petlyuk arrangement

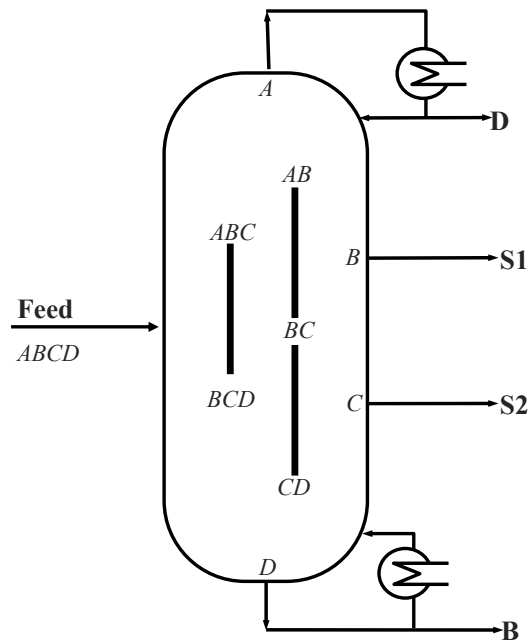


Figure 6.2: Dividing-wall implementation: Four-product extended Petlyuk arrangement in single column shell using double wall partition

ther, the liquid and vapor split ratios between pre-fractionator and the main column should be manipulated to get the optimal energy benefits. Nigge-mann et al. [26] conducted simulation and experimental studies for separation of a mixture of fatty alcohols into three high-purity products. They reported that the heat transfer across the dividing wall can be a factor in design and operation. Lestak et al. [21] argued that there may be some beneficial regions and the heat transfer across the dividing wall, should help decrease the overall energy consumptions. In non-beneficial regions however, the wall should be insulated. Mutalib et al. [25] reported experimental studies conducted on pilot plant and showed a two point control of the system. Ling and Luyben [23] explained that the liquid split valve must be manipulated and proposed a control structure with the use of four composition loops with the liquid split controlling the heavy key at the top stage of the prefractionator. Kiss and Bildea [19] gave some general control perspectives on dividing-wall columns. Ling et al. [22] suggested a control structure that can avoid remixing of intermediates leading to energy optimal operation. van Diggelen et al. [36] reported a study on dividing-wall columns giving emphasis on the controllability properties and dynamic responses. Some more works on the use of Model Predictive Control have been reported for divided wall columns [1, 4, 29].

Olujic et al. [27] reported recent advances on column internals for divided wall columns. Dejanovic et al. [9] reported simple design procedures for separating multicomponent aromatic mixtures into four products using energy efficient multiple partitioned dividing wall arrangements.

In this paper we report the very first work on control of a four-product extended Petlyuk column. We study, here the separation of A (methanol), B (ethanol), C (propanol) and D (*n*-butanol) using the four-product extended Petlyuk arrangement. For this case study, the energy saving is about 50 % compared to the conventional direct and indirect sequences [7].

Figure 6.1 shows the schematic of a four-product extended Petlyuk column. There are a total of six sub-columns making the Petlyuk arrangement and are numbered as C1, C21, C22, C31, C32 and C33 for convenience. This arrangement can also be fabricated in a single column shell using a double wall partition [7], as shown in Figure 6.2. Thermodynamically, the arrangements shown in Figure 6.1 and Figure 6.2 are equivalent. We shall refer to the arrangement shown in Figure 6.1 for the rest of the discussion.

In this study, we assume *ten* degrees of freedom (valves) available for composition control. The feed rate and feed conditions are assumed given. The distillate and the bottoms flow are used for level control of condenser and reboiler respectively, while the condenser duty is used for the pressure



control. We assume adiabatic column sections i.e., no heat transfer across the walls.

Note that we have included three vapor distribution valves (MV2, MV4 and MV6) as manipulated valves. This is unconventional [2] but can be implemented in real systems and development of vapor split valves for dividing-wall columns can be an area for future research as this can help to attain minimum energy usage when there are feed composition disturbances or changes in product specifications. A prototype of vapor split valves was demonstrated experimentally on a pilot plant recently [10]. Note that the valves, MV1, MV2, MV3, MV4, MV5, MV6, MV8 and MV9 (see Figure 6.1) do not specify direct molar flow rates, but are modelled as split ratios in the dynamic model. For example MV1 in Figure 6.1 manipulates ratio of liquid drawn out from sub-column C21 to the total molar liquid flow in sub-column C21.

We consider the separation of components A (lightest), B, C and D (heaviest). However, note that the letters B and D are also used to denote the bottom and distillate (top) products, respectively. To reduce the confusion, we will use subscripts for components and superscripts for products. For example,  $x_B^D$  denotes the mole fraction of component B in product D.

Table 6.1: Model details: four-product Petlyuk column

Relative volatilities [A B C D]	[7.1 4.43 2.15 1]
Number of stages in C1	30+30
Number of stages in C21	30+30
Number of stages in C22	30+30
Number of stages in C31	30+30
Number of stages in C32	30+30
Number of stages in C33	30+30
Feed flow rate(mol/min)	1
Feed composition	Equimolar
Nominal purity of distillate ( $x_A^D$ )	99.55 (mol %)
Nominal purity of upper side product ( $x_B^{S1}$ )	99.33 (mol %)
Nominal purity of lower side product ( $x_C^{S2}$ )	99.56 (mol %)
Nominal purity of bottom product ( $x_D^B$ )	99.62 (mol %)

## 6.2 Case Study

The data is given in Table 6.1. The process is modelled in Matlab using the simplifying assumptions of constant relative volatility and constant molar flows in each column section. The four components A, B, C and D have relative volatilities similar to the mixture of methanol, ethanol, propanol and *n*-butanol. We assume constant pressure, negligible vapor holdup, a total condenser and equilibrium on all stages. We assume linearized liquid flow dynamics. Compared to the specified purities given in Table 6.1, a large number of stages is assumed in each sub-column. This implies that the used energy for a near-sharp separation is close to the minimum energy using an infinite number of stages.

### 6.2.1 Steady state composition profiles

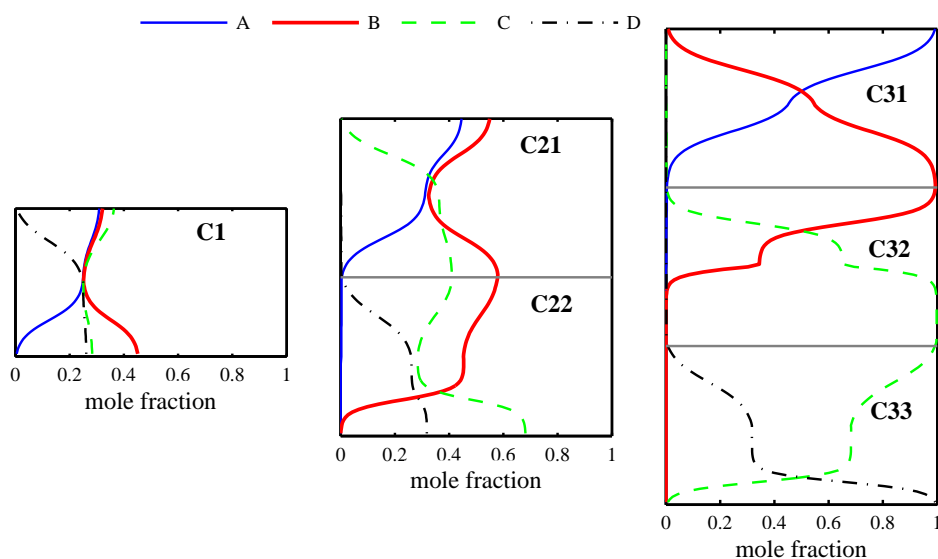


Figure 6.3: Steady state composition profiles in sub-columns C1, C21, C22, C31, C32 and C33

Figure 6.3 shows composition profiles at nominal steady state conditions of components A (methanol), B (ethanol), C (propanol) and D (*n*-butanol) in different sub-columns of the Petlyuk arrangement.

In a Petlyuk arrangement, the easiest separation is carried out first. The

more difficult splits, i.e, the splits between the immediate boiling components are carried out last. In the first sub-column C1, the easy split is between A and D, whereas the intermediate components, B and C, distribute in both products. The key impurity in the top stage of sub-column C1 is D and the key impurity in C1 bottoms is A. The feed to sub-column C21 is A, B and C. The easy split is between A and C, where B is allowed to distribute to both ends of sub-column C21. The key impurity at C21 top stage is C and the key impurity at C21 bottom stage is A.

The more difficult binary splits are done in sub-columns C31, C32 and C33. Sub-column C31 does the split between the two light components, A and B, sub-column C32 does the B/C split and sub-column C33 does the C/D split.

### 6.3 $V_{min}$ diagrams

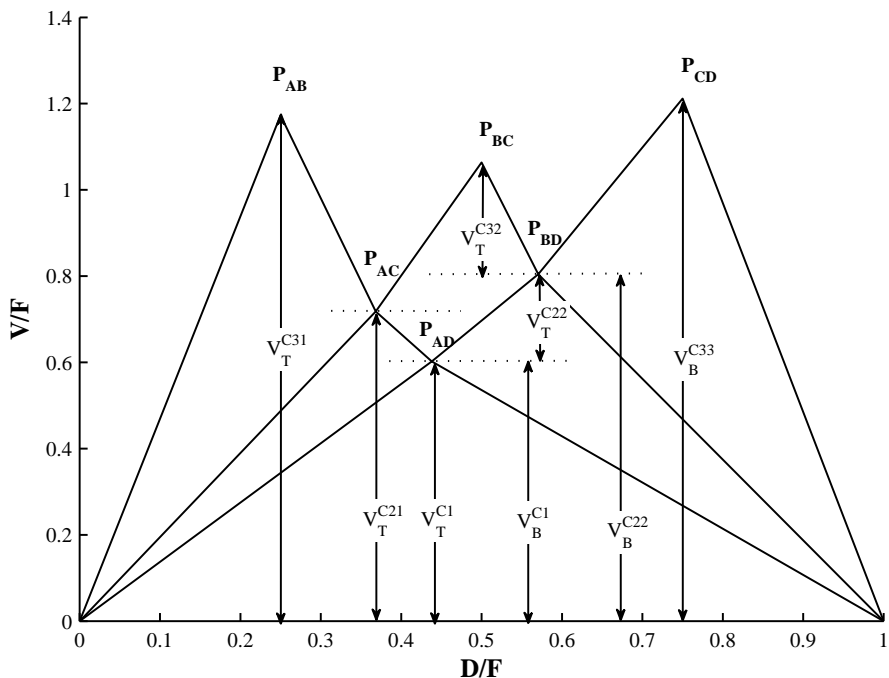


Figure 6.4:  $V_{min}$  diagram showing minimum vapor flows in various sections required for sharp separation of equimolar A-B-C-D feed

Halvorsen and Skogestad [15] have developed a graphical tool, the “ $V_{min}$ ” diagrams, to visualize the minimum energy requirement for sharp and non-sharp separations. For separation of ideal multicomponent mixtures the Underwood equations [35] are effective for generating the  $V_{min}$  diagrams, but the  $V_{min}$  diagram may also be generated for non-ideal mixtures using simulations with rigorous thermodynamic models [8].

Figure 6.4, shows the  $V_{min}$  diagram for an equimolar A-B-C-D mixture with a liquid feed. The  $y$ -axis shows the normalized minimum boilup ( $V/F$ ) and the  $x$ -axis shows the net product withdrawal ( $D/F$ ) in a conventional two-product column. Since, we are studying near-sharp separations, the peak points denoted by  $P_{AB}$ ,  $P_{AC}$ ,  $P_{AD}$ ,  $P_{BC}$ ,  $P_{BD}$  and  $P_{CD}$  are of interest. The peak  $P_{AB}$  gives the minimum vapor flow ( $V/F$ ), required for separating A and B. Note that the corresponding product split ( $x$ -coordinate)  $D/F = 0.25$ , since the feed is equimolar. Similarly point  $P_{AD}$  denotes the minimum vapor required to separate A and D.

Minimum energy is achieved when the prefractionator sub-columns C1, C21 and C22 are operated at their “preferred splits”, denoted by points  $P_{AD}$ ,  $P_{AC}$  and  $P_{BD}$  respectively. Thus, the internal flows in the sub-columns can directly be obtained from the  $V_{min}$  diagram. This can be used for the short cut design and preliminary sizing of column sections [7, 13]. In addition, with the minimum flows required for separation known, flows in a more detailed dynamic model for the process can be initialized.

Halvorsen [16] and Fidkowski [11] showed that in a Petlyuk arrangement, the minimum energy requirement to separate a multi-component feed is equal to the “most difficult binary separation”.

$$V_{min, Petlyuk} = \max(V_{AB}, V_{BC}, V_{CD}) \quad (6.1)$$

Here,  $V_{AB}$ ,  $V_{BC}$  &  $V_{CD}$  are the minimum boilup required for sharp separation of A/BCD, AB/CD and ABC/D in a conventional two-product distillation column with A-B-C-D feed. Note that,  $V_{AB}$ ,  $V_{BC}$  &  $V_{CD}$  depend on the feed conditions.

In Figure 6.4, the  $P_{CD}$  peak is the highest. This implies that the separation of C and D is the most difficult binary split in terms of energy usage. Thus, the minimum boilup required for sharp separation of the multicomponent feed using a Petlyuk arrangement is equal to the boilup required for this binary split ( $=V_{CD} = V_B^{33}$  in Figure 6.4).

In a generalized Petlyuk arrangement, the minimum vapor flow in sub-columns above and below a side product product may be different. This is equal to the difference in the heights of the peaks in the  $V_{min}$  diagram. A different vapor distribution in sub-columns can be realized by drawing side

products as both liquid and vapor or, alternatively, by using an intermediate heater or cooler between sub-columns. In this study, only liquid products are drawn and internal flows in sections C31 and C32 are recalculated for this more practical design. This modification does not lead to any additional energy requirements for a given separation, but it may allow for “over-purification” in some sections.

## 6.4 Control structures for three-product Petlyuk columns

Before we discuss the control structures for the four-product Petlyuk column, we present a short note based on the works published by previous workers [3, 6, 14, 20, 23] on the control structure design of three-product Petlyuk column. Figure 6.5 shows a general control structure for the three-product Petlyuk column with a ternary feed of A, B and C for the conventional case when the vapor split is not used for control.

To achieve the desired purity of the side stream (S) in the main column, the A/C split in the prefractionator (C1) must be controlled to avoid that too much C goes in the top or too much A goes in the bottom. The specifications for the split in the prefractionator (maximum values for  $x_C$  at  $C1^{TOP}$  and  $x_A$  at  $C1^{BOT}$ ) are indirectly determined by the purity specifications for the side stream (S). With a fixed vapor split ( $R_V$ ) one cannot control both at the same time, which is why Christiansen [6] and Halvorsen [14] propose to control the key impurity in the least pure end. Kiss and Rewagad [20], Ling and Luyben [23] propose to control  $x_C$  in the top of the prefractionator, which will be the best policy provided the top is the least pure end (i.e., when breakthrough of component A in the bottom of the prefractionator (C1) is not a problem).

We can now discuss the control of the final products (D, S, B) in the main column. For the distillate (D) and bottoms (B) product it is usually simple. These products have only one impurity each (the amount of B component), so for these we simply control the impurity ( $x_B$  in distillate (D) and  $x_B$  in bottoms (B)). However, for the side stream S, there are two impurities (components A and C), and we do not have enough degrees of freedom to control both.

One solution is to control the more “difficult” of the two and let the other be over-purified. For example, if the B/C split is more difficult than the A/B split, then one should control the amount of C in the side stream ( $x_C^S$ ). This is proposed by Ling and Luyben [23] and if we look at the vapor-liquid equilibria data of the components they studied, then we indeed find

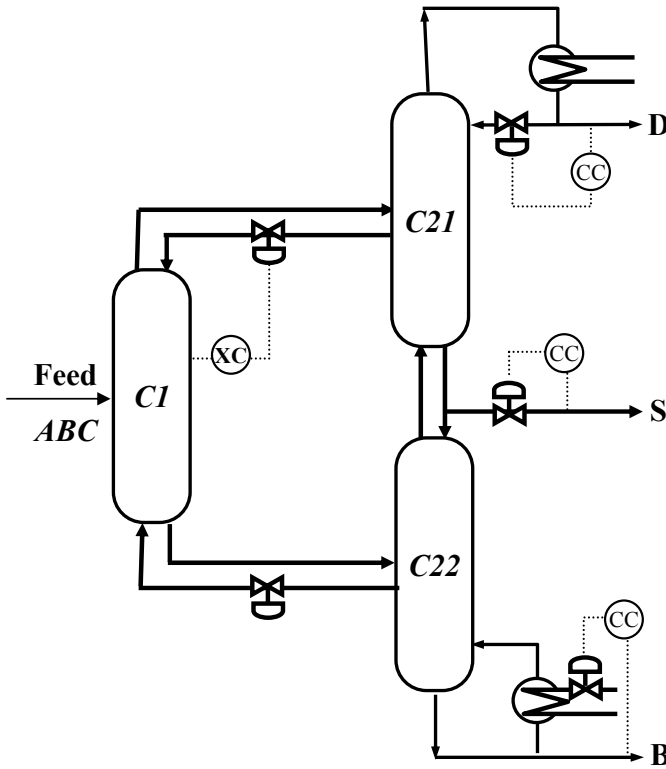


Figure 6.5: Proposed Control Structures for three-product Petlyuk columns

In prefractionator controller, XC can be a temperature controller [3] or a composition controller for the key impurity in the least pure end [6, 14] i.e., heavy key  $x_C$  at  $C1^{TOP}$  [20, 23] or, light key  $x_A$  at  $C1^{BOT}$

that toluene (B)/ *o*-xylene (C) is the more difficult separation. However, what would happen if the feed conditions change so that the benzene (A)/ toluene (B) split becomes the difficult one and we get too much A in the side product? To avoid this, we would need to increase the vapor flow in the top section C21, and since the vapor flow is the same in sections C21 and C22 we would get excess vapor in the bottom section C22. We resolve a similar issue in the four-product Petlyuk column by our proposed decentralized control structures described below.

### 6.5 Proposed control structures for the four-product extended Petlyuk column

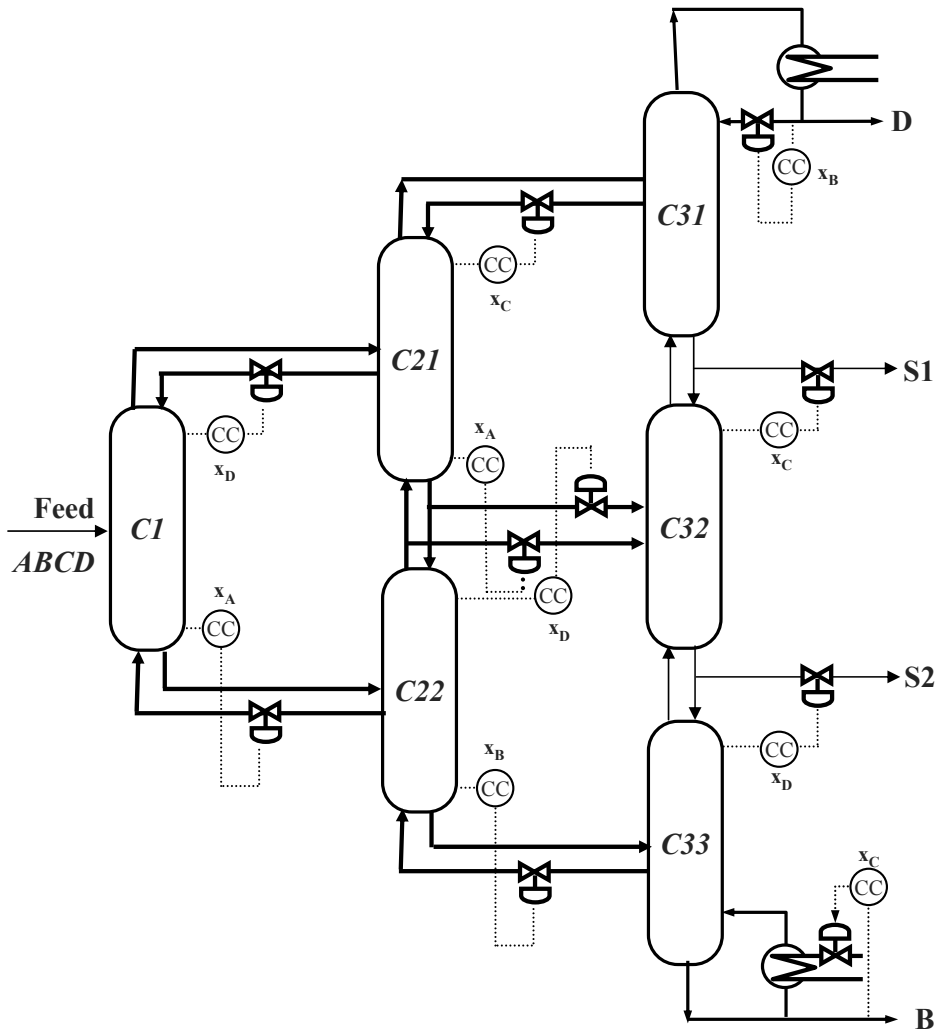


Figure 6.6: Schematic of Control Structure 1 (CS1)

A systematic design procedure [30] for plant-wide control structure should have emphasis on the overall economic objective. For this study, we use the minimization of the following general economic objective [32]:

$$J = \text{cost of feed} - \text{value of products} + \text{cost of energy} \quad (6.2)$$

Figure 6.1 shows the manipulated variables MV1, MV2, MV3, MV4, MV5, MV6, MV7, MV8, MV9 and MV10 used in designing control structure. The other manipulated variables not shown in Figure 6.1 are distillate flow rate (D), bottoms flow rate (B) and condenser duty. They are used to control the liquid level in condenser and reboiler and, for vapor inventory control respectively.

In this work, we use the six degrees of freedom in the prefractionator sub-columns C1, C21 and C22 to control the key impurities at their top and bottoms trays, to prevent them to escape as impurities in successive the sub-columns and hence in the final products.

Assuming all the products are about equally priced and that the price of energy is high, the final product purities are the active constraints as discussed by Skogestad [32]. In addition one may have constraints on individual impurities for side products. This leaves four degrees of freedom (MV7, MV8, MV9 and MV10) to control the “main” column i.e., the sub-columns C31, C32 and C33. A multivariable controller would get even better performance, but our main objective is to show the feasibility, even with a simple structure.

In this work, we consider four decentralized control structures and evaluate their control performance for a wide range of disturbances like feed rate, feed compositions changes and feed vapor fraction.

The four control structures are named CS1, CS2, CS3 and CS4 for convenience. Simple decentralized proportional-integral (PI) controllers are used. The complete list pairing of controlled variables and manipulated variables used in the control structures are shown in the Table 6.2.

Logarithmic transformation of compositions is used to reduce the effects of non-linearities [32, 33]. Therefore, in control structures CS1, CS2 and CS4, controlled composition variables are actually  $\ln x_i$ , where  $x_i$  is the key impurity being controlled.

### 6.5.1 Control Structure 1 (CS1)

In control structure 1 (CS1), we implement the basic two point LV structure [32] on each sub-column where reflux (L) is used to control the key impurity in the top and vapor (V) is used to control the key impurity in the bottom. For example, in sub-column C1 (see Figure 6.6), the key impurity on top tray is D (*n*-butanol) which is controlled using liquid reflux valve MV1.

At optimal (minimum energy) operation, sub-columns C31 and C32 have excess vapor for fractionation ( $V > V_{min}$ ) at the nominal feed conditions, thus a one-point control in these sections is sufficient [32]. Sub-columns C1,



C21, C22 and C33 should be at their minimum vapor conditions ( $V=V_{min}$ ), therefore these column sections have two-point control.

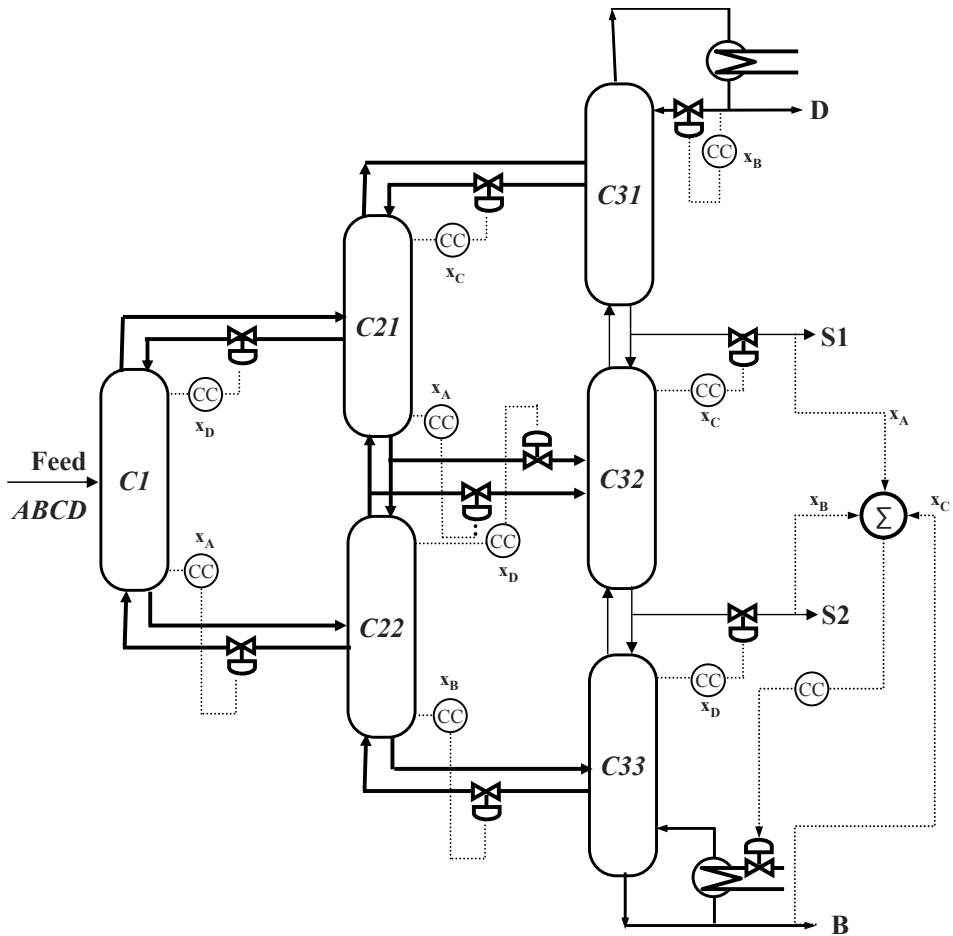


Figure 6.7: Schematic of Control Structure 2 (CS2)

### 6.5.2 Control Structure 2 (CS2)

Structure CS2 is identical to CS1, except that for the loop involving the boilup (MV10). Note that in CS1, A (methanol) composition at the C31 bottom and B (ethanol) composition at C32 bottom are not controlled. Thus for certain disturbances, these light keys can escape into the upper side product (S1) and lower side stream (S2) as impurity. This possibility is eliminated by ensuring that there is sufficient boilup for separation in the

column sections C31 and C32. A simple way to ensure this, is to pair the boilup, MV10 (see Figure 6.7) with sum of the light impurities at C31 bottom stage, C32 bottom stage and the C33 bottom stage (reboiler). Because the sum of the light keys is controlled with the boilup (MV10), there may be a small offset in the product purities.

6.5.3 Control Structure 3 (CS3)

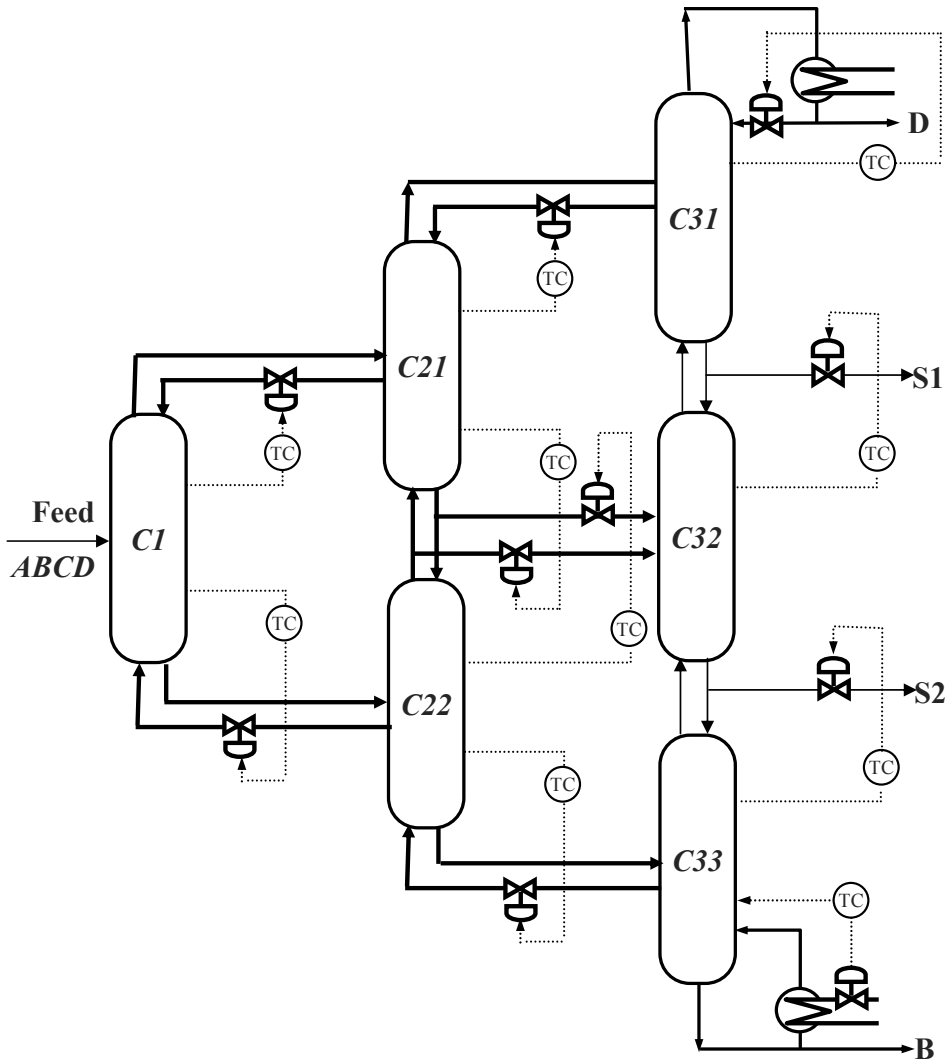


Figure 6.8: Schematic of Control Structure 3 (CS3)

This structure uses temperatures only, thus the idea is to infer compositions from temperature, which is not unique for multicomponent mixtures (see Figure 6.8). The controlled variables are a sensitive stage temperature in the stripping and rectifying sections of sub-columns C1, C21, C22 and C33, respectively (see Table 6.2 for details). Note that, there is only one temperature control loop in columns C31 and C32.

6.5.4 Control Structure 4 (CS4)

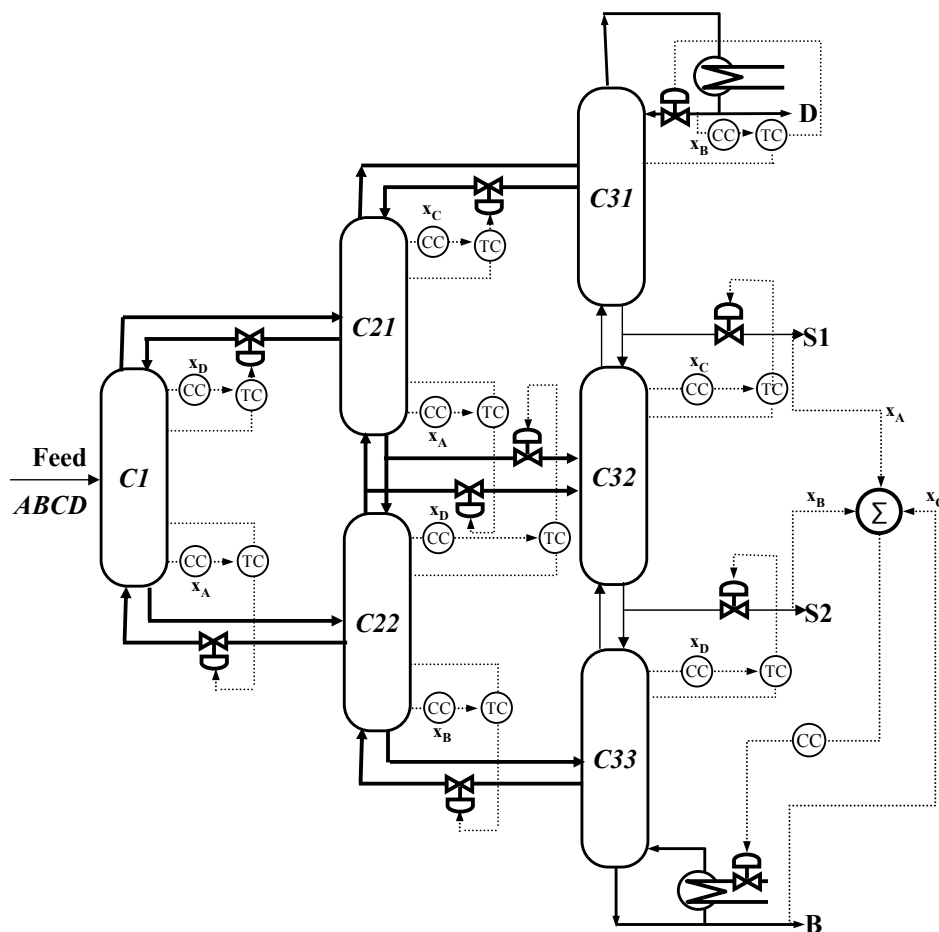


Figure 6.9: Schematic of Control Structure 4 (CS4)

This is a modification of CS3, with the addition of several outer composition loops. The temperature setpoints of slave temperature controllers are

set by master composition controller. The master composition loops control the same key impurities as in structures CS1 and CS2. For example, in sub-column C1, the setpoint of the top temperature controller is set by a master composition controller that controls the D (*n*-butanol) at top stage of column section C1. In addition, a modification same as the structure CS2 is that, the boilup (see Figure 6.9) controls sum of the light impurities at C31 bottom stage, C32 bottom stage and the C33 bottom stage (reboiler).

Table 6.2: Pairing of manipulated variables with controlled variables in the four control structures *a,b,c,d,e*

MV <sup>b</sup>	Controlled Variable			
	CS1 <sup>c</sup>	CS2 <sup>c</sup>	CS3	CS4 <sup>c</sup>
MV1	x <sub>D</sub> <sup>a</sup> at C1 <sup>TOP</sup>	x <sub>D</sub> at C1 <sup>TOP</sup>	T <sub>12</sub> <sup>C1</sup> <sup>d</sup>	x <sub>D</sub> at C1 <sup>TOP</sup> /T <sub>12</sub> <sup>C1</sup> <sup>e</sup>
MV2	x <sub>A</sub> at C1 <sup>BTM</sup>	x <sub>A</sub> at C1 <sup>BTM</sup>	T <sub>49</sub> <sup>C1</sup>	x <sub>A</sub> at C1 <sup>BTM</sup> /T <sub>49</sub> <sup>C1</sup> <sup>e</sup>
MV3	x <sub>C</sub> at C21 <sup>TOP</sup>	x <sub>C</sub> at C21 <sup>TOP</sup>	T <sub>19</sub> <sup>C21</sup>	x <sub>C</sub> at C21 <sup>TOP</sup> /T <sub>19</sub> <sup>C21</sup> <sup>e</sup>
MV4	x <sub>D</sub> at C22 <sup>TOP</sup>	x <sub>D</sub> at C22 <sup>TOP</sup>	T <sub>18</sub> <sup>C22</sup>	x <sub>D</sub> at C22 <sup>TOP</sup> /T <sub>18</sub> <sup>C22</sup> <sup>e</sup>
MV5	x <sub>A</sub> at C21 <sup>BTM</sup>	x <sub>A</sub> at C21 <sup>BTM</sup>	T <sub>48</sub> <sup>C21</sup>	x <sub>A</sub> at C21 <sup>BTM</sup> /T <sub>48</sub> <sup>C21</sup> <sup>e</sup>
MV6	x <sub>B</sub> at C22 <sup>BTM</sup>	x <sub>B</sub> at C22 <sup>BTM</sup>	T <sub>51</sub> <sup>C22</sup>	x <sub>B</sub> at C22 <sup>BTM</sup> /T <sub>51</sub> <sup>C22</sup> <sup>e</sup>
MV7	x <sub>B</sub> in condenser	x <sub>B</sub> in condenser	T <sub>12</sub> <sup>C31</sup>	x <sub>B</sub> at C31 <sup>TOP</sup> /T <sub>12</sub> <sup>C31</sup> <sup>e</sup>
MV8	x <sub>C</sub> at C32 <sup>TOP</sup>	x <sub>C</sub> at C32 <sup>TOP</sup>	T <sub>10</sub> <sup>C32</sup>	x <sub>C</sub> at C32 <sup>TOP</sup> /T <sub>10</sub> <sup>C32</sup> <sup>e</sup>
MV9	x <sub>D</sub> at C33 <sup>TOP</sup>	x <sub>D</sub> at C33 <sup>TOP</sup>	T <sub>47</sub> <sup>C33</sup>	x <sub>D</sub> at C33 <sup>TOP</sup> /T <sub>47</sub> <sup>C33</sup> <sup>e</sup>
MV10	x <sub>C</sub> at reboiler	x <sub>C</sub> at reboiler+ x <sub>B</sub> at C32 <sup>BTM</sup> + x <sub>A</sub> at C31 <sup>BTM</sup>	T <sub>56</sub> <sup>C31</sup>	x <sub>C</sub> at reboiler + x <sub>B</sub> at C32 <sup>BTM</sup> + x <sub>A</sub> at C31 <sup>BTM</sup>

<sup>a</sup> x: mole fraction; subscripts A: methanol, B: ethanol, C: propanol, D: *n*-butanol

<sup>b</sup> MV: Manipulated Variable

<sup>c</sup> logarithm of x is used as controlled variable in CS1, CS2 & CS4; for example ln(x<sub>D</sub>) at C1<sup>TOP</sup> is paired with MV1 in control structures CS1, CS2 and CS4

<sup>d</sup> T: tray temperature; superscript: column section; subscript: tray number (numbered from top to bottom)

<sup>e</sup> temperature setpoints of slave controllers corrected by master composition controller

## 6.6 Tuning

The tuning of the decentralized control structures was done using the SIMC tuning rules [31]. Because of the mainly sequential sequence of the columns, the controllers in the prefractionator sub-columns (C1, C21 and C22) are first closed. This is followed by the controllers in main column (C31, C32 and C33). Step changes in manipulated variables are made to identify the

Table 6.3: SIMC tuning parameter ( $\tau_C$ ) used in the four control structures <sup>a,b</sup>

Loop	CS1	CS2	CS3	CS4 <sup>a</sup>
MV1	5 min	5 min	5 min	4 min
MV2	3 min	3 min	3 min	4 min
MV3	5 min	5 min	5 min	4 min
MV4	5 min	5 min	5 min	4 min
MV5	3 min	3 min	3 min	8 min
MV6	3 min	3 min	3 min	8 min
MV7	20 min	20 min	5 min	12 min
MV8	20 min	20 min	5 min	8 min
MV9	20 min	20 min	5 min	8 min
MV10	5 min	5 min	3 min	5 min

<sup>a</sup>  $\tau_C$  for the master composition controllers;  $\tau_C$  for slave temperature controllers is same as in CS3 but without integral action

input-output steady state gain and dynamics. Most of the responses have only a small effective delay. The SIMC tuning factor,  $\tau_C$  was selected to get a smooth response (see Table 6.3).

## 6.7 Closed-loop simulation results

The proposed control structures were simulated with disturbances in feed rate, feed composition, feed vapor fraction and as well as product composition setpoint changes. The performance is analyzed by considering the response in the final product compositions as well as product flows (D, S1, S2 and B) and energy usage (V). The minimum theoretical boilup ( $V_{\min}$ ) required for sharp separation, for a new feed disturbance is also shown in the figures. Table 6.4 shows the summary of closed-loop responses using different control structures.

### 6.7.1 Performance of CS1 and CS2

Figure 6.10, shows the closed-loop response for various feed disturbances, in the sequence as listed in Table 6.4. For a feed rate disturbance of +10 % (t=0, Figure 6.10), all the product purities are restored and the molar flows of products increase from a nominal flow rate of 0.25 mol/min to 0.275 mol/min. This is followed by various feed composition disturbances.

Table 6.4: Summary of closed-loop response using different control structures <sup>a,b,c</sup>

Disturbance <sup>c</sup>	CS1	CS2	CS3	CS4
Feed, +10 %	OK	OK	OK	OK
$z_1^F$ (mol%) = [20 30 25 25]	OK	OK	OK	OK
$z_2^F$ (mol%) = [20 25 30 25]	OK	OK	OK	OK
$z_3^F$ (mol%) = [20 25 25 30]	OK	OK	Fail	OK
$z_4^F$ (mol%) = [25 20 30 25]	OK	OK	OK	OK
$z_5^F$ (mol%) = [25 25 20 30]	Fail	OK	Fail	OK
$z_6^F$ (mol%) = [25 20 25 30]	OK	OK	Fail	OK
+20% feed vapor fraction	Fail	OK	Fail	OK
$x_B$ in condenser, +5 %	OK	OK	–	OK
$x_C^{S1}$ , +5 %	OK	OK	–	OK
$x_D^{S2}$ , +5 %	OK	OK	–	OK

<sup>a</sup> OK: Closed-loop stable and purity of all products restored

<sup>b</sup> Fail: Closed-loop stable but purity of upper side product is not maintained ( $x_B^{S1}$  dropped considerably)

<sup>c</sup> Nominal feed rate:  $F=1$  mol/min  
 Nominal feed composition,  $z_F$  (mol%) = [25 25 25 25] (equimolar)

At  $t=7200$  minutes, we give changes in feed composition of components C (propanol) and D (*n*-butanol). The product purities of upper side product ( $x_B^{S1}$ ) deteriorate significantly and shows a long settling time. A similar deterioration in the product purity of S1 is seen in the figure at time,  $t=9600$  minutes, for a disturbance affected by increasing the vapor fraction of the feed by 20 %. As explained in section 6.2.1, the two side products have two key impurities. Since the light key on C31 bottom tray is not controlled, it can leak into the side product 1 (S1) for certain disturbances. These responses are discussed in more detail later in section 6.8.1. Figure 6.11 shows the performance for setpoint changes of +5% in the heavy keys of products D, S1 and S2 (at  $t=0, 1200$  and  $2400$ , respectively) using CS1.

Figure 6.12 shows the closed-loop response using CS2 for a feed rate and feed composition disturbances. At  $t=0$ , we give a feed rate disturbance and the purities of four products can be restored like CS1. Unlike CS1, the purities of all the products including the upper side product ( $x_B^{S1}$ ) can be restored for all the feed composition disturbances. In Figure 6.13, we show a +5% composition setpoint changes in the heavy keys of products D, S1 and S2.

### 6.7.2 Performance of CS3 and CS4

Figure 6.14 shows the response for a feed rate increase by 10%, at  $t=0$ . All the product purities are restored and the molar flows of products increase from a nominal flow rate of 0.25 mol/min to 0.275 mol/min. Since we are studying a multicomponent separation, for feed composition changes, temperature control alone may not be sufficient for sharp separation. For example, the closed-loop response for a feed composition disturbance in components A (methanol) and D (*n*-butanol), at  $t=3600$ , there is a large deterioration in the product purity of upper side product ( $x_B^{S1}$ ). For this disturbance, the energy usage is more than the “minimum or  $V_{min}$ ”. There is a similar deterioration in purity of S1 for the feed vapor fraction disturbance at  $t=9600$ , for which the energy loop decreases the boilup, less than the  $V_{min}$ .

The control structure CS4 uses composition/ temperature cascade controllers. Note that unlike the response using structure CS1 (see Figures 6.10) and structure CS3 (see Figure 6.14), purity of all the products can be restored after initial transient. Figures 6.15 shows that all the disturbances under study can be rejected and product purities are restored. Similarly, Figure 6.16 shows composition setpoint changes in products D, S1 and S2.

## 6.8 Discussion

### 6.8.1 Impact of feed disturbances & the $V_{min}$ diagram

As discussed in section 6.7.1, the closed-loop responses were stable for all disturbances using CS1. However, for a feed composition disturbance with 20 % C (propanol) and 30 % D (*n*-butanol), although the response was closed-loop stable, the purity of upper side product ( $x_B^{S1}$ ) deteriorated considerably (see Figure 6.10, at  $t=7200$  minutes). A similar deterioration in the purity of upper side product (see Figure 6.10, at  $t=9600$  minutes) is seen when the vapor fraction was increased by 20 %. This can be explained using the “ $V_{min}$ ” tool.

Figure 6.17 shows the  $V_{min}$  diagram for nominal feed mixture, in solid lines. As explained in section 6.3, the minimum boilup for sharp separation is set by the “most difficult binary split”. This is denoted in the Figure 6.17 by peak points  $P_{AB}$ ,  $P_{BC}$  and  $P_{CD}$ . For the nominal feed, the peak  $P_{CD}$  is highest. This implies that the separation of C/D is the most difficult. For separation of this feed using the Petlyuk arrangement, the minimum boilup is set by this split.

At an operating point close to minimum energy, the sub-column C33

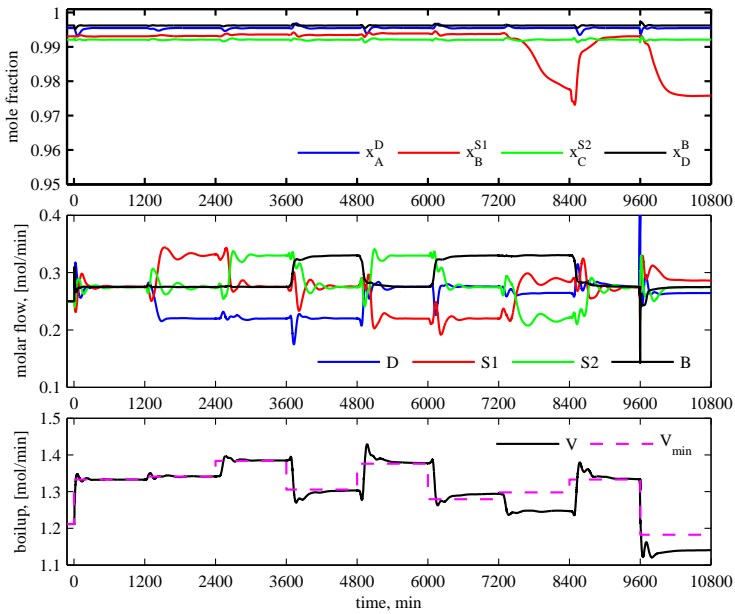


Figure 6.10: CS1: Closed-loop results for feed disturbances. Purity of upper side product ( $x_B^{S1}$ ) drops at time 7200 and 9600 (**not acceptable**).

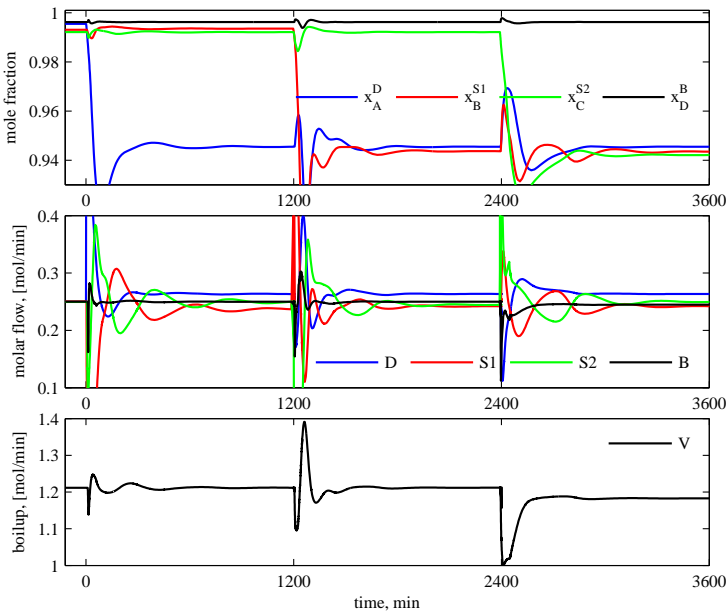


Figure 6.11: CS1: Closed-loop results for setpoint Changes



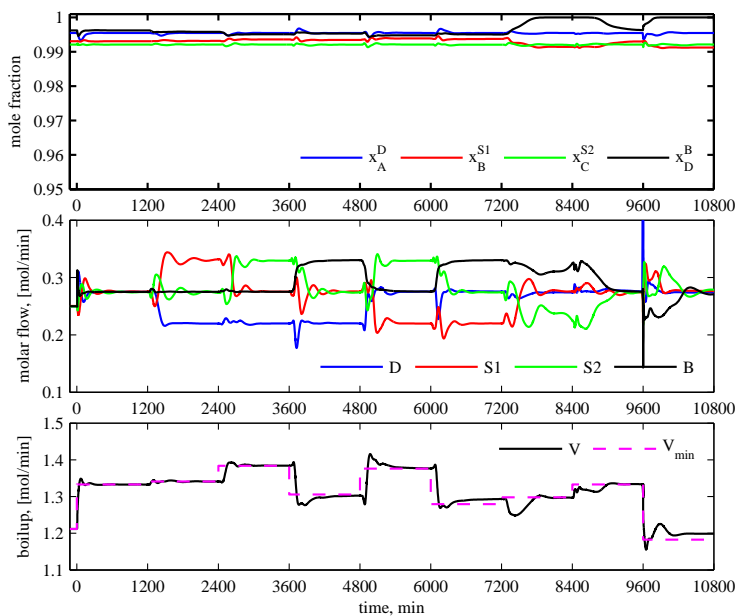


Figure 6.12: CS2: Closed-loop results for feed disturbances.

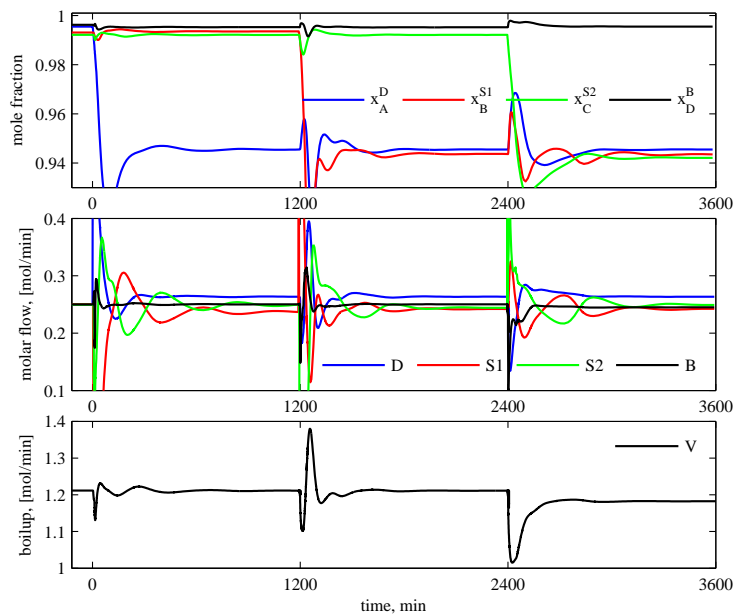


Figure 6.13: CS2: Closed-loop results for setpoint Changes

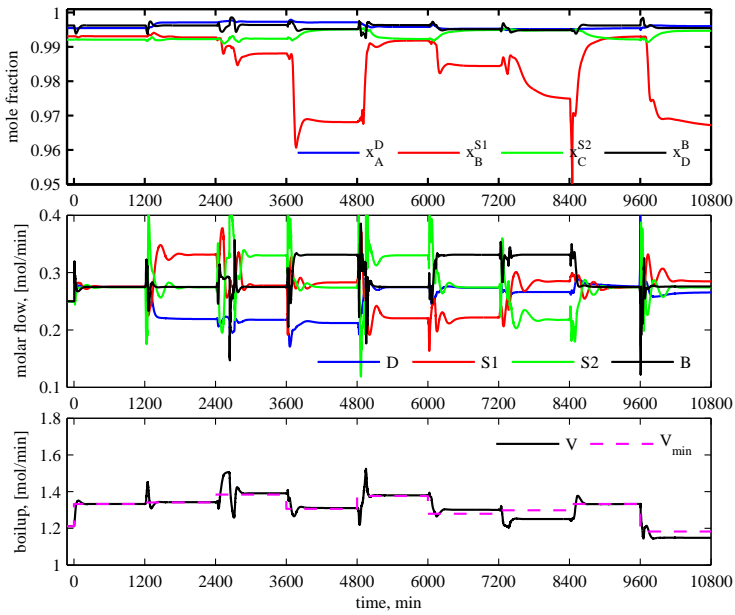


Figure 6.14: CS3: Closed-loop results for feed disturbances. Purity of upper side product ( $x_B^{S1}$ ) drops at time= 3600, 4800, 6000, 7200 and 9600 (not acceptable).

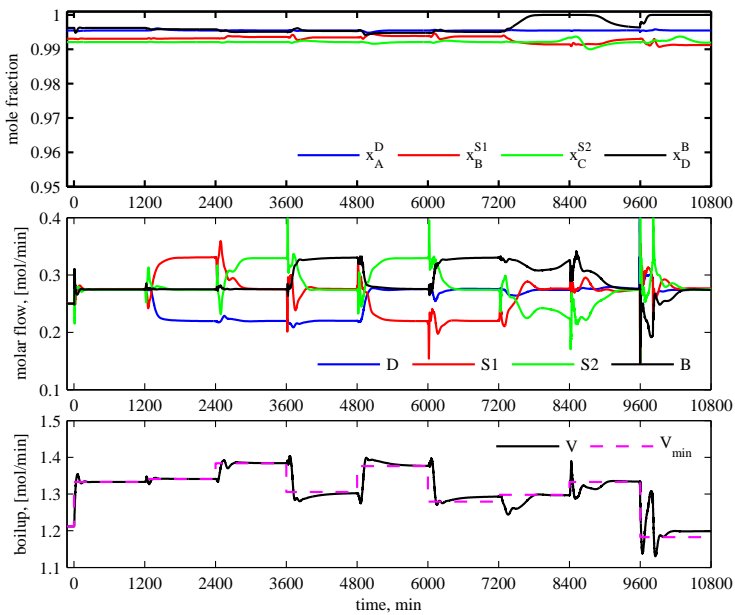


Figure 6.15: CS4: Closed-loop results for feed disturbances

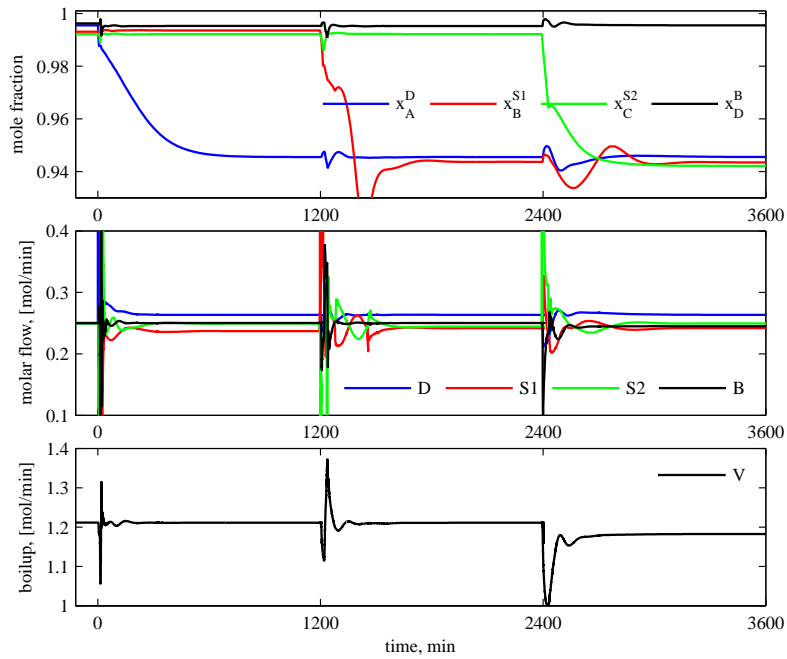


Figure 6.16: CS4: Closed-loop results for setpoint Changes

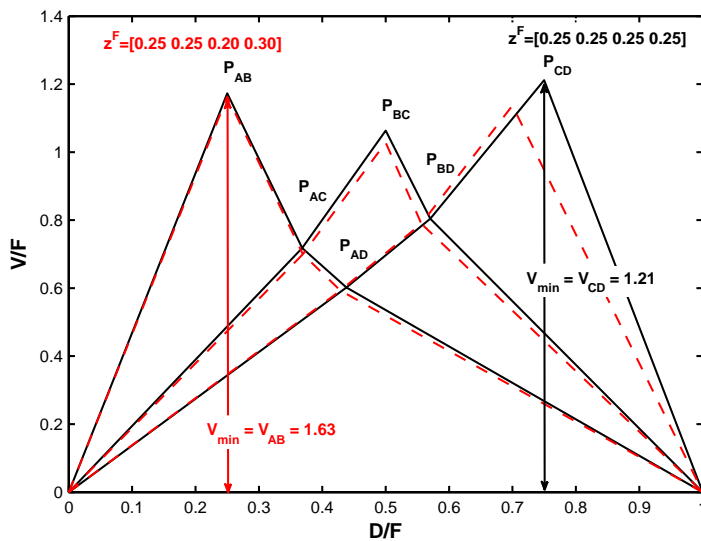


Figure 6.17:  $V_{min}$  diagrams: nominal feed composition,  $z^F$  (mol %) = [25 25 25 25] (solid-black line)  $z^F$  (mol%) = [25 25 20 30] (dashed-red line)

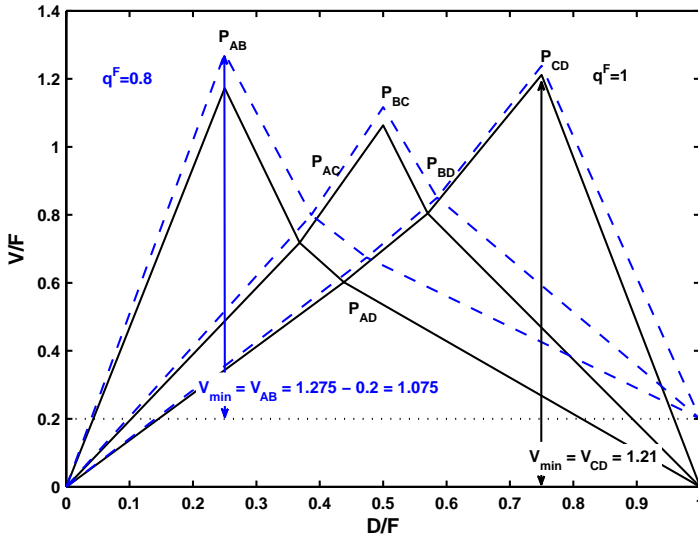


Figure 6.18:  $V_{\min}$  diagrams: nominal feed vapor fraction,  $q^F = 1$  (solid-black line) and for  $q^F = 0.8$  (dashed-blue line)

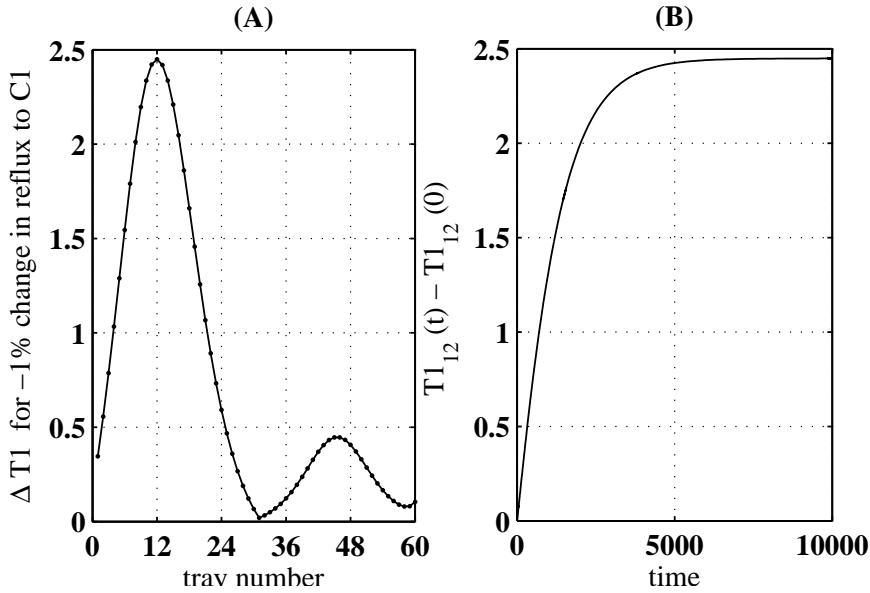


Figure 6.19: (A) Change in temperatures of column section, C1 for -1% change in reflux. (B) Column C1, tray 12 temperature ( $T1_{12}$ ) for -1% change in reflux to C1

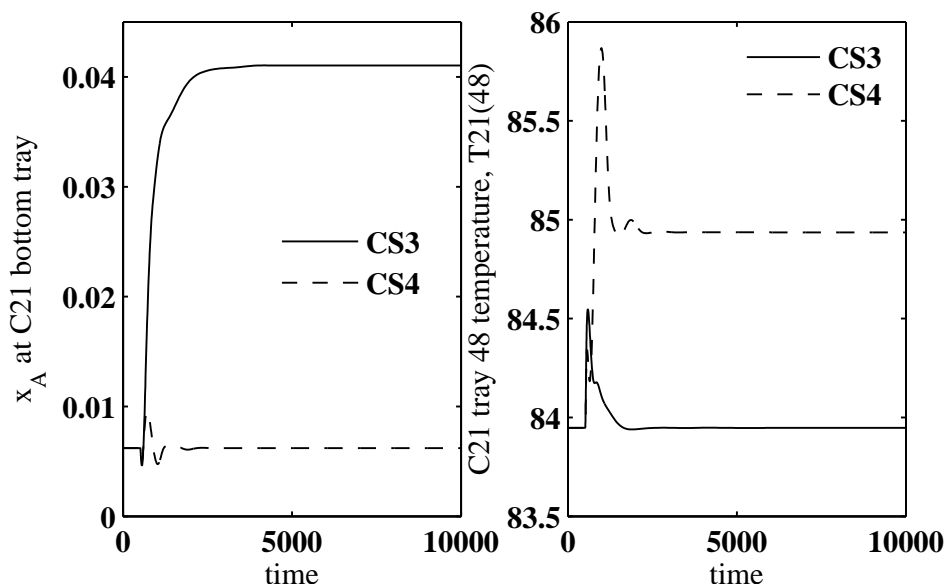


Figure 6.20: Regulatory response using CS3 and CS4 for a feed composition of  $z^F$  (mol %) = [20 25 25 30] on prefractionator column (C21) separation

(doing C/D split) is at the limiting reflux while sub-columns C32 and C31 have some excess reflux. Because the sub-column C33 has a two point control in structure CS1, for any disturbance that does not cause change the order of these peaks, structure CS1 can give pure side products. In other words, a disturbance that may cause A/B or B/C split to demand more boilup than the C/D split, the upper side product (S1) or the lower side product (S2) may become impure, respectively.

Figure 6.17 shows the  $V_{min}$  plot (in dashed line) for a new feed composition with 20 % C and 30 % D. Now, peak  $P_{AB}$  is highest, which makes the A/B separation the most difficult split. The structure CS1 has only one point control of sub-column C31. There is an insufficient boilup for a A/B separation and A (methanol) escapes from the bottom tray of column section C31, to contaminate the upper side product (S1). The similar reasoning can be given for a feed vapor fraction disturbance. See Figure 6.18, there is a change in the order peak points, resulting in the drop in the purity of upper side product (S1).

For the disturbances leading to changes in the peaks in  $V_{min}$  diagrams, a maximum-select controller with boilup can be used to implement a two point control in sub-columns C31, C32 and C33. Alternately in CS2 and

CS4, we propose a single controller that pairs boilup with the sum of the composition of light impurities at the bottom stages of the sub-columns C31, C32 and C33.

### 6.8.2 Temperature control

The control structures CS3 and CS4 use temperature controllers. The most sensitive tray temperature corresponding to a manipulated variable is chosen as the control variable. The manipulated variables are perturbed in manual mode from steady state to identify the sensitive tray temperatures. Figure 6.19 shows the effect of 1% change in reflux (MV1) to sub-column C1. The first plot shows the difference in the temperature of sub-column C1 from the initial state to the new steady state after perturbation. Tray 12 ( $T_{12}^1$ ) is clearly the most sensitive. The second plot shows the dynamics of tray temperature 12 of sub-column C1. This stage temperature ( $T_{12}^1$ ) is paired with MV1, and tuned for a good closed-loop response.

The control structure, CS3 uses temperature control alone. In a multi-component separation, the setpoints of temperature controllers should be changed for the feed composition disturbances. Figure (see Figure 6.14, at  $t=3600$  minutes) shows the regulatory response using CS3 when the composition of the components A (methanol) and D (*n*-butanol) in feed is changed. The purity of upper side product ( $x_B^{S1}$ ) drops considerably. As temperature setpoint of the controller is constant, a significant amount of A (methanol) escapes the sub-column C21 bottoms and appears in upper side product (S1) as impurity.

For a feed composition change from a nominal equimolar feed to one containing 20 % A and 30 % D, Figure 6.20 shows the composition of A (methanol) at the bottom tray of sub-column C21 using control structures CS3 and CS4. The second subplot shows the temperature of tray 48 in C21, which is paired with manipulated variable MV5. In structure CS4, the setpoint of the slave temperature controller is corrected using a master composition controller, which controls A (methanol) at the C21 bottom stage at its nominal value. Any key impurities escaping from sub-columns C1, C21 and C22 may make the final product impure. However for feed rate changes with fixed composition, the temperature control alone may be sufficient.

### 6.8.3 Composition control

The prefractionator “sub-column” C1 separates the components A and D. We thus control *n*-butanol,  $x_D$  (heavy impurity) in the top (or more precisely

in the liquid on the top stage) and methanol,  $x_A$  (light impurity) in the bottom liquid product. The optimal purities may vary and/or be difficult to find, but since this is an easy separation and we assume a relatively large number of stages. It will not cost much energy to over-fractionate, so it is suggested to set the setpoints for  $x_A$  and  $x_D$  at low values (for example,  $10^{-4}$ ). Similarly, in sub-column C21 we control the key components A (methanol) and propanol (C), and in column C22 we control key components B (ethanol) and D (*n*-butanol). Again, the setpoints for these may be set to low values, because the separations are expected to be easy compared to the number of stages.

For the sub-columns C31, C32 and C33, with the four end products, the choice on control variable is more difficult. For the top three products (D, S1 and S2), we suggest to control the corresponding heavy key impurity ( $x_B$ ,  $x_C$  and  $x_D$ , respectively) at the top stage in each sub-columns, by manipulating the liquid reflux into these sub-columns. The setpoints for these impurities are set by product specifications or by optimization. Three light key impurities now remain uncontrolled; namely  $x_C$  in the bottom product (B),  $x_B$  in the lower side product (S2) and  $x_A$  in the upper side product (S1). However, these three impurities cannot be controlled independently [37] because they are all determined by the boilup (V), which sets the vapor flow in the sub-columns C31, C32 and C33. The standard solution to this is to have three composition controllers (and three setpoints) with a max-selector that implements the largest controller output (boilup). This will imply that two of the products are over-purified. Alternatively, we propose a simpler solution with only one controller, which is to control the sum of the impurities,  $\ln(x_A + x_B + x_C)$ . The setpoint of this sum can then be adjusted to achieve the desired purities of the “limiting” product. Notice that when the boilup is used to control the sum of the light keys (in control structures CS2 and CS4), for the disturbances making A/B becomes the most difficult split (at time = 7200, 9600 in Figures 6.12 and 6.15), the bottom product gets over-purified, while other products are at their specifications.

There may also be a possibility of infeasibility in the setpoints of the key impurities in the two-point control of sub-columns. But this is eliminated by the choice of large number of stages. Another problem using composition control of keys at the column ends with composition pinch zones is that, the steady state gain for the corresponding manipulated variable can be nearly zero and there may be strong non-linearity effects as also discussed by previous workers [12, 24]. Therefore, their control using a feed back controller can be impossible. For sub-columns with limiting internal flows, there are no composition pinch zones at the ends and consequently, there

is a large steady state gain with the manipulated variables. Therefore, composition control is feasible with a feedback controller. However, in the sub-column C32 because of excess internal vapor and liquid flows (see Figure 6.3), there is a long pinch in the stripping section. B (ethanol) at C32 bottom tray was not chosen as a controlled variable, because of severe non-linearity effects. A composition on a sensitive tray and not a tray in the pinch zone can be a better candidate control variable.

## 6.9 Conclusions

In this paper, we propose simple decentralized control structures for minimum energy operation of the four-product Petlyuk column arrangement shown in the figure 6.1 or, its equivalent arrangement as shown in the Figure 6.2.

The proposed composition control scheme CS2 is shown in the Figure 6.7. It requires composition measurements or estimates for most internal and external flows in the column. If these composition measurements are not available, one may use the control structure CS4 in Figure 6.9, where the inner temperature loops are sufficient to stabilize the operation. The outer cascade composition loops are required in order to maintain product compositions and achieve minimum energy operation. The three prefractionator columns perform three easy splits (A/D, A/C and B/D), and the corresponding six key impurities may usually be controlled at low values without a noticeable increase in energy consumption. The remaining four degrees of freedom are used to control the three difficult splits (A/B, B/C and C/D) in the main column. We propose to control the amount of heavy impurity in the three light products (D, S1, S2) by adjusting the three liquid flows into the corresponding sections. Boilup (V) is then left to control the light impurity in the three heavy products (S1, S2 and B), and, in accordance with the  $V_{min}$ -diagram, we propose to control the most difficult split, for example, by using boilup to control the “maximum” of the three impurities (control structure, CS4) or their sum (control structure, CS2). This will result in “over-purification” of two of the products, but this will not generally increase the energy consumption because, as known from the  $V_{min}$ -diagram, we will optimally have excess energy in two of the sections.

## References

- [1] Adrian, T., Schoenmakers, H., Boll, M., 2004. Model predictive control of integrated unit operations: Control of a divided wall column.



- Chemical Engineering and Processing 43 (3), 347–355.
- [2] Agrawal, R., Fidkowski, Z. T., 1998. More operable arrangements of fully thermally coupled distillation columns. *AIChE Journal* 44 (11), 2565–2568.
- [3] Alstad, V., 2005. Studies on selection of controlled variables. Ph.D. thesis, Norwegian University of Science and Technology, Department of Chemical Engineering.
- [4] Buck, C., Hiller, C., Fieg, G., 2011. Applying model predictive control to dividing wall columns. *Chemical Engineering & Technology* 34 (5), 663–672.
- [5] Cahn, R. P., DiMiceli, A. G., 1962, US 3058893, United States Patent Office. Separation of multicomponent mixture in single tower.
- [6] Christiansen, A. C., 1997. Studies on optimal design and operation of integrated distillation arrangements. Ph.D. thesis, Norwegian University of Science and Technology, Department of Chemical Engineering.
- [7] Dejanovic, I., Matijaevic, L., Halvorsen, I., Skogestad, S., Jansen, H., Kaibel, B., Olujic, ., 2011. Designing four-product dividing wall columns for separation of a multicomponent aromatics mixture. *Chemical Engineering Research and Design* 89 (8), 1155 – 1167.
- [8] Dejanovic, I., Matijaevic, L., Halvorsen, I., Skogestad, S., Jansen, H., Kaibel, B., Olujic, Z., 2011. Designing four-product dividing wall columns for separation of a multicomponent aromatics mixture. *Chemical Engineering Research and Design* 89 (8), 1155 – 1167.
- [9] Dejanovic, I., Matijasevic, L., Olujic, Z., 2010. Dividing wall column—a breakthrough towards sustainable distilling. *Chemical Engineering and Processing: Process Intensification* 49 (6), 559–580.
- [10] Dwivedi, D., Halvorsen, I., Skogestad, S., 2011. Control structure design for optimal operation of thermally coupled columns. In: *Heritage Distillation Symposium*. Dr James Fair. topical Conference at the 2011 AIChE Spring Meeting. Curran Associates Inc.
- [11] Fidkowski, Z., Królikowski, L., 1987. Minimum energy requirements of thermally coupled distillation systems. *AIChE Journal* 33 (4), 643–653.

- [12] Fuentes, C., Luyben, W. L., 1983. Control of high-purity distillation columns. *Industrial & Engineering Chemistry Process Design and Development* 22 (3), 361–366.
- [13] Ghadrdan, M., Halvorsen, I. J., Skogestad, S., 2011. A shortcut design for Kaibel columns based on minimum energy diagrams. In: 21st European Symposium on Computer Aided Process Engineering. Vol. 29 of *Computer Aided Chemical Engineering*. Elsevier, pp. 356 – 360.
- [14] Halvorsen, I. J., Skogestad, S., 1999. Optimal operation of Petlyuk distillation: steady-state behavior. *Journal of Process Control* 9 (5), 407 – 424.
- [15] Halvorsen, I. J., Skogestad, S., 2003. Minimum energy consumption in multicomponent distillation. 1. vmin diagram for a two-product column. *Industrial & Engineering Chemistry Research* 42 (3), 596–604.
- [16] Halvorsen, I. J., Skogestad, S., 2003. Minimum energy consumption in multicomponent distillation. 2. three-product Petlyuk arrangements. *Industrial & Engineering Chemistry Research* 42 (3), 605–615.
- [17] Halvorsen, I. J., Skogestad, S., 2003. Minimum energy consumption in multicomponent distillation. 3. more than three products and generalized Petlyuk arrangements. *Industrial & Engineering Chemistry Research* 42 (3), 616–629.
- [18] Kaibel, G., 1987. Distillation columns with vertical partitions. *Chemical Engineering & Technology* 10 (1), 92–98.
- [19] Kiss, A. A., Bildea, C. S., 2011. A control perspective on process intensification in dividing-wall columns. *Chemical Engineering and Processing: Process Intensification* 50 (3), 281 – 292.
- [20] Kiss, A. A., Rewagad, R. R., 2011. Energy efficient control of a btx dividing-wall column. *Computers & Chemical Engineering* 35 (12), 2896 – 2904.
- [21] Lestak, F., Smith, R., Dhole, V., 1994. Heat transfer across the wall of dividing wall columns. In: *Trans. Inst. Chem. Eng.* 1994, 72A, 639–644.
- [22] Ling, H., Cai, Z., Wu, H., Wang, J., Shen, B., 2011. Remixing control for divided-wall columns. *Industrial & Engineering Chemistry Research* 50 (22), 12694–12705.

- [23] Ling, H., Luyben, W. L., 2009. New control structure for divided-wall columns. *Industrial & Engineering Chemistry Research* 48 (13), 6034–6049.
- [24] Moczek, J. S., Otto, R. E., Williams, T. J., 1963. Control of distillation column for producing high-purity overheads and bottoms streams. *Industrial & Engineering Chemistry Process Design and Development* 2 (4), 288–296.
- [25] Mutalib, M. I. A., Zeglam, A. O., Smith, R., 1998. Operation and control of dividing wall distillation columns: Part 2: Simulation and pilot plant studies using temperature control. *Chemical Engineering Research and Design* 76 (3), 319–334.
- [26] Niggemann, G., Hiller, C., Fieg, G., 2010. Experimental and theoretical studies of a dividing-wall column used for the recovery of high-purity products. *Industrial & Engineering Chemistry Research* 49 (14), 6566–6577.
- [27] Olujic, Z., Jdecke, M., Shilkin, A., Schuch, G., Kaibel, B., 2009. Equipment improvement trends in distillation. *Chemical Engineering and Processing: Process Intensification* 48 (6), 1089–1104.
- [28] Petlyuk, F., Platonov, V., Slavinskii, D., 1965. Thermodynamically optimal method for separating multicomponent mixtures. *International Chemical Engineering* 5 (3), 555–561.
- [29] Rewagad, R. R., Kiss, A. A., 2012. Dynamic optimization of a dividing-wall column using model predictive control. *Chemical Engineering Science* 68 (1), 132 – 142.
- [30] Skogestad, S., 2000. Plantwide control: the search for the self-optimizing control structure. *Journal of Process Control* 10 (5), 487–507.
- [31] Skogestad, S., 2003. Simple analytic rules for model reduction and pid controller tuning. *Journal of Process Control* 13 (4), 291–309.
- [32] Skogestad, S., 2007. The do’s and dont’s of distillation column control. *Chemical Engineering Research and Design* 85 (1), 13 – 23.
- [33] Skogestad, S., Morari, M., 1988. LV-control of a high-purity distillation column. *Chemical Engineering Science* 43 (1), 33 – 48.

- [34] Stupin, W., 1972. Thermally coupled distillation- a case history. *Chemical Engineering Progress* 68 (10).
- [35] Underwood, A. J. V., 1949. Fractional distillation of multicomponent mixtures. *Industrial & Engineering Chemistry* 41 (12), 2844–2847.
- [36] van Diggelen, R. C., Kiss, A. A., Heemink, A. W., 2010. Comparison of control strategies for dividing-wall columns. *Industrial & Engineering Chemistry Research* 49 (1), 288–307.
- [37] Wolff, E. A., Skogestad, S., 1995. Operation of integrated three-product (Petlyuk) distillation columns. *Industrial & Engineering Chemistry Research* 34 (6), 2094–2103.

# Chapter 7

## Conclusions and further work

### 7.1 Main Conclusions

This thesis reports results carried out for control and operation of three fully-coupled distillation arrangements, namely, the three-product Petlyuk column, the four-product Kaibel column and the four-product Petlyuk column. These arrangements are/will most commonly be realized at industrial scale using a dividing-wall in a single columns shell.

The main contribution of this thesis are described below.

- Three-Product Petlyuk Column

Single loop decentralized control structure strategies for a three-product Petlyuk arrangement is explored in Chapter 3. The message of this chapter is that a control structure that can ensure sufficient energy in all sub-columns may lead to products within the purity constraints. This can be ensured by feedback control of the key component in the most critical sub-column from energy point of view. Another proposed control structure is when vapor split is not available as a degree of freedom. This may come at the expense of some penalty, i.e., in the form of higher energy consumption. However, this loss is inevitable and the proposed control structure is close to the optimal energy usage with fixed vapor split.

- Four-product Kaibel Column

Experimental works carried on the four-product Kaibel column are described in Chapter 4. A four-point temperature control structure

is verified for steady-state operation as well for transient conditions during startup and disturbances due to feed changes and setpoint changes to temperature loops. A systematic method to fit an equilibrium based model to steady state experimental data is also described in this chapter.

- Four-product Petlyuk Column

The inferences drawn from the work carried out on the four-product Petlyuk arrangement is similar to the first study on three-product Petlyuk arrangement. The decentralized control structure can perform well and shows reasonable closed-loop performance. The main conclusion is that all the sub-columns should perform their separation task easiest split to ensure minimum energy operation and to obey the purity constraints. To ensure this, a LV configuration in each sub-column is recommended. In addition, the boilup should be paired with the light key at the bottoms of the column performing the most difficult binary split in the main column. This can be ensured by paring up the reboiler duty with sum of the light keys at the last stage of the three sub-columns constituting the main column.

- Active vapor split control

The experimental use of a vapor split valve as a degree of freedom for diving-wall columns is shown for the very first time. We also propose that the vapor split valve shall work best with a feed back loop. The feedback action removes any uncertainties in the vapor split between the prefractionator and the main column. There is no need for measuring the vapor flows to set the valve position. The use of vapor split valve in closed-loop is shown for operation of the four-product Kaibel column.

## 7.2 Further works

There are several areas of improvements and possibilities for further works as listed under:

- In Chapter 3, for selection of the control structures for the three-product Petlyuk columns, it was highlighted that there are four key impurities ( $x_B^D$ ,  $x_A^S$ ,  $x_C^S$  and  $x_B^B$ ) in the main column. Since all four compositions can not be specified simultaneously, it was recommended to fix two of compositions ( $x_B^D$  and  $x_C^S$ ) at their specifications. One

Table 7.1: Alternate control structures for three-product Petlyuk columns with two of the keys in the main column fixed at specifications (denoted by X)

	$x_B^D$	$x_A^S$	$x_C^S$	$x_B^B$
Alternative 1 <sup>a</sup>	X		X	
Alternative 2		X	X	
Alternative 3	X	X		
Alternative 4	X			X
Alternative 5		X		X
Alternative 6			X	X

<sup>a</sup> used in Chapter 3

of the remaining keys was controlled and the other was allowed to overpurify using a selector switch. However, this is only one of the six alternatives and there are a total of  ${}^4C_2 = 6$  possible alternatives. One can fix two of the keys and choose to overpurify or keep at specification the remaining two. Some these combinations leading to alternative decentralized control structures can be an interesting future work. Table 7.1 shows the six alternatives, where two of the alternative keys are fixed at their specifications.

- Chronologically speaking, works reported in Chapter 3 were done last while work on the four-product Petlyuk column were done earlier. Some of the findings made during the study of three-product Petlyuk column may also be relevant for the four-product Petlyuk column and should guide future works on four-product Petlyuk column, for example,

The setpoints for the prefractionator should be overpurified to avoid infeasibility in event of disturbances (as explained in Section 3.3.2). This finding should be useful also in case of the operation of four-product Petlyuk column. The discussion on “impossibility” of infeasible specifications of key impurities is correct in Section 6.8.3 for the prefractionator *only*, owing to large number of stages. However, there may still be infeasibility in the main column, due to “loose” specifications in the prefractionator column. Hence, some overpurification is good for the prefractionator.

Some structures *without* the use of the vapor split manipulation may be explored for the four-product Petlyuk arrangements as a future

work.

- Some future works related to simulation studies on Petlyuk arrangements reported in Chapters 3 and 6 are listed as follows.

We studied mainly LV control structures for the sub-columns constituting the Petlyuk arrangement. Some other variations like DV, L/D-V/B etc. are also possible which may offer superior dynamic performance and should be chosen appropriately on a case to case basis.

Distillation is a highly non-linear process and the point of operation may also have an impact on controllability. For example, a high purity column is more difficult to control. The design parameters of the column like number of stages may also have an impact on the controllability. These factors have not been studied in this work and should be treated as future work.

Direct composition measurement was used as controlled variable. Composition measurements are usually expensive. Therefore, a soft sensor based on temperature measurements may be developed and tested. This may be especially useful in the control of the prefractionator.

- We have reported only decentralized control structures. The simulation models and the experimental setup may also be used for testing a multivariable controller.
- As reported in Chapter 4, the number of stages in the experimental setup were not sufficient to yield high purity products. This can be improved by the use of structure packing. However, in practice, it was difficult to insert the thermocouple in the column sections together with the structured packing. So either, a solution to measure temperature with structured packing should be found or, a superior random packing may be used in place of Raschig rings.
- The vapor split valve used for experimental works can be improved by sizing it better. New designs of vapor split valves may be tested using current experimental setup.
- The experimental setup can be used for studying the control properties of four-product Kaibel column and three-product Petlyuk column. In this thesis, only works were carried out for separating four products. The same setup can be exploited to study operation of three-product Petlyuk arrangement.



- Further improvements may be done to the design of the experimental setup. For the products, swinging funnels may be replaced with metered-pumps. The level controller in the reboiler may be fixed for further experiments. The safety of the setup should be improved and methanol may be replaced by a more benign component.



# Joint Declaration by Co-Workers



### Joint Declaration by Co-workers

Chapter 3 in the doctoral thesis, “*Control and operation of dividing-wall columns with vapor split manipulation (2012)*”, by Deeptanshu Dwivedi is a joint work which has been submitted as the following article:

**Dwivedi D.**, Halvorsen I.J., Skogestad S., Control structure selection for three-product Petlyuk (dividing-wall) column”, *submitted to Chemical Engineering and Processing: Process Intensification*, 2012.

The contribution of each co-worker is as follows:

- Deeptanshu Dwivedi (Author 1): Wrote model for simulation studies, performed all the simulations and wrote the manuscript.
- Ivar J. Halvorsen (Author 2): Supervised the overall work and helped in analysis of results.
- Sigurd Skogestad (Author 3): Supervised the overall work, helped in analysis of results and in revision of the manuscript.



(Deeptanshu Dwivedi)  
PhD Candidate  
NTNU



(Ivar J. Halvorsen) (Sigurd Skogestad)  
Senior Scientist Professor  
SINTEF ICT NTNU



### Joint Declaration by Co-workers

Chapter 4 in the doctoral thesis, "*Control and operation of dividing-wall columns with vapor split manipulation (2012)*", by Deeptanshu Dwivedi is a joint work which has been submitted as the following article:

**Dwivedi D.**, Standberg J., Halvorsen I.J., Skogestad S., Steady state and dynamic operation of four-product dividing-wall (Kaibel) columns: Experimental Verification", *submitted to Industrial & Engineering Chemistry Research*.

The contribution of each co-worker is as follows:

- Deeptanshu Dwivedi (Author 1): Performed all the experimental runs, helped in later modification & maintenance of setup, performed experimental data- simulation fitting and wrote the manuscript.
- Jens Stranberg (Author 2): Built and contributed to design of the experimental setup and proposed the control structure.
- Ivar J. Halvorsen (Author 3): Supervised the overall work, helped in planning & running of experiments, trouble shooting during experimental runs and modifications of experimental setup.
- Sigurd Skogestad (Author 4): Supervised the overall work, helped in planning of experiments, helped in the design of the experimental setup & in analysis of the results and, in revision of the manuscript.



(Deeptanshu Dwivedi)  
PhD Candidate  
NTNU



(Jens P Strandberg)  
Senior Process Engineer  
Aker Solutions



(Ivar J. Halvorsen)  
Senior Scientist  
SINTEF ICT



(Sigurd Skogestad)  
Professor  
NTNU






### Joint Declaration by Co-workers


Chapter 5 in the doctoral thesis, "*Control and operation of dividing-wall columns with vapor split manipulation (2012)*", by Deeptanshu Dwivedi is a joint work which has been submitted as the following article:

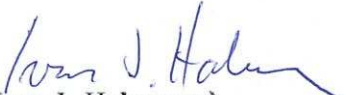
**Dwivedi D.**, Standberg J., Halvorsen I.J., Preisig, H.A., Skogestad S., Active vapor split control for dividing-wall columns", *submitted to Industrial & Engineering Chemistry Research*.

The contribution of each co-worker is as follows:


- Deeptanshu Dwivedi (Author 1): Performed all the experimental runs, helped in later modification & maintenance of setup and wrote the manuscript.
- Jens Stranberg (Author 2): Built and contributed to design of the experimental setup.
- Ivar J. Halvorsen (Author 3): Supervised the overall work, helped in planning & running of experiments, trouble shooting during experimental runs and modifications of experimental setup.
- Heinz Preisig (Author 4): Contributed to design of the experimental setup and helped in revision of the manuscript.
- Sigurd Skogestad (Author 5): Supervised the overall work, helped in planning of experiments, helped in the design of the experimental setup & in analysis of the results and, in revision of the manuscript.

  
(Deeptanshu Dwivedi)  
PhD Candidate  
NTNU

  
(Jens P Strandberg)  
Senior Process Engineer  
Aker Solutions

  
(Ivar J. Halvorsen)  
Senior Scientist  
SINTEF ICT

  
(Heinz Preisig)  
Professor  
NTNU

  
(Sigurd Skogestad)  
Professor  
NTNU



## Joint Declaration by Co-workers

Chapter 6 in the doctoral thesis, “*Control and operation of dividing-wall columns with vapor split manipulation (2012)*”, submitted by Deeptanshu Dwivedi is a joint work which has been accepted as the following article:


**Dwivedi D.**, Halvorsen I.J., Skogestad S., “Control structure selection for four-product Petlyuk column”, *Accepted for publications in Chemical Engineering and Processing: Process Intensification*, doi: “10.1016/j.cep.2012.07.013”.

The contribution of each co-worker is as follows:

- Deeptanshu Dwivedi (Author 1): Wrote the model for simulation studies, performed all the simulations and wrote the manuscript.
- Ivar J. Halvorsen (Author 2): Supervised the overall work and helped in analysis of results.
- Sigurd Skogestad (Author 3): Supervised the overall work, helped in analysis of results and in revision of the manuscript.



(Deeptanshu Dwivedi)  
PhD Candidate  
NTNU



(Ivar J. Halvorsen)  
Senior Scientist  
SINTEF ICT



(Sigurd Skogestad)  
Professor  
NTNU